NASA-CR-193731

NASA CONTRACTOR REPORT

NASA CR

(NASA-CR-193731) APPLICATION OF POWDER METALLURGY TECHNIQUES TO PRODUCE IMPROVED BEARING ELEMENTS FOR LIQUID ROCKET ENGINES Final Report, Feb. 1982 - Aug. 1992 (Compressor Components Textron) 115 p

N94-10804

Unclas

G3/26 0179801

APPLICATION OF POWDER METALLURGY TECHNQUES TO PRODUCE IMPROVED BEARING ELEMENTS FOR LIQUID ROCKET ENGINES

D. J. MORACZ, ET AL
COMPRESSOR COMPONENTS TEXTRON
MATERIALS & MANUFACTURING TECHNOLOGY CENTER
23555 EUCLID AVENUE
CLEVELAND, OHIO 44117

FINAL REPORT

AUGUST, 1992

PREPARED FOR
NASA - GEORGE C. MARSHALL SPACE FLIGHT CENTER
MARSHALL SPACE FLIGHT CENTER, ALABAMA 35812

TECHNICAL REPORT STANDARD TITLE PAGE

1. REPORT NO.	2. GOVERNMENT ACCESSION NO.	3. RECIPIENT'S CATALOG NO.
NASA CR		

4. TITLE AND SUBTITLE	5. REPORT DATE
Application of Powder Metallurgy Techniques to Produce Improved Bearing Elements for Liquid Rocket Engines	August 1992
	6. PERFORMING ORGANIZATION CODE
7. AUTHOR(S) D.J. Moracz, R.J. Shipley, V.S. Moxson, R.J. Killman and H.E. Munson	8. PERFORMING ORGANIZATION REPORT # EER-1041
9. PERFORMING ORGANIZATION NAME AND ADDRESS Compressor Components Textron Inc. Materials & Manufacturing Technology Center 23555 Euclid Avenue Cleveland, Ohio 44117-1798	10. WORK UNIT NO.
	11. CONTRACT OR GRANT NO. NAS8-34763
12. SPONSORING AGENCY NAME AND ADDRESS National Aeronautics and Space Administration Washington, D.C. 20546	13. TYPE OF REPORT & PERIOD COVERED Final February, 1982 - August, 1992
	14. SPONSORING AGENCY CODE NAS-MSFC

15. SUPPLEMENTARY NOTES

Prepared by Materials & Manufacturing Technology Center

16. ABSTRACT

The objective of this program was to apply powder metallurgy techniques for the production of improved bearing elements, specifically balls and races, for advanced cryogenic turbopump bearings. The materials and fabrication techniques evaluated were judged on the basis of their ability to improve fatigue life, wear resistance, and corrosion resistance of Space Shuttle Main Engine (SSME) propellant bearings over the currently used 440C.

An extensive list of candidate bearing alloys in five different categories; tool/die steels, through hardened stainless steels, cobalt-base alloys and gear steels; was considered. Testing of alloys for final consideration included hardness, rolling contact fatigue, cross cylinder wear, elevated temperature wear, room and cryogenic fracture toughness, stress corrosion cracking and five-ball (rolling-sliding element) testing.

Results of the program indicated two alloys that showed promise for improved bearing elements. These alloys were MRC-2001 and X-405. 57mm bearings were fabricated from the MRC-2001 alloy for further actual hardware rig testing by NASA-MSFC.

17. KEY WORDS	18. DISTRIBUTION STATEMENT
Powder Metallurgy Cryogenic Bearing Elements Turbopumps	Unlimited

19. SECURITY CLASSIF. (of this report)	20. SECURITY CLASSIF. (of this page)	21. NO. OF PAGES	22. PRICE
Unclassified	Unclassified	106	NTIS

MSFC - Form 3292 (Rev December 1972) For sale by National Technical Information Service, Springfield, Virginia 22151

TABLE OF CONTENTS

LIST OF ILLUSTRATIONS

LIST OF ILLUSTRATIONS

LIST OF ILLUSTRATIONS

LIST OF ILLUSTRATIONS

LIST OF TABLES

LIST OF TABLES

SECTION I. INTRODUCTION

Traditionally, high-performance bearings for aerospace applications are made from vacuum-melted M-50 steel. However, this 4% chromium alloy lacks corrosion resistance. For applications in which corrosion resistance is a major concern, such as cryogenic systems in which condensation can form, the trend has been to use 440C stainless steel. This alloy has been used successfully in less demanding cryopump applications. For the Space Shuttle Main Engine (SSME), however, 440C performance in the high-pressure turbopumps has been marginal. Detailed analyses have indicated that service life of the bearings is limited by wear as a result of poor lubrication conditions.

This performance is not acceptable because economic feasibility of the shuttle is based on reusability without extensive tear down and rebuilding. In the SSME, bearings are expected to withstand repeated firings with extensive idle period between. The cost of disassembly and reassembly to replace high pressure oxygen turbine pump (HPOTP) bearings is far greater than the cost of the bearings themselves.

Bearings which have been removed from the pump often show discoloration indicating oxidation and surface temperatures over $538^{o}C$ ($1000^{o}F$) (1). The bearings are designed to be cooled by liquid oxygen and lubricated with PTFE transfer from the ball separator. The cooling and lubrication are inadequate to support more than typically three missions. The heating of the bearing surface is partially due to micro-welding and tearing resulting from inadequate lubrication and partially due to the reduced cooling efficiency of the oxygen when it vaporizes upon contact with the frictionally heated bearing.

The purpose of this program was to select an improved bearing alloy for demanding cryogenic applications such as the HPOTP of the SSME. At present, the time between overhaul of the HPOTP, which delivers liquid oxygen to the SSME, appears to be limited by the life of its cryogenic bearings, made from vacuum melted, heat treated 440C stainless steel.

A basic premise of this program was that powder metallurgy (P/M) processing, rather than conventional cast/wrought processing, would provide a superior metallurgical microstructure, regardless of the bearing alloys being considered. During powder manufacture, individual powder particles solidify very rapidly. Therefore, when properly consolidated, the microstructure of a P/M alloy is fine and homogeneous. The primary carbide particles in a P/M bearing alloy are very small and uniformly distributed. Furthermore, P/M processing provides the potential for alloy compositions which are simply not practical through conventional processing. Thus, advanced P/M technology is a viable approach to produce bearing materials that are resistant to oxidation, wear, and rolling contact fatigue, thereby extending the service life of the SSME cryogenic bearings.

Note that as used here, P/M refers to hot consolidated, fully dense material, rather than material that has been cold-pressed and sintered or cold-pressed, sintered, and forged.

To accomplish the objective of developing a superior bearing alloy for cryogenic applications such as the HPOTP, a three phase program was performed. Phase 1 of this program compiled an extensive list of candidate bearing alloys in five different categories, i.e. tool/die steels, through hardened stainless steels, cobalt-base alloys and gear steels. The list of fifty-six alloys was narrowed down to eleven P/M alloys which were evaluated for hardness, rolling contact fatigue life, cross cylinder wear, fracture toughness, and corrosion resistance. Based on the results, six alloys were selected for further study in Phase 2.

Phase 2 efforts were directed at further corrosion resistance and rolling contact fatigue testing, elevated temperature wear testing, cryogenic fracture toughness testing, stress corrosion cracking testing and five-ball (rolling-sliding element) testing.

In Phase 3, two alloys were selected for fabrication and testing of full-scale bearing assemblies.

SECTION II. DESCRIPTION

A. Phase 1 - Material and Fabrication Technique Evaluation and Selection

The Phase 1 objective was to generate appropriate selection criteria and then apply these criteria to identify candidate materials and fabrication techniques for high pressure oxygen turbopump (HPOTP) bearing applications.

Phase 1 was divided into two tasks which were performed sequentially. In Task 1, analytical studies were performed in which the cryogenic pump bearing requirements at 2.5×10^6 DN were defined, examination and analysis of failed 440C bearings were performed, and selection and evaluation criteria were established. In Task 2, these criteria were used to identify candidate bearing materials and fabrication techniques for subsequent evaluation in Phase 2. Properties of the current 440C bearing material were used as the baseline for all comparisons.

1. Experimental Procedures and a Discussion of Results

a. Task 1. Analytical Studies. Several bearing parts from HPOTP 440C bearings were obtained from NASA/MSFC for analyses to better define cryogenic pump bearing requirements and to assist in the selection and evaluation criteria for proposed new bearing alloys. The following bearing parts from HPOTP 440C bearings shown in Table 1 below were examined by the TRW Bearings Division Laboratory (now known as MRC Specialty Bearings a division of SKF Bearings).

Table 1
HPOTP 440C Bearings Analyzed

Bearing S/N	Run in Pump S/N	Pump Position	Part
8549531	9008	3	Section from inner race
8549531	9008	3	Section from outer race
8557044	2110	4	Section from inner race
8557044	2110	4	Section from outer race
8557044	2110	4	Two balls
8517824	2007	4	Section from inner race

TRW Bearings Division Laboratory also received reports on Rocketdyne personnels' examination of bearings from ten pumps. These reports are briefly summarized in Table 2 to indicate basic failure patterns. In addition, TRW had access to "HPOTP Bearing Consultant Review" Rockwell International report BC 81-52, dated March 25, 1981 (2), which described the pump application and reviewed numerous failures. In October, 1981, TRW Bearings Division personnel examined the No. 4 bearing from Pump S/N 9008 at the request of Rocketdyne personnel. A literature survey identified several reports (3,4,5) of importance to the problem.

The HPOTP is a turbine driven pump which delivers liquid oxygen to the main rocket engine. Another pump delivers liquid hydrogen to the engine and the reaction of oxygen and hydrogen provides thrust for the Space Shuttle. A part of the liquid oxygen being pumped is bypassed into the bearing compartment to cool the bearings. The pump shaft is supported by two pairs of preloaded, angular contact ball bearings, as shown in Figure 1.

Shaft speed is approximately 30,000 RPM. The two sets of bearings are preloaded by Belleville washers. To facilitate sliding of outer rings in housings under the influence of the spring washers, outer rings are coated with a dry film lubricant. Both bearing pairs are subject to radial loads from three sources: weight of components, reaction to the torque of the pump, and unbalances in the rotating system. Ideally, the only axial loads are those produced by the preload springs because the balance piston arrangement equalizes the axial forces produced by turbine and pump. In practice, there are high axial forces on the No. 3 bearing during transient conditions, such as starts and stops.

Basic lubrication of the bearings is by transfer film of PTFE from the "Armalon" cages. Several of the bearings which were covered in Rocketdyne's reports of bearing examinations had dry film lubricant on internal surfaces in a further attempt to improve lubrication.

The cryogenic environment plus the fact that bearings return to normal ambient temperatures and atmospheres between tests or firings require corrosion resistant materials for the bearings. When cold bearings are returned to a normal environment, moisture condenses on the surfaces. Most bearings in the HPOTP application have been made of AISI 440C steel. One set of bearings covered in Rocketdyne's examination was made from BG-42, which is a modified 440-type steel with higher hot hardness and, generally, improved fatigue endurance life.

Data in Table 2 was abstracted from observations of bearings removed from test by Rocketdyne personnel. Ten pumps were involved. Each pump was subjected to more than one run, and runs were of varying duration. A number of these tests involved experimental hardware, such as variations in preload springs. The No. 3 and 4 bearings in Pump S/N 9308 were made from BG-42 steel. All other bearings were made of 440C steel. Some bearings had dry filmed races and balls while others did

Table 2
Summary of Bearing Condition After HPOTP Testing
Inspection by Rocketdyne Personnel

Pump S/N	No. Seconds Operation	Bearing Position	Overall Condition	Inner Race	Inner Shoulder	Outer	Balls	Cage
2011R1	1231	1	Dented					Lt.Contact
(4 Starts)		2	Failed		Rolled Over		Small & Dark	Hvy.Contact
		3	Failed	Distress		Distress	Golden Colored	Lt.Contact
		4	Failed	Distress	Rolled Over	Distress	Small & Spalled	Hvy.Contact
9308	101.5	1	Reusable	Scuffed		Dents		Med.Contact
(2 Starts)		2	Reusable	Scuffed		Dents		Med.Contact
		3	Failed	Scuffed		Dents	Micro-Spalls	Med.Contact
		4	Failed	Scuffed			Micro-Spalls	Delamination
0405R1	900*	1	Not Reusable	Dented				Lt.Contact
(3 Starts)		2	Failed	Distress			Small & Dark	Hvy.Contact
		3	Failed	Spalled		Dents	Small & Gray	Hvy.Contact
		4	Failed	Spalled			Small & Dark	Hvy.Contact
0209R1	2522.2	1	Reusable					Lt.Contact
(9 Starts)		2	Reusable					Lt.Contact
		3	Failed	Spalled		Distress	Shallow Spalls	Hvy.Contact
		4	Failed	Distress	Rolled Over	Distress	Small & Dark	Hvy.Contact
0108	850	1	Reusable					Lt.Contact
(3 Starts)		2	Reusable					Lt.Contact
		3	Failed	Spalled		Spalled	1 Spall	Med.Contact
		4	Failed	Spalled		Spalled	Small & Black	Med.Contact
2111	1250	1	Not Reusable					Delamination
(3 Starts)		2	Not Reusable	Light Distress				Hvy.Contact
		3	Not Reusable				Dark Colored	Hvy.Contact
		4	Failed		Rolled Over		Small & Black	Erosion
2110	1250	1	Failed				Dark Colored	Delamination
(3 Starts)		2	Failed				Small & Dark	Hvy.Contact
		3	Not Reusable					Hvy.Contact
		4	Failed		Rolled Over		Small	Delamination
9305	102	1	NOT LISTED					
(7 Starts)		2	NOT LISTED					
		3	Reusable	Scuffed		Dents		
		4	Reusable	Scuffed		Dents		

*Apparently the bearings in Pump 0405R1 had been subjected to additional running, perhaps under different conditions, before the three starts totalling 900 seconds listed here.

Table 2 (Cont'd)
Summary of Bearing Condition After HPOTP Testing
Inspection by Rocketdyne Personnel

Pump S/N	No.Seconds Operation	Bearing Position	Overall Condition	Inner Race	Inner Shoulder	Outer	Balls	Cage
2110	1760	1	Probably Reusable					
(5 Starts)		2	Probably Reusable					
		3	Failed	Spalled		Spalled	7 Spalls	Hvy.Contact
		4	Failed	Spalled	Rolled Over	Spalled	Small & 9 Spalls	Delamination
0010R1	1147	1	Reusable	Discolored			Discolored	
(5 Starts)		2	Reusable	Discolored			Discolored	
		3	Failed	Spalled		Spalled	Small & 4 Spalls	
		4	Failed	Spalled		Spalled	1 Spall	Hvy.Contact

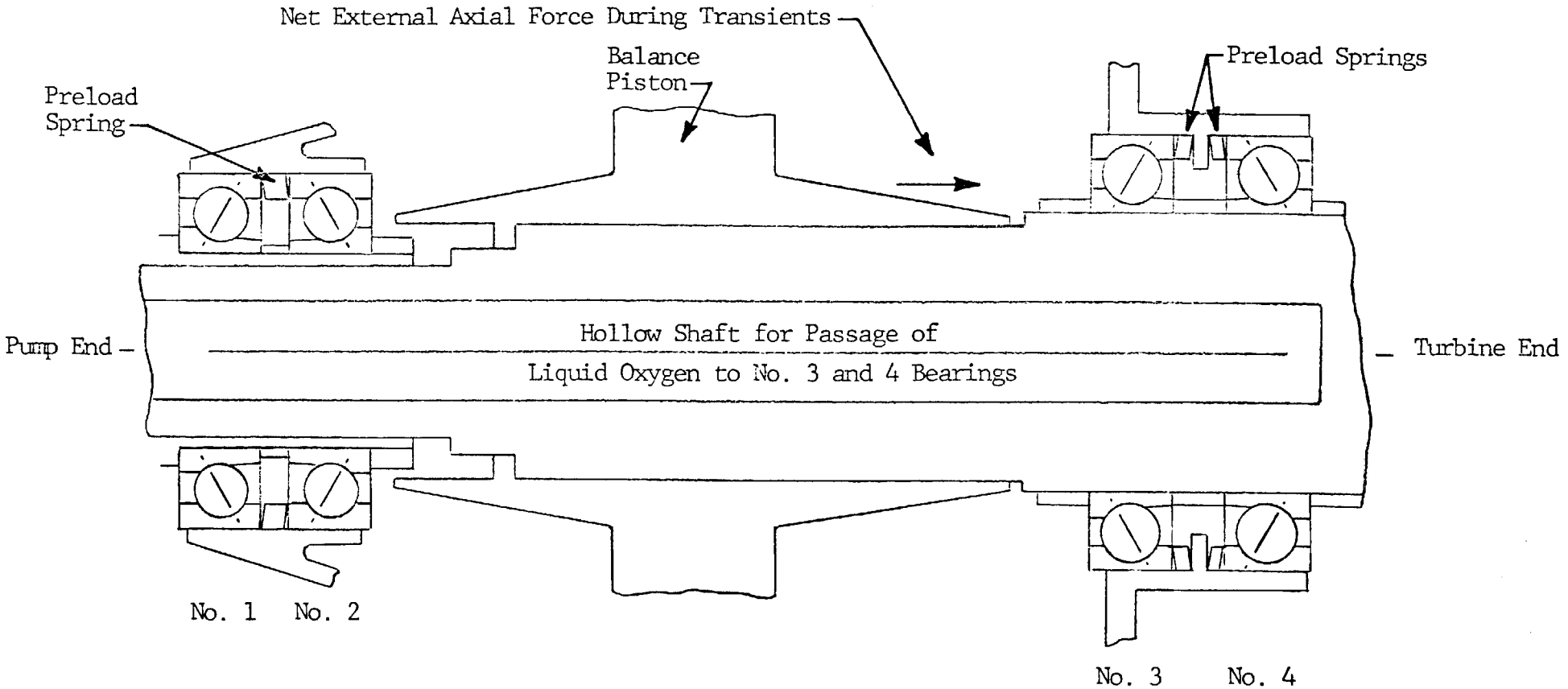

Figure 1. Schematic of bearing set-up in HPOTP.

not. Pump operating levels were varied so that some pumps never reached rated conditions, some ran for a substantial percentage of time at full design load, and two (S/N 2110 and 2111) ran part of the time at 111% of design load. Thus, a fully quantitative analysis of bearing condition versus operating conditions is not feasible.

Data in Table 3 summarizes examinations made by TRW Bearings Division personnel on bearings or parts of bearings submitted to TRW for analysis. All raceway spalls appear to have been of the shallow, surface-initiated type. Figure 2 shows a spalled raceway in which surface distress is becoming microspalling. In Figures 3 and 4, microspalling has become more extensive, and somewhat larger, but still shallow spalls have developed. In Figure 5, sections of balls show both shallow surface spalling and deep spalling (left ball only). All components in Figures 3, 4, and 5 show significant discoloration, apparently from oxidation. In Figure 3, the inner raceway corners have been rolled over, with some chipping of the rolled edge, during operation.

Raceway and ball surfaces demonstrated typical results of inadequate lubricant films. In a usual oil-lubricated ball bearing application, an oil film is developed which prevents most metal-to-metal contact between balls and races. This oil film is a function of fluid viscosity, rotational speed, and applied load. The success of the film in preventing metallic contact is a function of the film's thickness and the smoothness of the contacting surfaces. When the film is of insufficient thickness to prevent metallic contact, the high points of the surfaces intermesh, causing microwelding and tearing. Surfaces become rougher so that the deterioration is accelerated and microspalls develop. Cracks emanate from the microspalls and more material breaks away, creating larger spalls. This same phenomena is observed in the HPOTP bearings. In this case, the extremely low viscosity of liquid oxygen prevents a sufficiently thick film from developing. While solid lubricant films can also prevent metal-to-metal contact (and an attempt is being made to do this through the "Armalon" cages and dry filming surfaces) it has not been adequate.

A second problem is inadequate cooling. This is indicated by the low contact angle on the inner races of many bearings and discoloration of races and balls. The low contact angle develops because the inner ring and/or the balls become warmer than the outer ring and expand. This expansion decreases the internal clearance and the bearing operating contact angle is reduced. Discoloration is produced by high temperature oxidation of surfaces; work performed at NASA's Marshall Space Flight Center indicates that these surface temperatures sometimes exceed 538^{o}C (1000^{o}F).

As contacting surfaces become rough they generate more heat. Some of the liquid oxygen striking the contact areas is vaporized, greatly reducing its cooling ability. The gas bubbles have a pressure which probably interferes with liquid oxygen getting to the affected areas.

Table 3
Summary of HPOTP Bearing Inspection by TRW Personnel

Pump S/N	No.Seconds Operation	Bearing Position	Overall Condition	Inner Race	Inner Shoulder	Outer	Balls	Cage
0008	2180	4	Failed	Spalled		Spalled	Spalled	*
9008	2406	3	Failed	Spalled	Rolled Over	Spalled	Spalled*	*
2110**	1760	4	Failed	Spalled	Rolled Over	Spalled	Small & Spalled	*
2007	6092	4	Failed	Microspalled		*	*	*

*Not available for examination by TRW
**Note that this bearing is included in Table 2

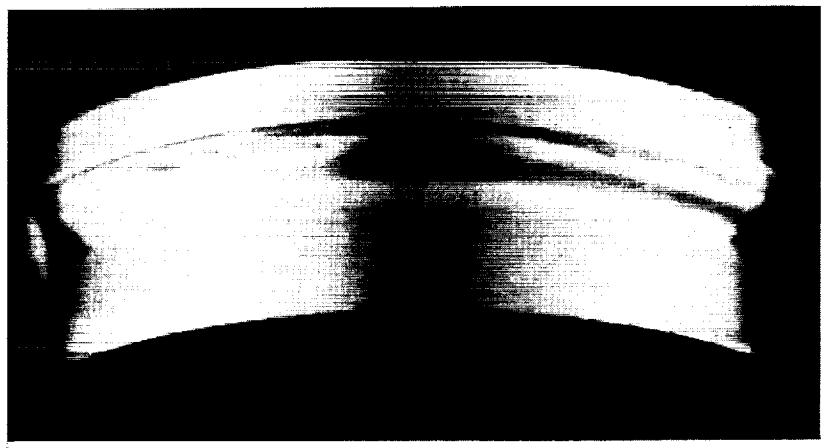

Figure 2. Inner race from No. 4 bearing, HPOTP S/N 2007.

Microspalling can be seen in band in normal location on raceway. Some burnishing can be seen high on raceway, near shoulder. Color variations in raceway are not as pronounced as they appear in picture.

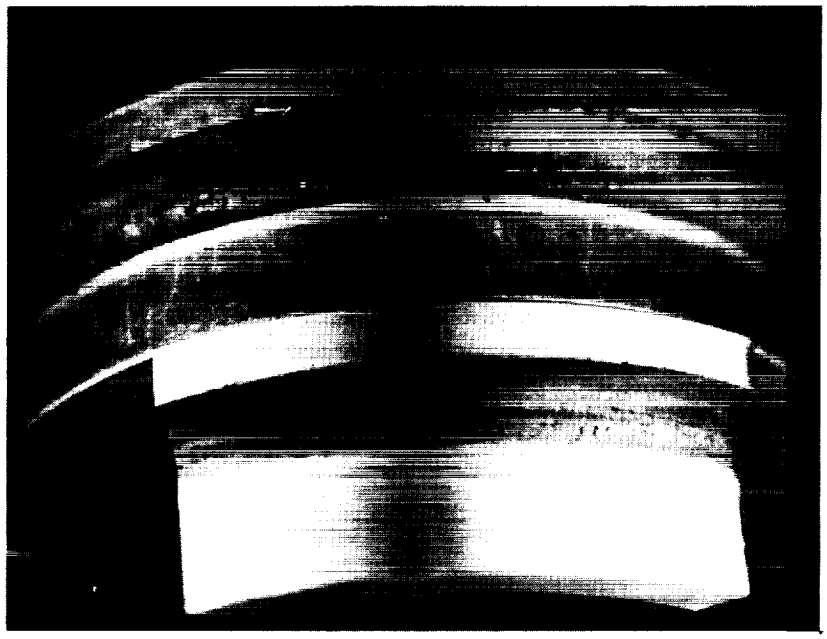

Figure 3. Sections of inner races from No. 4 bearing HPOTP S/N 2110 (top) and No. 3 bearing HPOTP S/N 9008 (bottom).

Dark shoulders of No. 4 bearing are from dry film lubricant applied to race. Both races have extensive shallow spalling at low contact angle (near bottom of race). The corner of the high shoulder (thrust-carrying side of race) of each bearing is rolled over and somewhat chipped. Races are somewhat discolored, but the brown hue is accentuated by the photographic film.

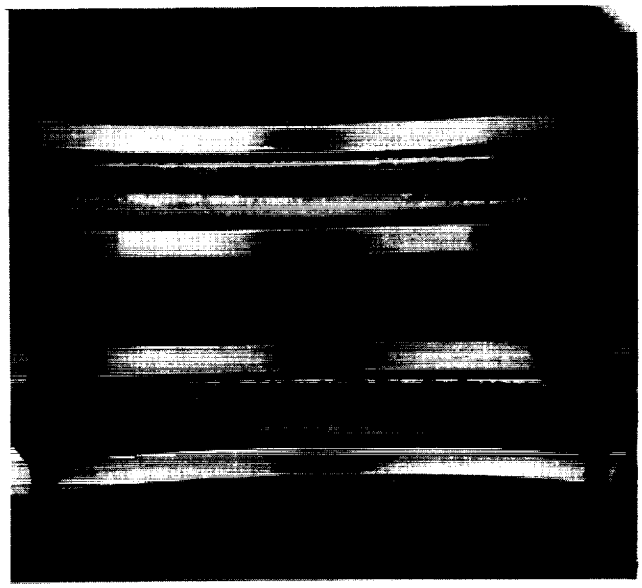

Figure 4. Sections of outer races from No. 4 bearing HPOTP S/N 2110 (top) and No. 3 bearing HPOTP S/N 9008 (bottom).

Both raceways have multiple ball tracks. Microspalling exists in a narrow band just below center of race in each race. The most heavily loaded area in No. 3 bearing, near lower shoulder, is not spalled. Races are discolored in ball tracks.

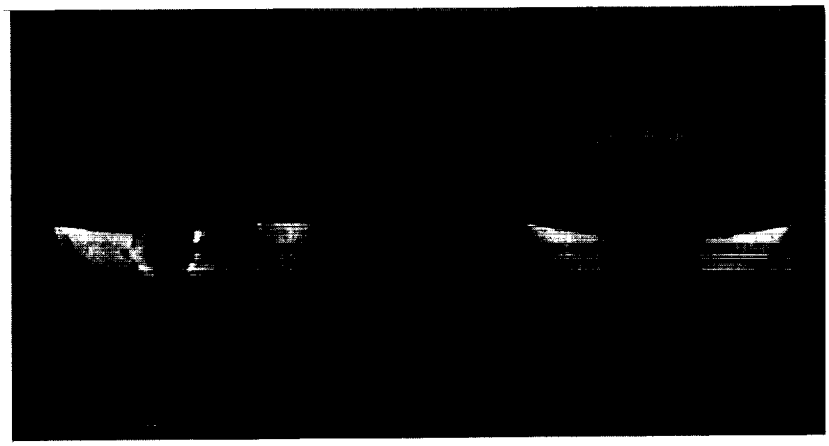

Figure 5. Sections of two balls from No. 4 bearing, HPOTP S/N 2110.

Both balls show microspalling. Left ball shows a deep spall also. Both balls are discolored.

Thus, another regenerative situation occurs, which once underway proceeds at an accelerated pace.

It may be argued that if the above scenario is correct, there should be frequent catastrophic failures. In these, all internal clearance is lost, the cages are broken, and balls may become grossly misshapen. Instead, there have been no reports of any catastrophic failures in this application. It is believed that the extreme cold of the immediate environment plus the short duration of individual runs has prevented complete bearing breakdown at failure. Although surfaces become hot, the bulk of bearing material remains cool, analogous to the condition which occurs during a typical machining operation; therefore, loss of clearance develops relatively slowly.

It may be further argued that the low contact angle is caused by an excessive, externally applied, radial load. However, this argument is doubted for three reasons. In all of the failed bearings examined, there were indications that there was considerable operation at "normal" or higher than normal contact angles before entering the low contact angle mode. Secondly, the inner race condition is so typical of the loss-of-clearance-type failures which have been observed often in more conventional bearings. Finally, if an excessive radial load was applied to the No. 3 and 4 bearings one also would expect to see indications of heavier loading on the No. 1 and 2 bearings.

The low contact angle in a bearing operating under axial load results in an increased stress, since the normal force applied to the ball raceway contact is inversely proportional to the sine of the contact angle. As a consequence, the surface initiated spalls become more pronounced at the lower contact angles.

Another problem occurring in these bearings is gross wear of balls and races. This is a situation which also occurs in more conventional applications, typically from operation at high speed under light loads. In the HPOTP application there is an additional probable source of wear: oxidation of surfaces followed by more running. Of the nine each No. 1 and 2 bearings and ten each No. 3 and 4 bearings which are listed in Table 2, one No. 2 bearing and four No. 4 bearings have rolled-over inner race shoulders. Two No. 2 bearings, two No. 3 bearings and seven No. 4 bearings have balls that have worn undersize. In Table 3 it may be observed that a No. 3 bearing also has a rolled-over race shoulder; this may have been caused by an excessive axial load.

In the HPOTP application, shown in Figure 1, the No. 1 and No. 2 bearings are preloaded as a pair, as are the No. 3 and No. 4 bearings. External axial loads from pump and turbine are supposed to be equalized by the balance piston, but under transient conditions, the unbalanced load will be applied to the No. 3 bearings. This action moves the shaft to the right (Figure 1). Ideally, the outer ring of each bearing slides in its housing under the influence of the preload springs, and axial preload is maintained. In practice, both in the HPOTP application and

in conventional applications, some of the bearing outer rings do not slide; in that case No. 2 and/or No. 4 bearings tend to lose axial load. When the unbalanced load is overcome by forces on the balance piston, the shaft apparently remains in the offset position so that unloaded bearings are still essentially unloaded. The bearing in the pair which receives the external axial load tends to receive most of the radial load also, because of the greater effective clearance in the unloaded bearing. When a ball bearing operates at high speed under a lightly loaded condition, centrifugal force drives the balls into the center of the outer race, while the balls tend to approach the shoulder of the inner race. If the applied load is insufficient to maintain traction, ball speed will vary continuously, producing severe sliding action between balls and the inner race. Under poor lubrication there will be erosive wear. As balls become undersize their contact on the inner race reaches the corner. Even a small axial force is sufficient to roll a ridge of metal over the corner. As soon as balls in one bearing of a pair are undersize the radial load will be concentrated on the other bearing, even if the outer ring is now able to slide under the influence of the preload spring.

In Table 2, two No. 3 bearings are noted as having undersize balls. It is possible to explain this as being caused by the same basic mechanism which occurs in the No. 2 and No. 4 bearings; however, this time one assumes that the external axial load is very small and the preload spring is unable to apply a preload. In Pump No. 0405 R1, however, both No. 3 and No. 4 bearings have undersize balls, suggesting that the two bearings would have had to take turns carrying the applied radial load. As long as a substantial radial load is present, the bearing supporting it will tend to possess tractive forces which reduce slippge.

A possible explanation for the undersize balls in the No. 3 bearings, and perhaps in some of the others, is that the oxidized surfaces eroded under rolling contact. All undersize balls are noted as being discolored.

The inner race of bearing No. 3 from Pump No. 9008 (Table 3 and Figure 3) had a rolled-over corner. This is the only case of a No. 3 bearing with a rolled-over corner that was observed. The "HPOTP Bearing Consultant Review" report (2) referenced earlier noted that balls from this bearing showed spalling and mechanical wear. It was TRW's understanding at that time that bearings in Pump No. 9008, and others tested before March 1981, may have been subjected to heavier transient loads than subsequent bearings. Ultimate failure occurred at a low contact angle. It was suspected that the rolled-over corner in this bearing occurred during a transient high load condition after balls had already become undersize.

All but two of the pumps whose bearing data are summarized in Table 2 were run after March 1981. Bearings which were available for examination by TRW, except for No. 4 bearing from Pump No. 2110, were run before March 1981. Reference (2) describes a number of changes

which were being made in bearings and assembly to improve bearing life. It was not known when some of these changes were incorporated, but it appeared that most of the same failure mechanisms were at work in the more recent tests as in the earlier ones. A possible exception is the transient axial overload condition which may have been improved. From the descriptions it could not be determined if dry film lubricant applied to internal surfaces made any significant improvement in performance. One set of bearings, in Pump No. 9308, was made from BG-42 corrosion resistant steel. Test duration was too short to make a direct comparison with other data, but bearings failed with microspalls in the balls.

Data indicate that the No. 1 bearing experiences the least amount of problems in the application. This bearing receives radial load, axial preload, and possibly external axial load. Apparently the preload spring works, to the extent that the bearing always has an adequate load. The No. 2 bearing fares almost as well as the No. 1 bearing, but sometimes loses preload. It can be concluded from the No. 1 and No. 2 bearing experiences that radial load is not excessive.

The No. 3 and No. 4 bearings fail rapidly. They would seem to be exposed to the same sort of conditions as the No. 1 and No. 2 bearings, except for external axial load on bearing No. 3. Axial preload is somewhat higher than on the No. 1 and No. 2 bearings, but it is proportional to their higher capacity. The radial load may be higher on No. 3 and No. 4 bearings, but it is not believed to be excessive or one would not see manifestations of slippage which occur in bearing No. 4. The most critical differences may be cooling. No. 1 and No. 2 bearings receive a greater liquid oxygen flow than do No. 3 and No. 4 bearings and they receive it more directly. No. 1 bearings may be better cooled than No. 2. No. 3 and No. 4 bearings are cooled by liquid oxygen which must first pass through a hollow shaft, and this would appear to be capable of being reduced by pressure from vaporizing liquid in the bearing chamber. The worst problem with bearing No.'s 3 and 4 appears to be a thermal one.

In an attempt to upgrade bearing performance, BG-42 has been substituted for 440C in one test of which was known at that time. This one test is inconclusive. BG-42 is reported to have higher fatigue endurance life than 440C, higher hardness, and retains that hardness at higher temperatures. BG-42 has corrosion resistance comparable to 440C. Hot hardness has apparently not been a problem in this application. Even though surfaces become hot, the bulk metal remains relatively cool because of the ambient environment and the brevity of the runs; macro-hardness checks of discolored rings and balls reveal no measurable softening. Improvement in fatigue endurance has always been a primary aim of bearing material technology which suggests BG-42 should be preferable in this regard. However, all raceway spalling and most of the ball spalling seems to have been of the surface-induced type. This failure mechanism is not addressed by improvements in conventional fatigue endurance. Some balls have deep spalls which may have resulted from repeated stressing of surface-spalled areas.

The evidence presented at that time suggested that a material with better wear resistance could significantly improve bearing life. Bench tests at TRW demonstrated that some bearing materials of comparable hardness differ from others in wear resistance by an order of magnitude. Wear of balls has been a major failure mechanism. If wear could be reduced there would be less debris to initiate surface distress, load sharing could improve, and thermal excursions might be slowed.

There is some evidence that corrosion resistance at a high surface temperature may be important. Problems created by erosion of corroded surfaces may be approached by improved corrosion resistant materials or by reducing temperatures within the application.

The conclusion reached from these analytical studies is that the fundamental problem in the HPOTP bearings is lubrication, but this has several facets. In more conventional applications, lubrication problems have sometimes been solved by simply reducing the load or stress. Any improvement which interrupts the regenerative chain of events which one observed in the HPOTP failure modes will improve life. At the present time, wear resistance, resistance to micro-spalling, and perhaps corrosion resistance at high temperatures appear to be the most important material characteristics to be considered.

Improved fatigue endurance of the bearing material will reduce subsurface initiated spalling, which may be currently present in balls, and may reduce micro-spalling. If primary failure modes can be reduced or eliminated, bearings will last longer and conventional fatigue endurance will become more and more significant.

It would appear also, from work done at Rocketdyne and NASA, that crack arresting properties of the material may be important in preventing small spalls from progressing to fracture.

b. Task 2. Selection of Candidate Materials and Fabrication Techniques

(1) Listing of Candidate Materials. Based on the analytical studies performed in Task 1 and discussions with bearing experts at NASA MSFC a list of candidate bearing materials was compiled as shown in Table 4. The criteria used to select the candidate bearing materials was wear resistance, corrosion resistance, toughness and hardness. These materials represented five generic families of materials: tool/die steels, through-hardened stainless steels, surface hardened stainless steels, cobalt-based alloys, and gear steels. From this selection, eleven alloys, X-405, MRC-2001, T-440V, 14-4/6V, D-5, Vanadium-modified Pyromet 350, Stellite 3, FerroTic CS-40, Triballoy 800, WD-65 and CBS-600, were selected for evaluation.

(2) Material Procurement and Processing. As was stated previously, all materials evaluated would be processed by powder metallurgy. Powders were purchased from four sources. Nitrogen

Table 4
Candidate Materials

Alloy	Composition(%), Typical*										Typical Hard.(Rc)	Impact Strength	Wear Resistance	Other
	Base	Cr	Mo	V	Co	Ni	Mn	Si	C	Other				
1. Tool/Die Steels														
D-1	Fe	11.5	0.45	0.3	-	-	-	-	1.0		60	CCN 209		
D-2	Fe	11.5	0.8	0.4			0.3	0.4	1.5		60-64	IZOD 24-60		
D-3	Fe	12	-	0.25			0.6	0.5	2.2		61-62	IZOD 25-30	Good	
D-4	Fe	12	0.8	0.4			0.2	0.3	2.2		59-61		Good	
D-5	Fe	12.5	1.5		2.75		0.3	0.3	1.25		60	IZOD 62 CCN 25	Good	Rust Resist.
D-6	Fe	13					0.75	0.3	2.05	1.25W	60-66		Good	
D-7	Fe	13	1.1	4		(0.5)	0.4	0.4	2.4		60-64	IZOD 18		
COBALT CHROM	Fe	12.5	0.7		3	(0.6)	(0.35)	(0.6)	1.35		61	LOW	Good	Rust Resist.
CHROMOVAN	Fe	12.5	0.8	1					1.6		62-65	IZOD 44-57	Good	Abrasion Resist.
DOUBLE-SIX SUPER	Fe	12.5	0.8	0.25					1.9		60-66	IZOD 38-42		
CHROMEWEAR 300	Fe	8.25	1.12	4.5			0.7	0.4	2.7		60-67		4 to 5 times D-2	
CPM-M4	Fe	4.25	4.5	4			0.3	0.3	1.35	5.75W	61-63	CCN 32		
CPM-9V	Fe	5.25	1.3	9			0.5	0.9	1.8		56-58	CCN 20	Excellent	
FERROTIC CS-40	Fe	17.5	0.5						0.8		66-68			+45% TiC
M-50	Fe	4	4.25	1			0.25	0.2	0.85		58-64	M/CVN 22-25	.0073	B_{10}=4.5
2. Stainless Steels (Through-Hardened)														
440B	Fe	17	(0.75)				(1)	(1)	0.85		58-59			
T440V	Fe	17.5	0.5	5.75			0.5	0.5	2.2		58-63	CCN 11		
BG-42	Fe	14.5	4	1.2			0.45	0.3	1.15		60-63			
MRC-2001	Fe	15	6	2			0.5		1.2	.1Cb	60-62	M/CVN 8	.0023	
WD-65	Fe	14	4	2.75	5.75				1.15	2.5W	58-62	M/CVN 7-8.5	.0623	B_{10}=2
CRB-7	Fe	14	2	1			0.4	0.3	1.1	.25Cb	61	M/CVN 12	.0733	B_{10}=15
14-4/6V	Fe	14.5	4.5	6			0.5	0.5	2					B_{10}=4.7
X-405	Fe	19	2	1					1.25					
NM-100	Fe	17.5		0.75	9.5				1.25	10.5W				
AEB-L	Fe	13.2					0.6	0.38	0.68		60			
WB-49	Fe	4.2	3.7	1.9	5.2				1.09	6.7W	61			

* (X) - Maximum

Table 4
Candidate Materials

Alloy	Composition(%), Typical*										Typical Hard.(Rc)	Impact Strength	Wear Resistance	Other
	Base	Cr	Mo	V	Co	Ni	Mn	Si	C	Other				
3. Stainless Steels (Surface Hardened)														
CARPENTER 636	Fe	13	1	0.35		0.75	1	1	0.22	1W	43	CVN 20		
410-Cb	Fe	12.5					1	1	0.15	0.25Cb	43	CVN 65		
PYROMET X-12	Fe	10.5	4.75		6		0.9	0.5	0.12	1.25Cu	48	CVN 11		
COOPER 14-S	Fe	12.5				0.75	1	1.5	0.15			CVN 5-16		
AFC-77	Fe	14	5	0.2	13.5				0.15		53	CVN 9		
CR-1	Fe	11.75				10.5	0.25	0.3		1.2Al 0.4Ti	48			
PYROMET 350	Fe	16.5	2.8			4.5	0.75	0.5	0.1		48	CVN 14		
1420 WM	Fe	12	1	0.25		8	0.75		0.22	1W	50	CVN 5		
4. Cobalt-Base Materials														
STELLITE 3	Co	30.5				3	1	1	2.45	12.5W 1Fe	60	CCN 4 IZOD 6		
STELLITE 6B	Co	30	1.5			3	2	2	1.2	4.5W 3Fe	38		Excellent	Non-Galling
STELLITE 6K	Co	30	1.5			3	2	2	1.65	4.5W 3Fe	38-47		Very Good	
STELLITE 19	Co	31							1.8	10.5W 3Fe	55	IZOD 11.5		
STELLITE 21	Co	27.5	5			2.5	1	1	0.3	2Fe		CVN 2.9		
STELLITE 98 (M2)	Co	30	0.8	4		3.5	1	1	2	18.5W 2.5Fe	63	IZOD 3		
STELLITE 100	Co	34							2	19W	61-66			Non-Galling
ALX	Co	33					0.5	0.5	2	16.5W 5Fe	58-61			
TANTUNG G	Co	30					2		3	17W 1Ta5Cb	55-63			
TANTUNG 144	Co	28					1	1	3	20W 5Cb	60-62			
REXALLOY 33	Co	33						0.75	2.25	17W	60-63			
WALLEX 50	Co	19				18		2.75	0.8	10W 3.5B	56-61	CVN 2		
AMDRY 850	Co	19				18		3.5	0.7	10W 3.25B	55-60	CVN 2		
COBENIUM/DYNAVAR	Co	20	7			15	2		0.15	16Fe 0.04Be	55-60			
TRIBALOY 400	Co	8	28						.08	2Fe	58-60	CCN 5	Good	
TRIBALOY 800	Co	17	28						.08	3Fe	54-60	CCN 1		

Table 4
Candidate Materials

Alloy	Composition(%), Typical*										Typical Hard.(Rc)	Impact Strength	Wear Resistance	Other
	Base	Cr	Mo	V	Co	Ni	Mn	Si	C	Other				
5. Gear Steels														
CBS-600	Fe	1.5	1				0.6	1.1	0.19		60-62	CVN 30	Case Hardened	
CBS-1000	Fe	1.1	4.5	0.35		3	0.5	0.5	0.13		60	CVN 20		Case Hardened
X-2	Fe	5.0	1.4	4.5			0.3	0.9	0.2	1.4W	48-52	CVN 18		Case Hardened
8620	Fe	0.5	0.2			0.55	0.8	0.3	0.2		63-64	IZOD 26-56		Case Hardened
9310	Fe	1.2	0.1			3.25	0.5	0.3	0.1		60-62	IZOD 57		Case Hardened
52100	Fe	1.5					0.35	0.3	1		60-63			

atomized MRC-2001, X-405, T440V, 14-4/6V, D-5, and CBS-600 powders were purchased from Crucible Steel Company. The particle size distributions for these powders are shown in Figures 6 through 11. Crucible also supplied WD-65 powder in a hot isostatically pressed (HIP)-plus-rolled form. The vanadium-modified Pyromet 350 and Stellite 3 were supplied by Homogeneous Metals. Sintercast produced the FerroTic material (FerroTic is a blend of titanium carbide in a martensitic stainless steel matrix), and Cabot supplied the Tribaloy 800. Powder particle morphology is shown in Figure 12.

All powders were screened to -100 mesh (>150 microns) prior to consolidation. Consolidation to full density of all powders was accomplished by HIP at 1149^{o}C (2100^{o}F) and 138 MPa (20 Ksi), prior to heat treatment at TRW Bearings Division.

(3) Preliminary Material Screening. Screening of the candidate bearing materials included evaluation of the homogeneity and cleanliness of their microstructure, hardness, rolling contact fatigue, cross cylinder wear, fracture toughness, and corrosion resistance. The current bearing material, 440C, was used as the baseline for all evaluations.

(a) Microstructural Evaluations. Representative microstructures of the candidate bearing materials after HIP and HIP plus heat treatment where applicable are shown in Figures 13 through 23. In general, all samples were fully dense; those made from gas atomized powders exhibited a fine uniform distribution of carbides. Prior particle dendritic structure was evident in the as-HIP X-405, MRC-2001, and Stellite 3. Even after heat treatment, this structure was retained in samples of the MRC-2001. The CBS-600 is a case-hardened alloy and, therefore, lacks the carbide content of the through-hardened alloys. As a consequence of being a blended product, the FerroTic CS-40 exhibited more variability in the carbide size and distribution. The Tribaloy 800 contained inclusions and showed prior-particle outlining not present in the other candidate bearing materials.

(b) Hardness. A comparison of Rockwell C hardness for the candidate bearing materials is shown graphically in Figure 24 with actual values shown in Table 5. The vanadium-modified Pyromet 350 was eliminated from the program for insufficient hardness. All other materials met or exceeded the hardness of the baseline 440C, making them suitable for further testing.

(c) Corrosion Resistance. Three methods were used to evaluate the corrosion resistance of the candidate materials. The first two methods involved alternately submerging the test specimens in liquid nitrogen and exposing them to ambient atmosphere. The primary difference between the two methods was the change from stainless steel wire to non-metallic contacts to suspend the test specimens, thereby eliminating any corrosion resulting from the fixturing device. Samples were cycled until corrosion became evident. Corrosion resistance was measured in terms of cycles to visible oxidation (discoloration/rust).

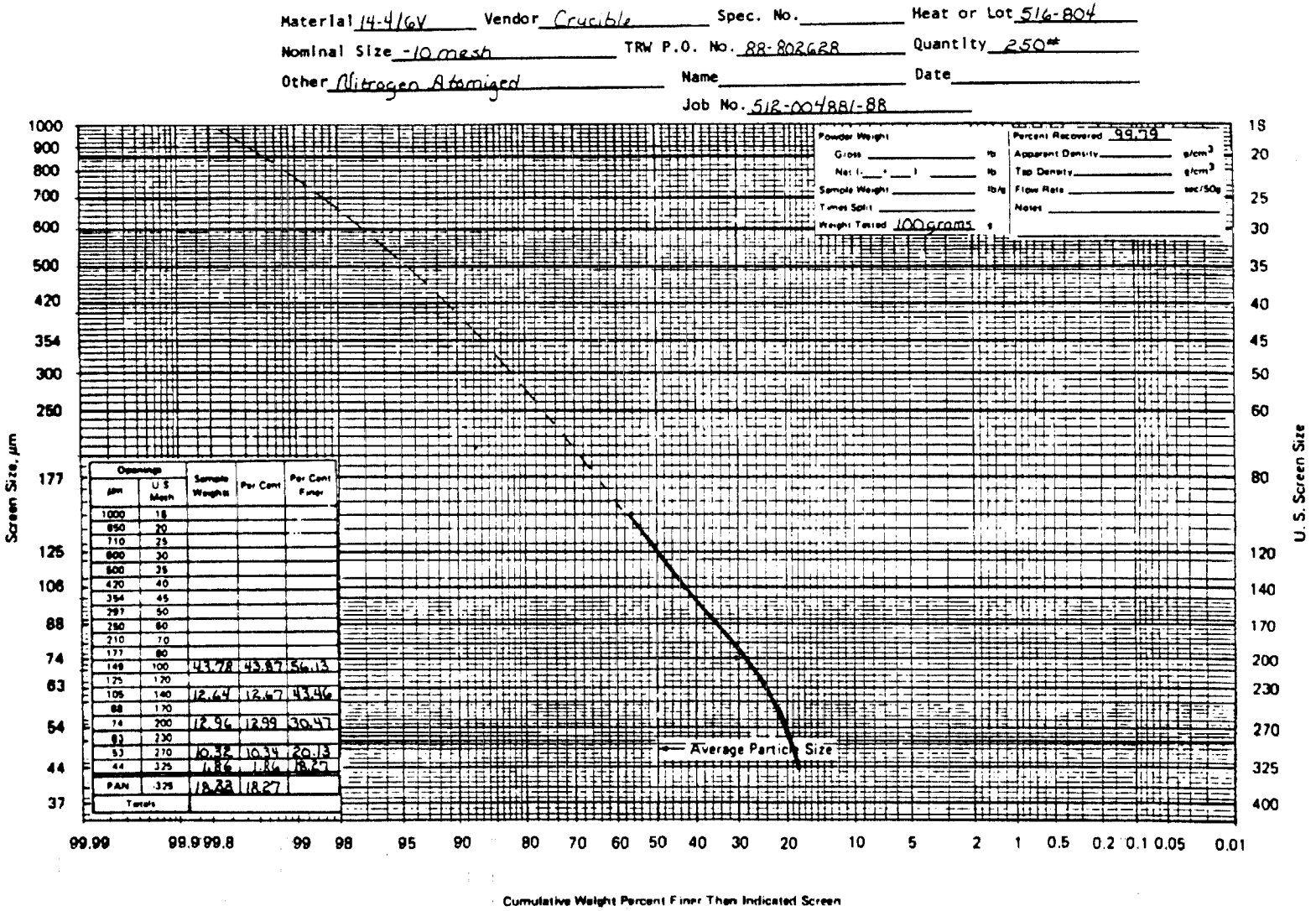

Figure 6. Particle size distribution of Crucible 14-4/6V powder plotted as screen size versus cumulative weight percent finer than indicated screen.

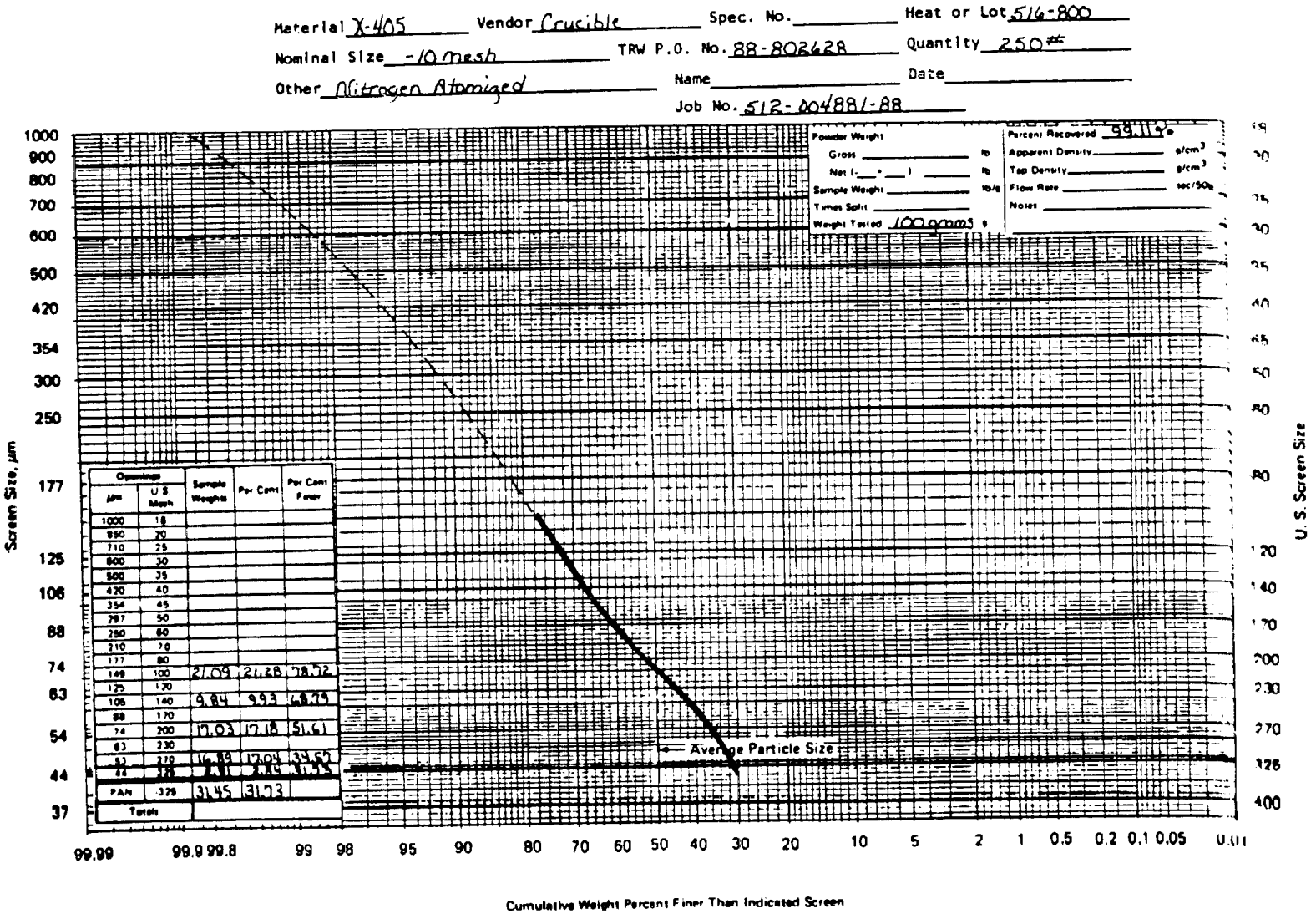

Figure 7. Particle size distribution for Crucible X-405 powder plotted as screen size versus cumulative weight percent finer than indicated screen.

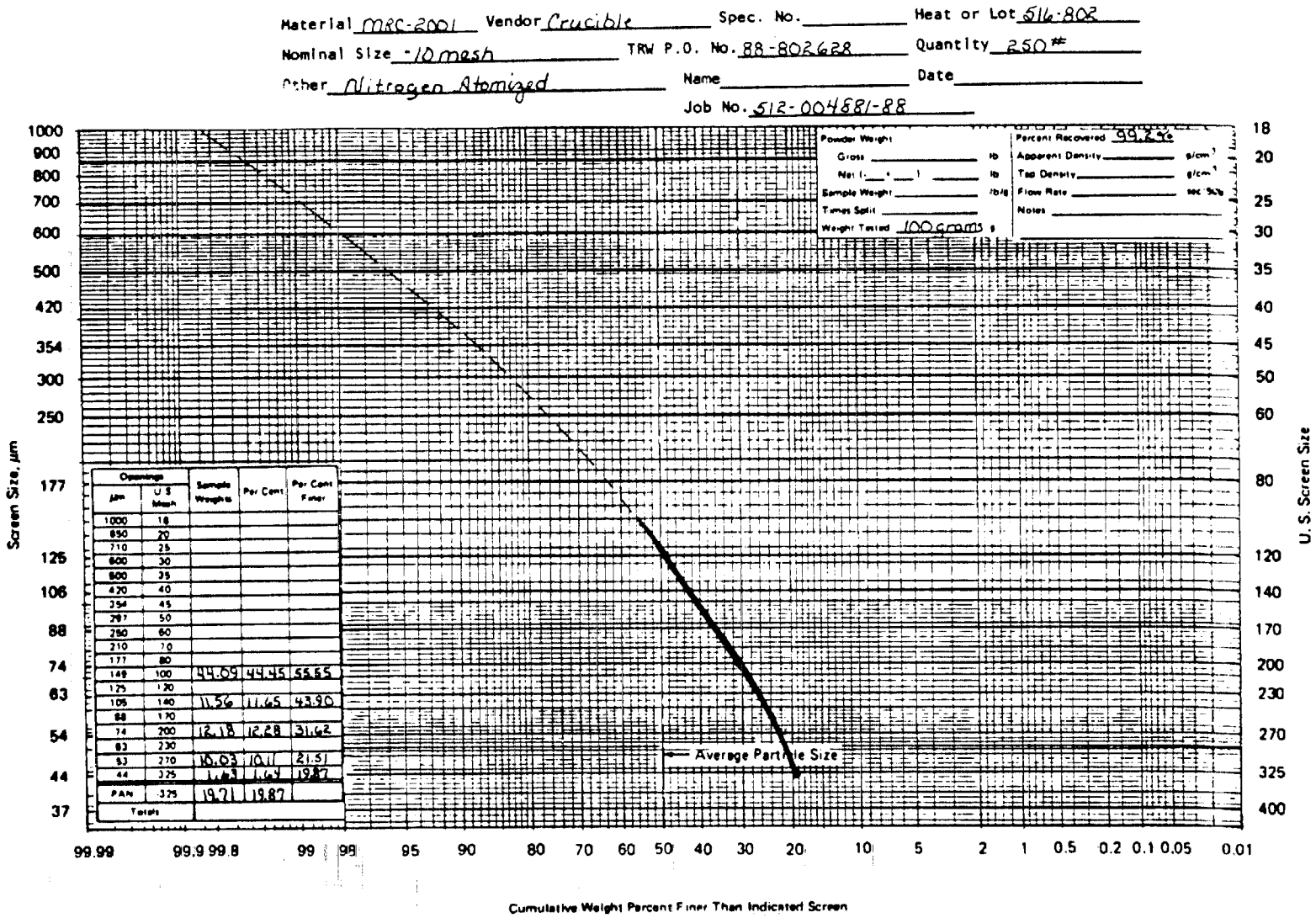

Figure 8. Particle size distribution of MRC-2001 powder plotted as screen size versus cumulative weight percent finer than indicated screen.

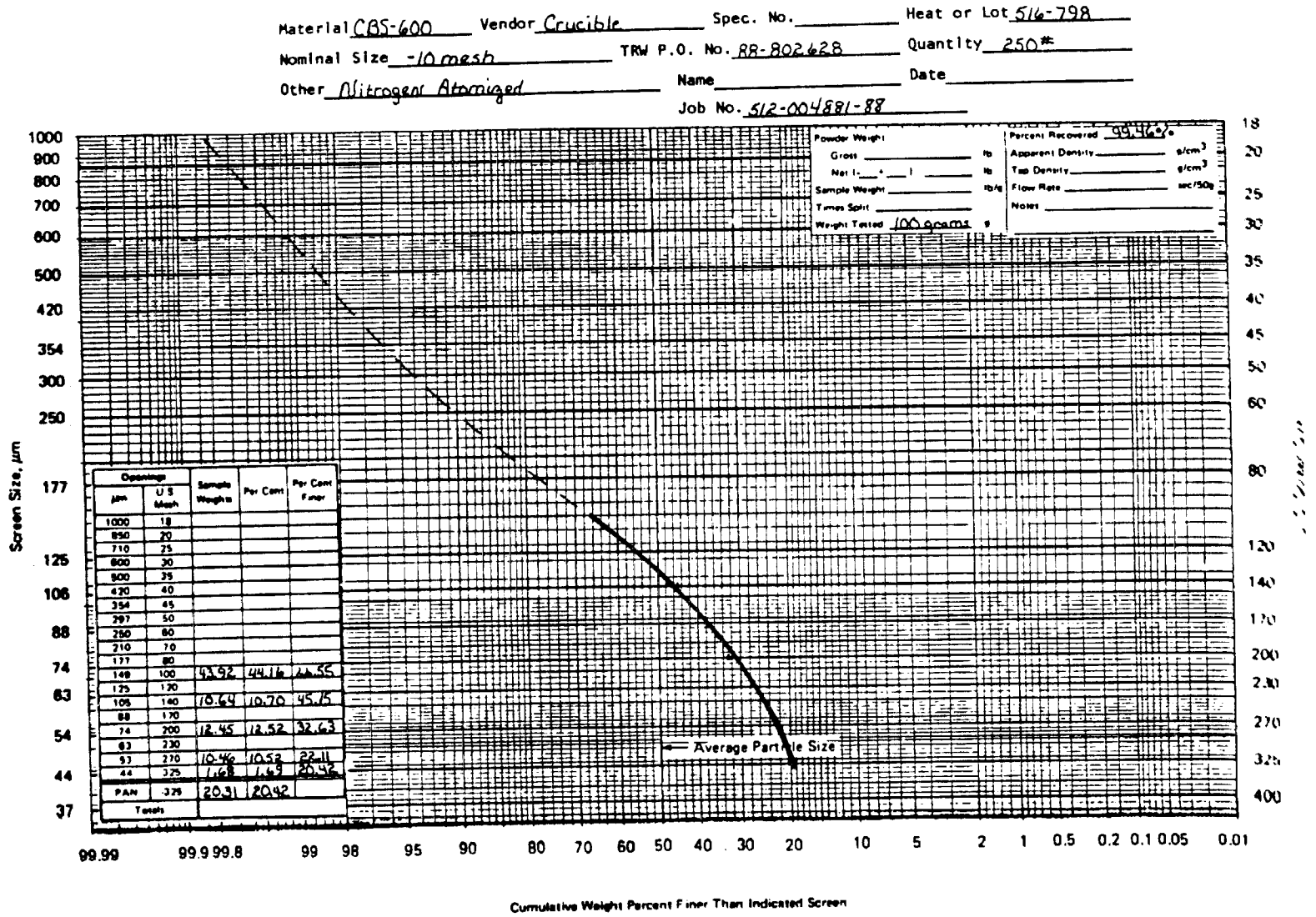

Figure 9. Particle size distribution of CBS-600 powder plotted as screen size versus cumulative weight percent finer than indicated screen.

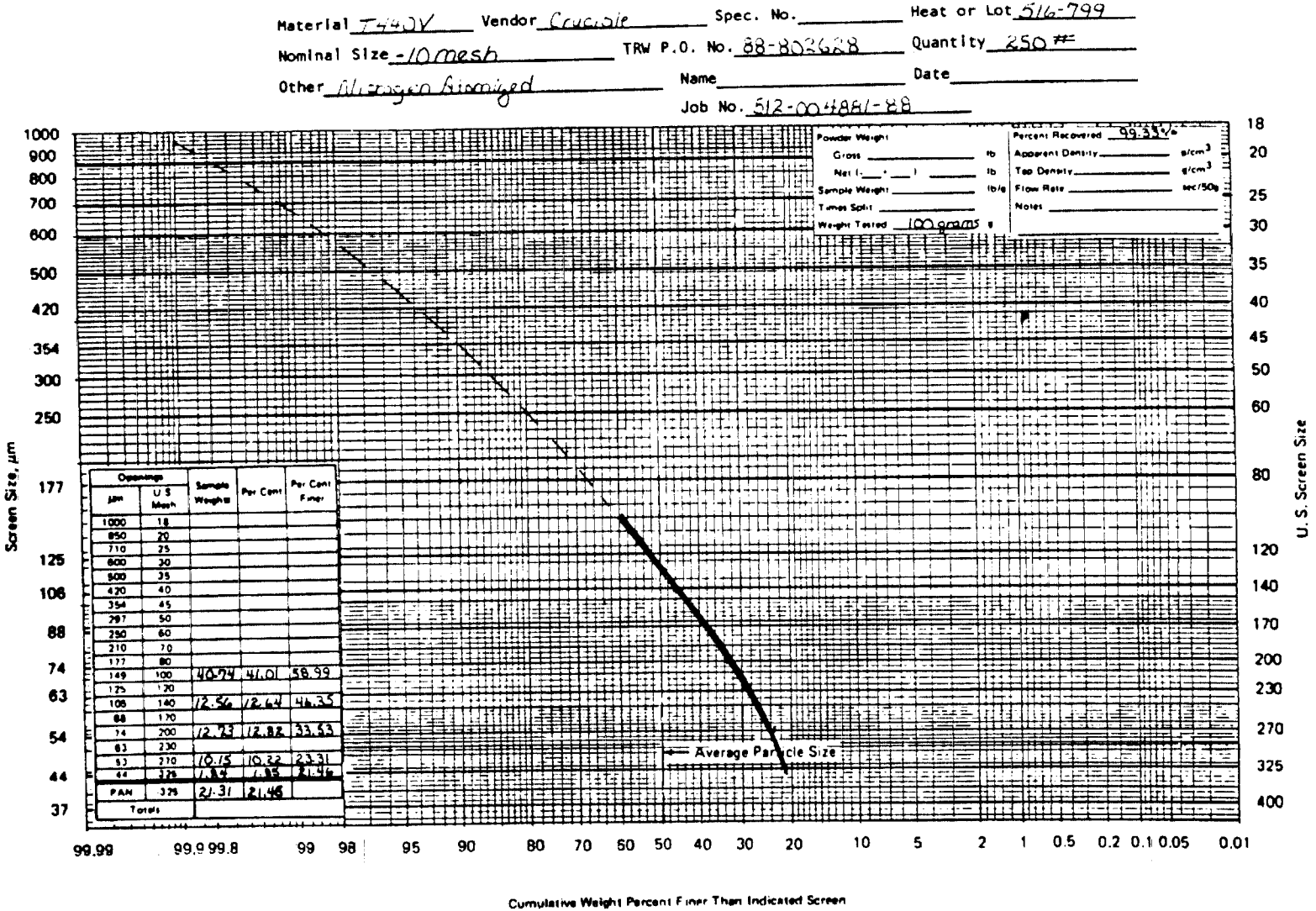

Figure 10. Particle size distribution of T-440V powder plotted as screen size versus cumulative weight percent finer than indicated screen.

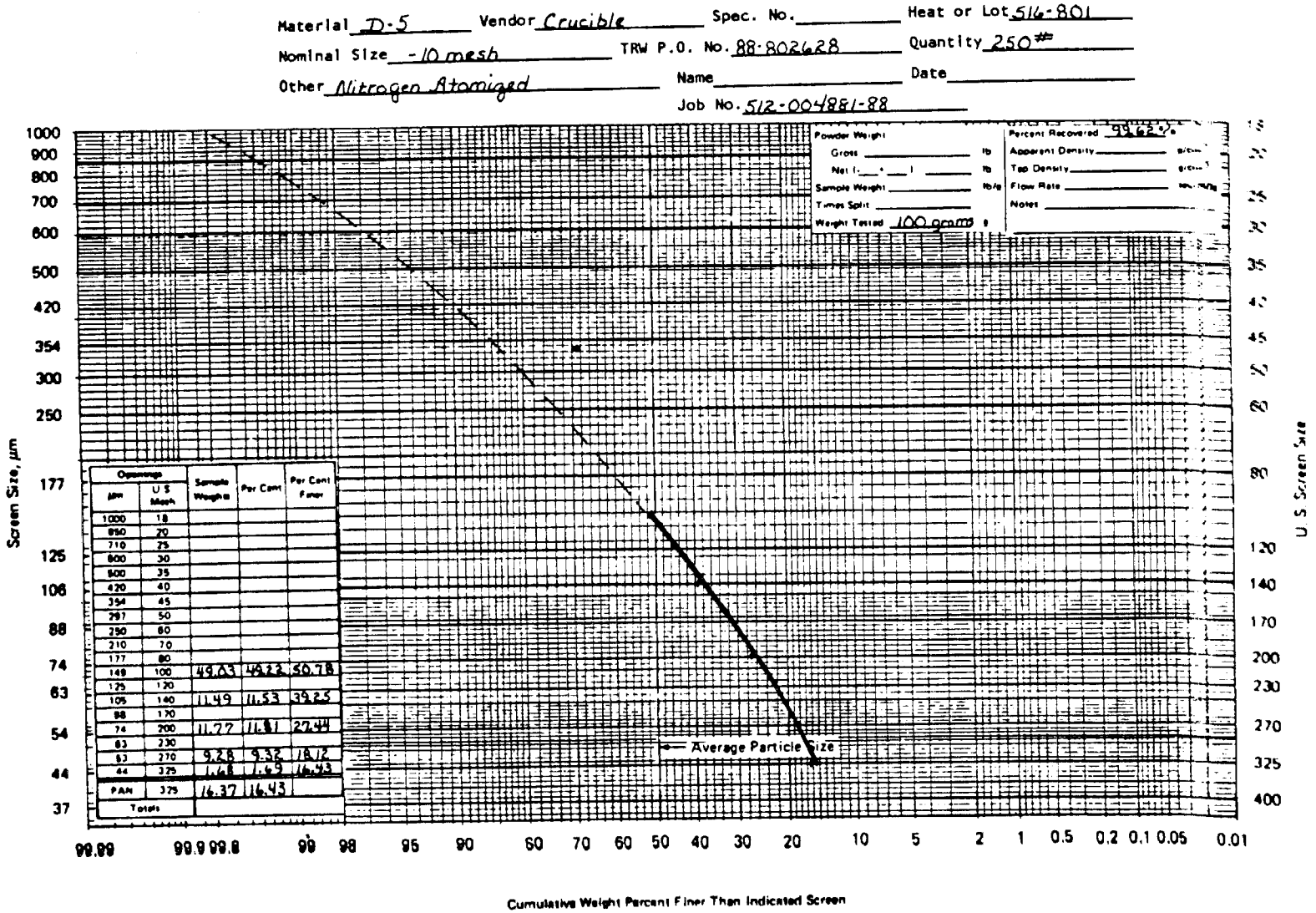

Figure 11. Particle size distribution of D-5 powder plotted as screen size versus cumulative weight percent finer than indicated screen.

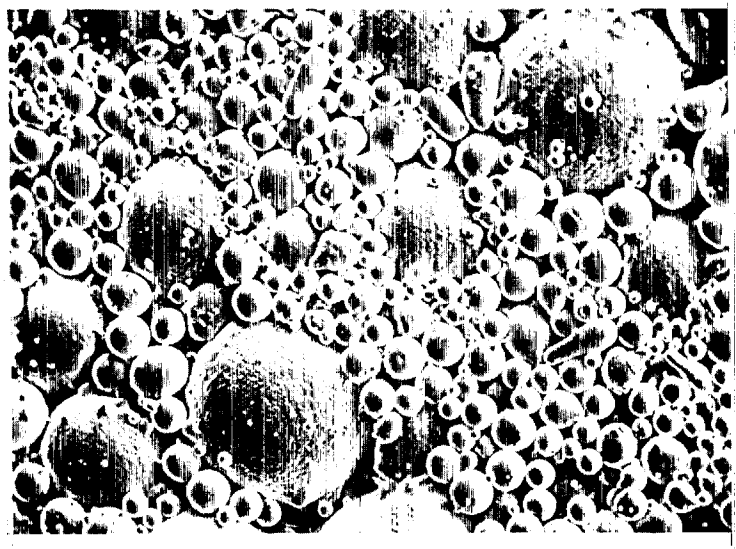

a. MRC-2001

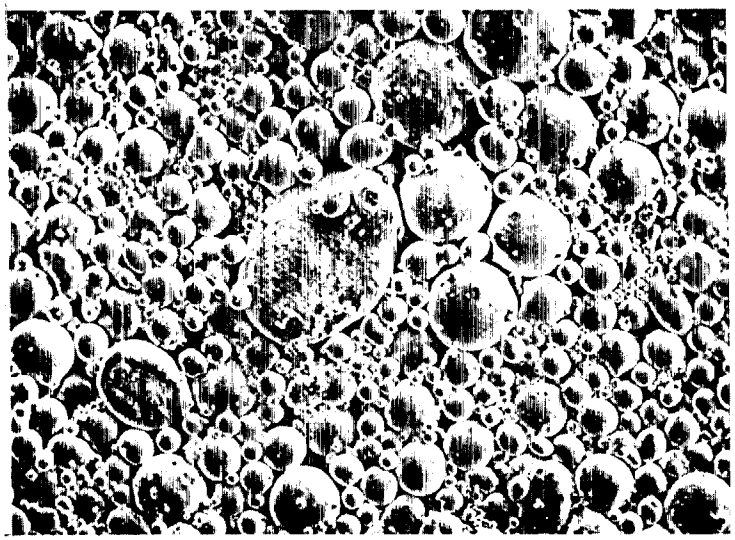

b. X405

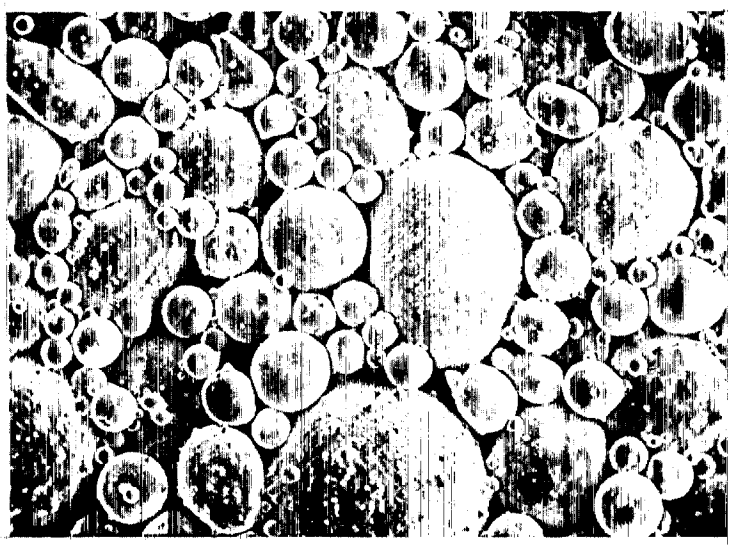

c. T440V

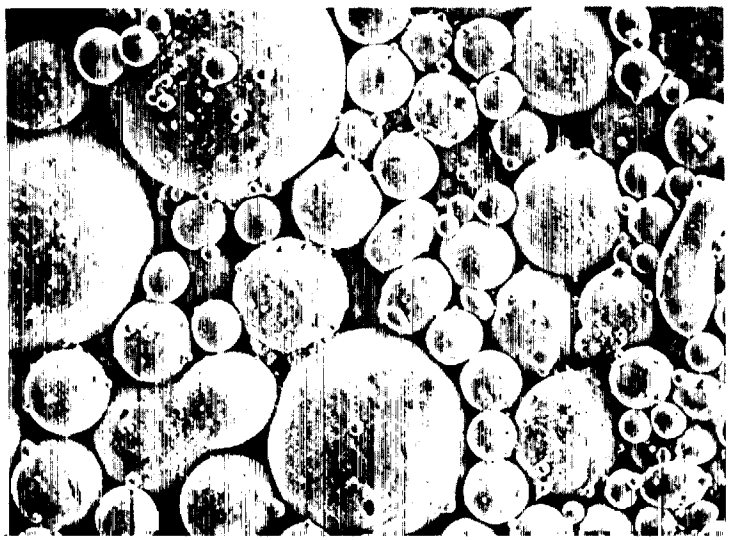

d. 14-4/6V

Figure 12. Scanning electron micrographs of powder samples (100X).

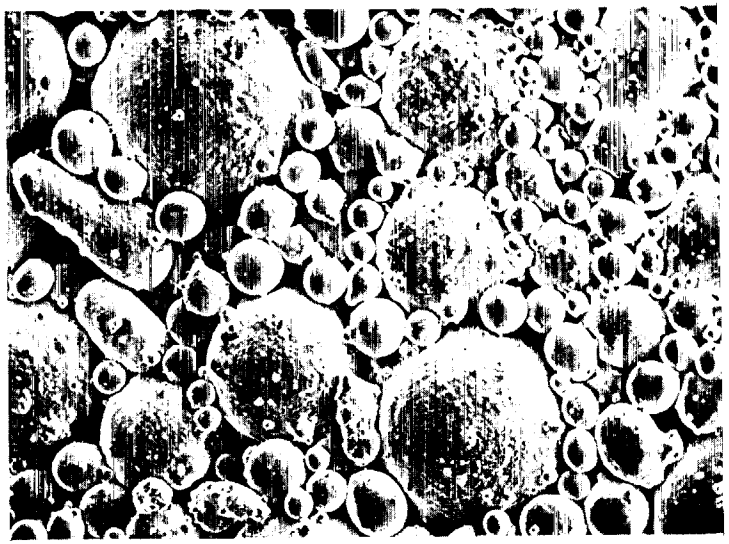

e. D-5

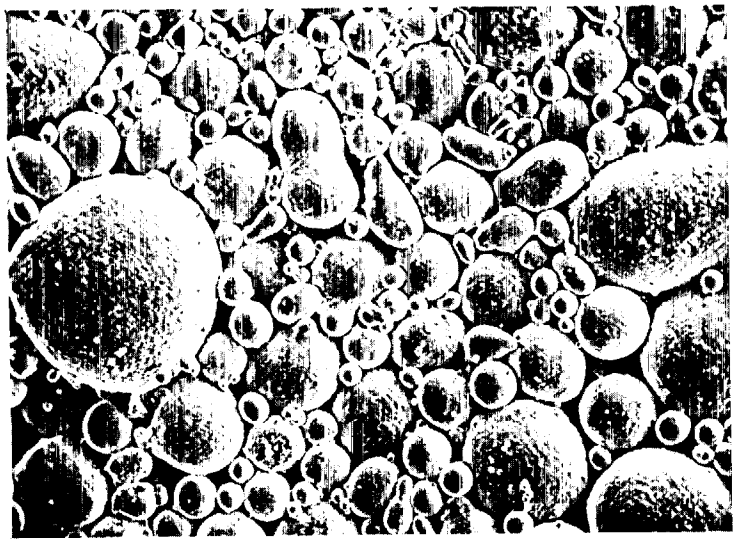

f. CBS-600

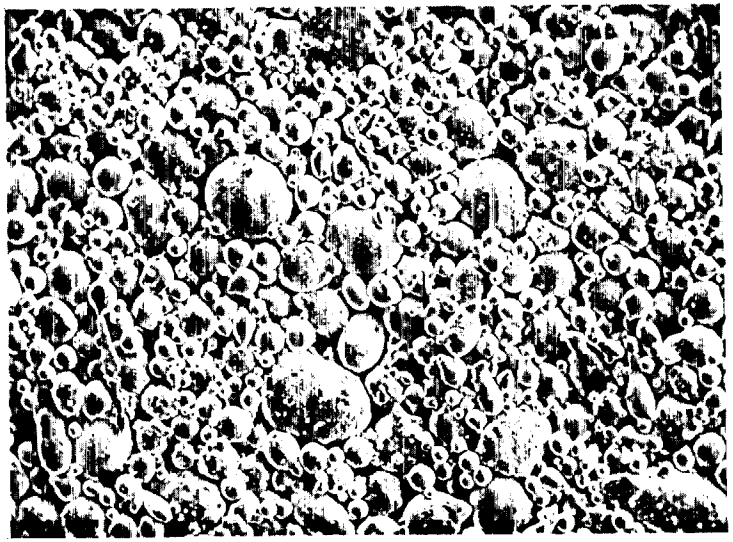

g. Modified Pyromet 350

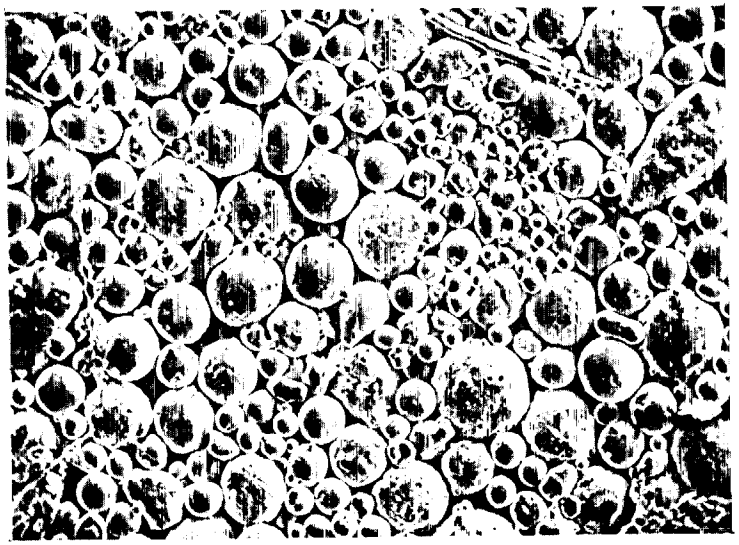

h. Stellite 3

Figure 12. (continued) Scanning electron micrographs of powder samples (100X).

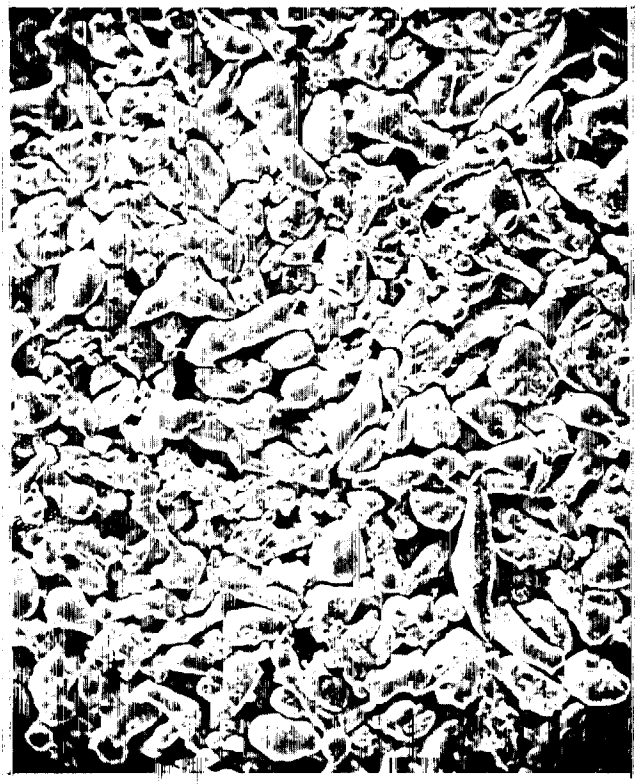

i. Triballoy 800

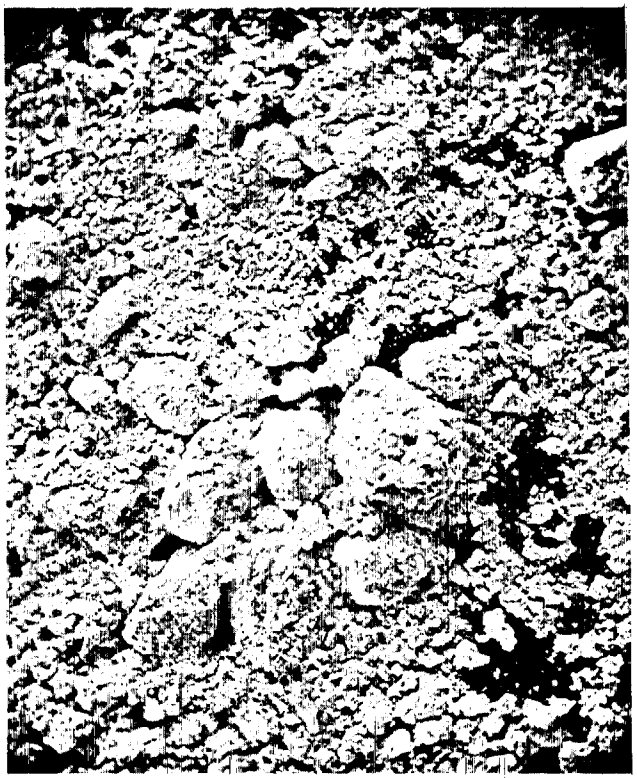

j. Ferro-TiC CS-40

Figure 12. (continued) Scanning electron micrographs of powder samples (100X).

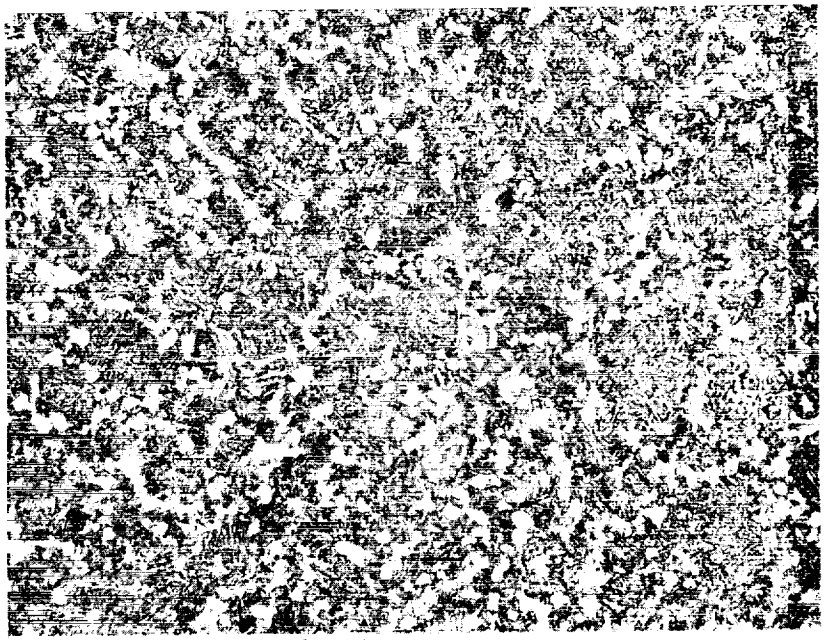

100X

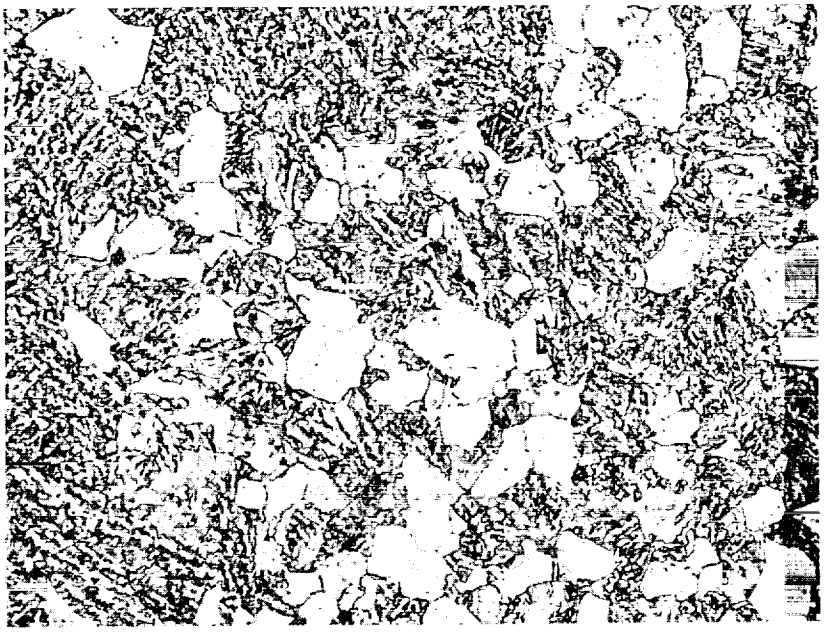

500X

Figure 13. As-HIP CBS-600.
Etchant: Electrolytic Chromic.

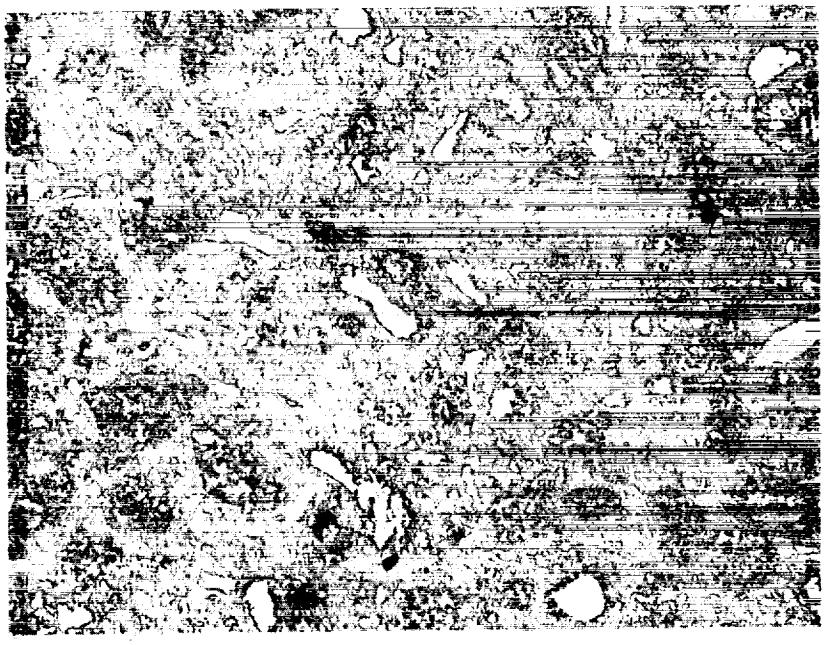

100X

500X

Figure 14. As-HIP Ferrotic CS-40.
Unetched.

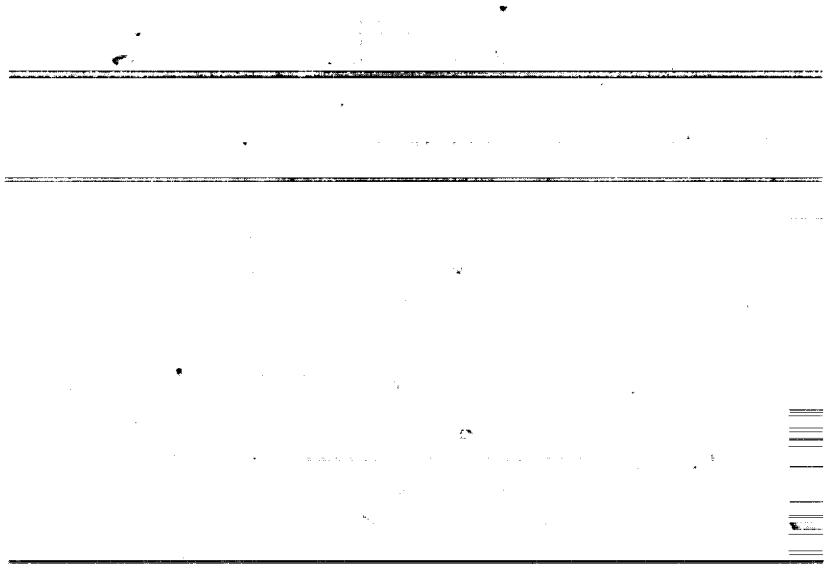

100X

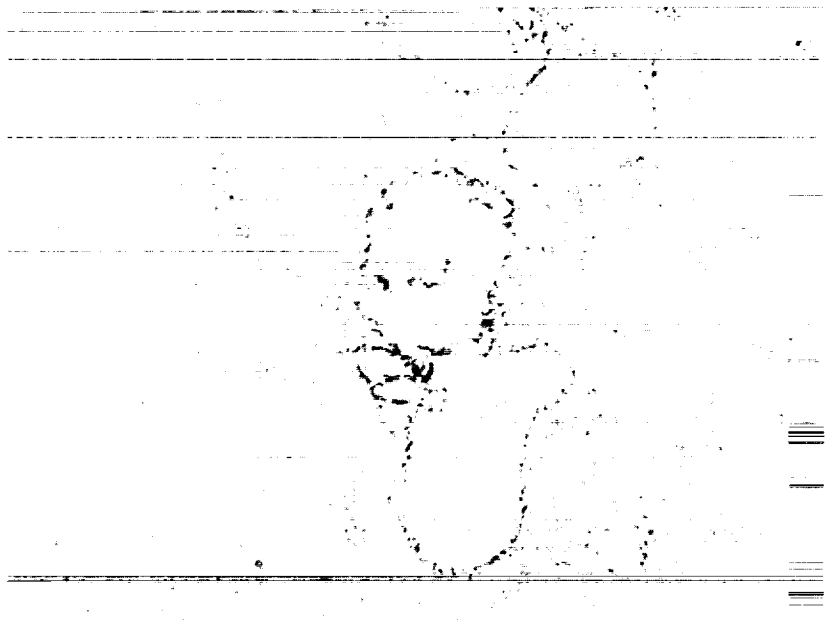

500X

Figure 15. As-HIP Tribaloy T-800.
Etchant: Nital.

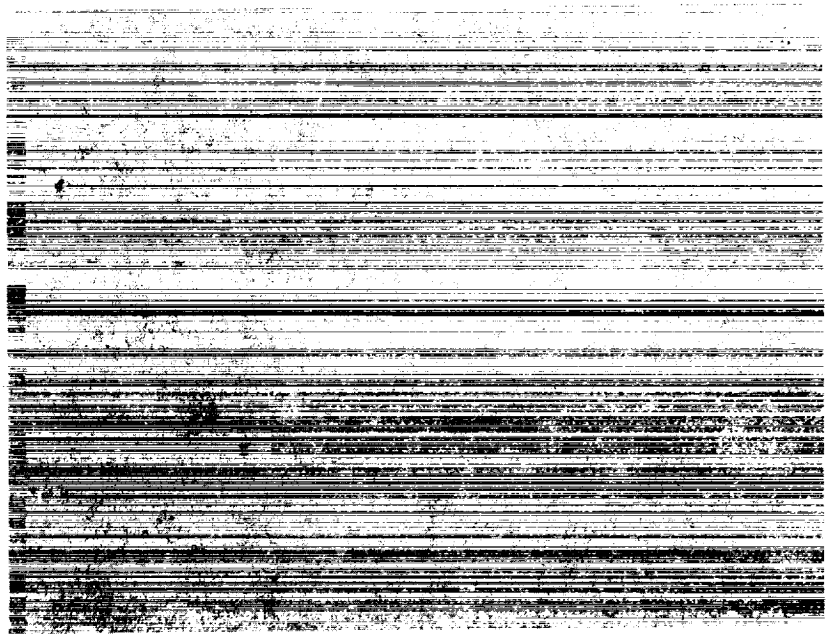

100X

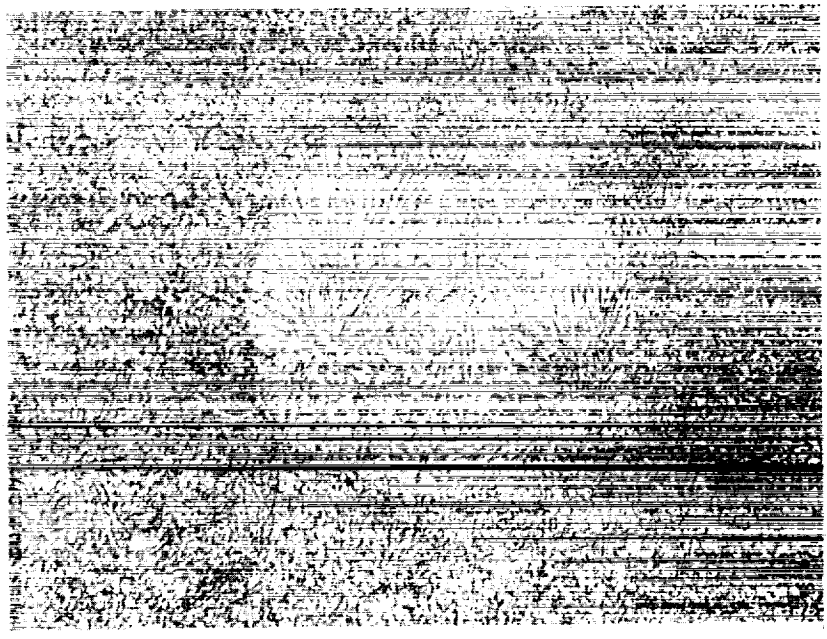

500X

Figure 16. As-HIP Stellite 3.
Etchant: Electrolytic Chromic.

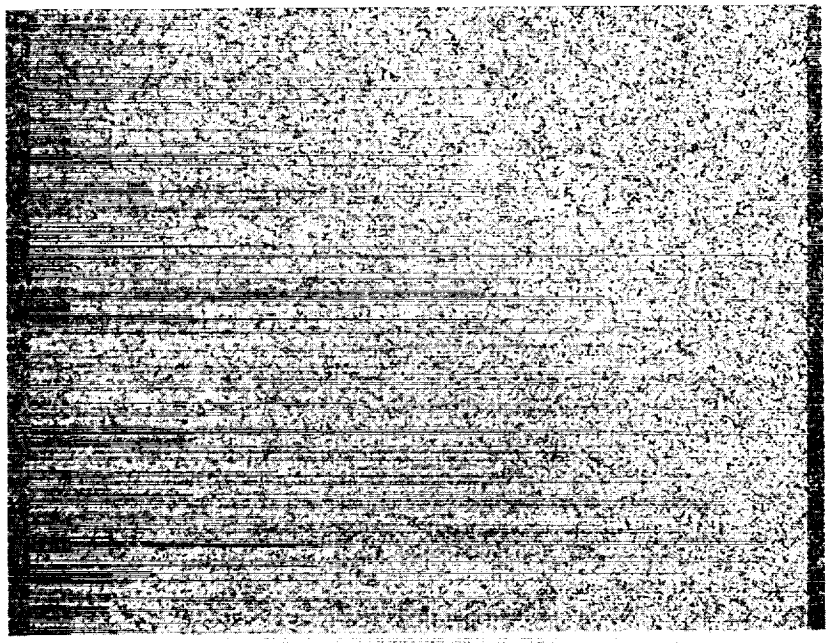

100X

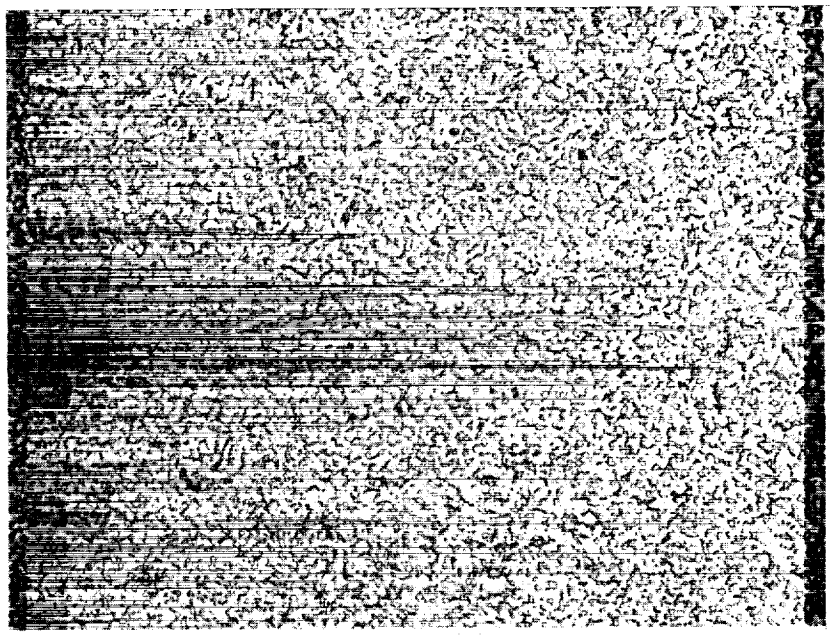

500X

Figure 17. As-HIP Modified Pyromet 350.
Etchant: Electrolytic Chromic.

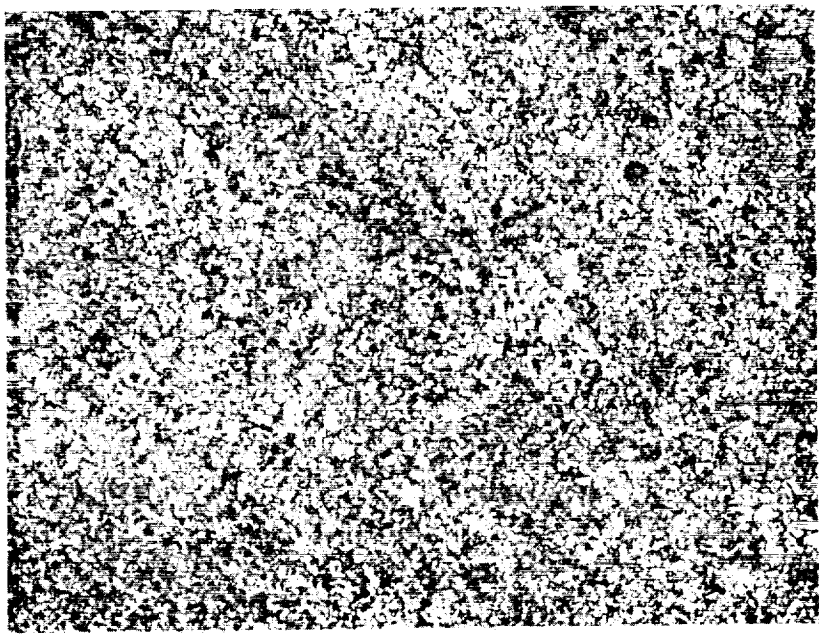

(a) 500X

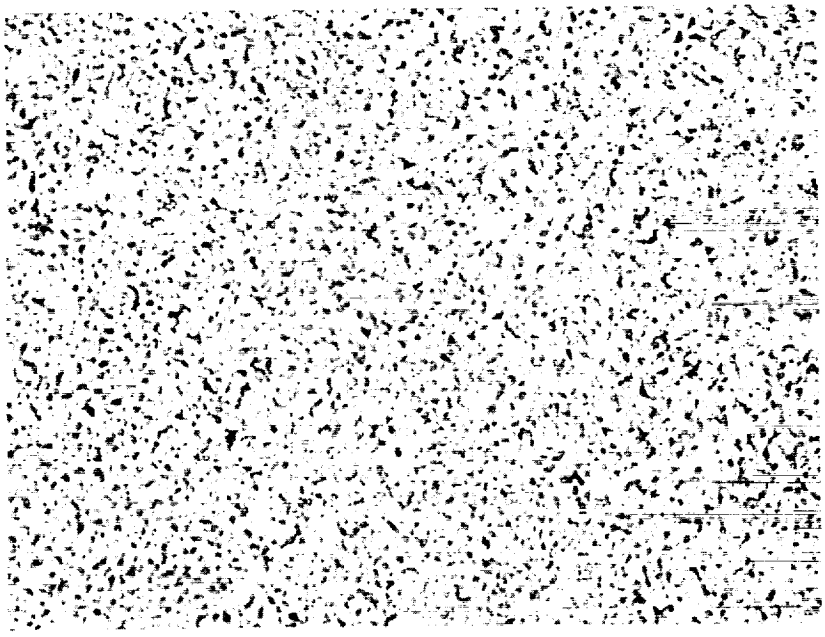

(b) Hardened, R_c63. 500X

Figure 18. Microstructure of 14-4/6V.
Etchant: Electrolytic Chromic.

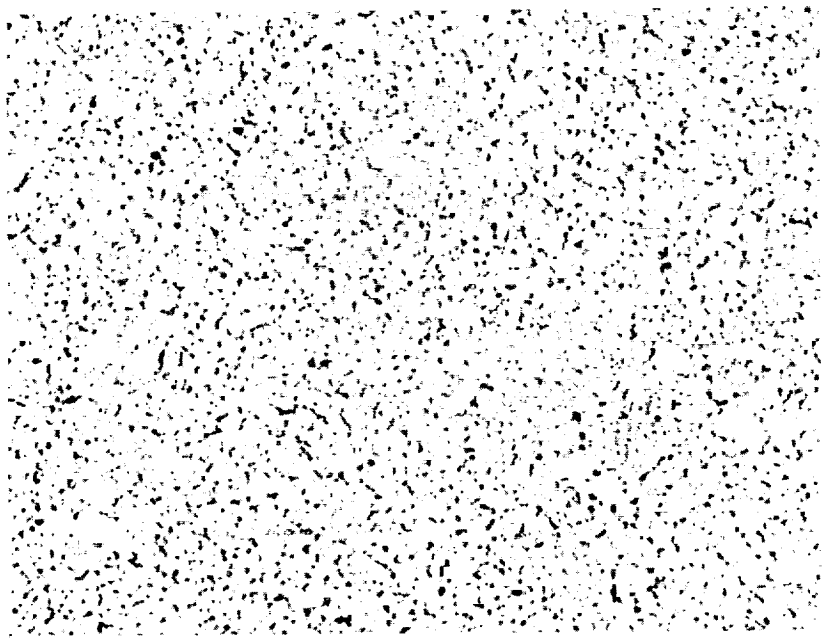

(a) As-HIP 500X

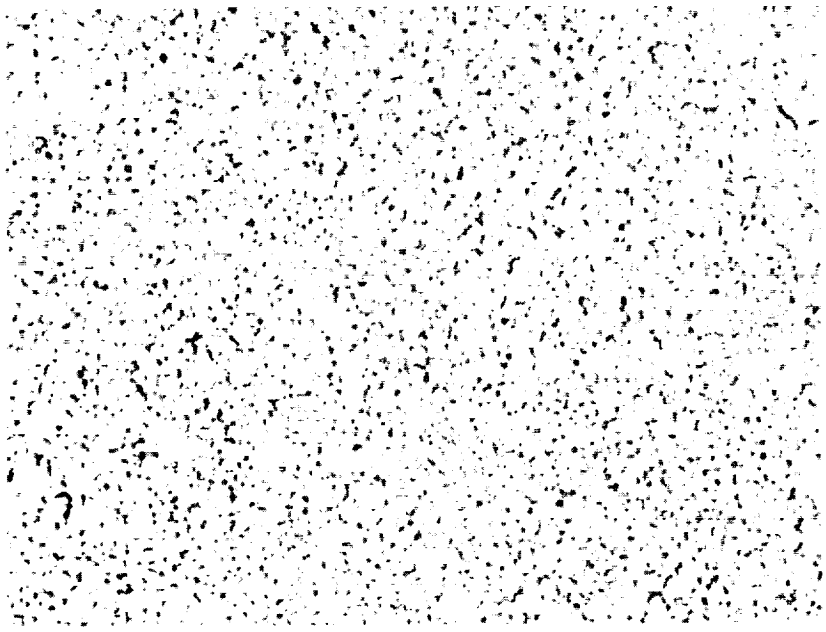

(b) Hardened, $R_c 60$ 500X

Figure 19. Microstructure of D-5.
Etchant: Electrolytic Chromic.

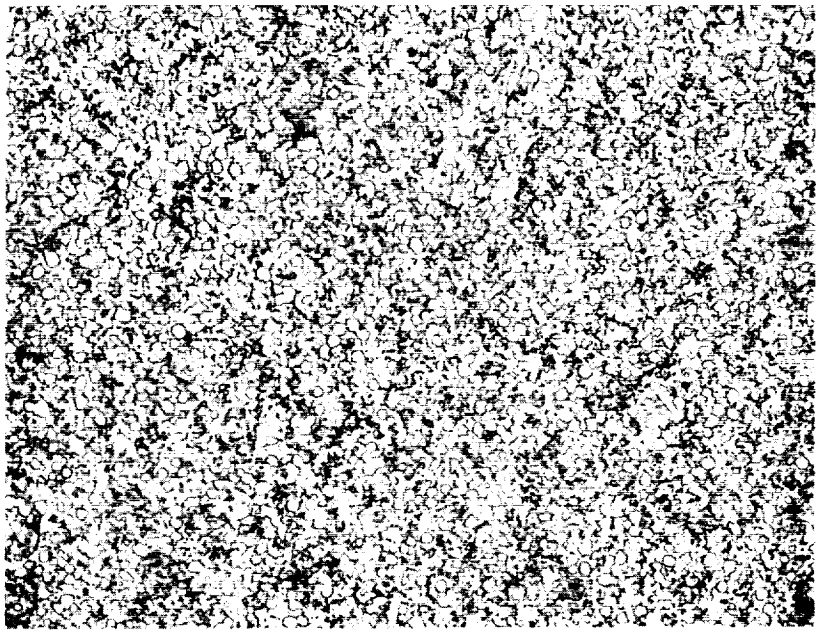

(a) As-HIP 500X

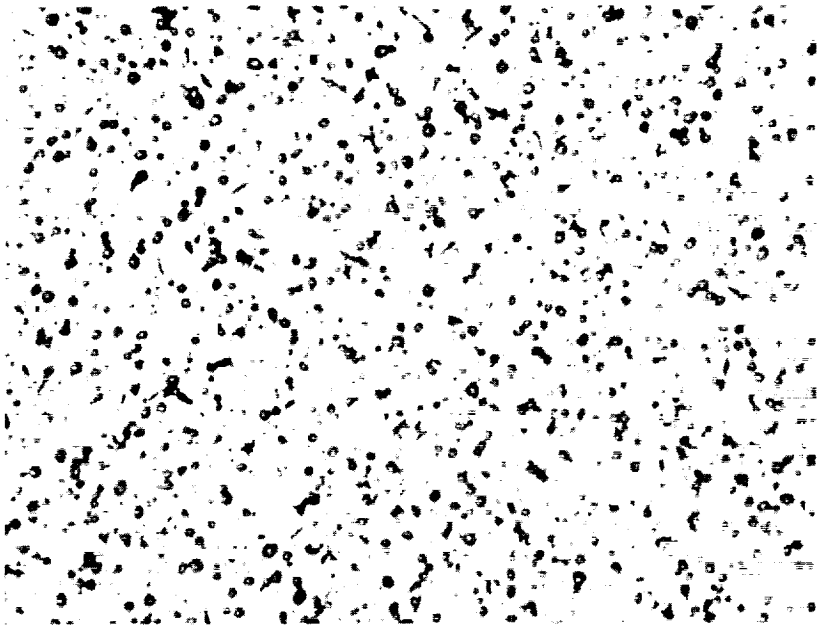

(b) Hardened, R_c62 500X

Figure 20. Microstructure of WD-65.
Etchant: Electrolytic Chromic.

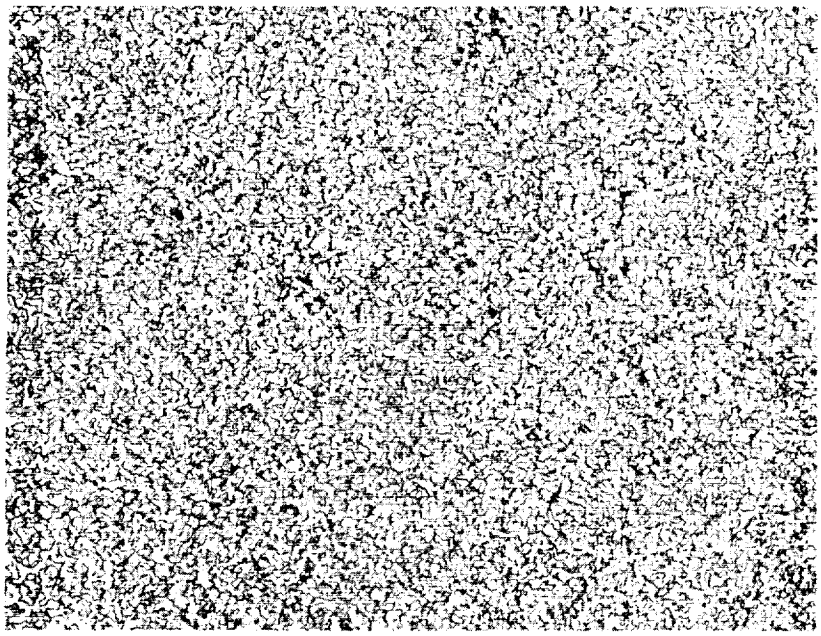

(a) As-HIP 500X

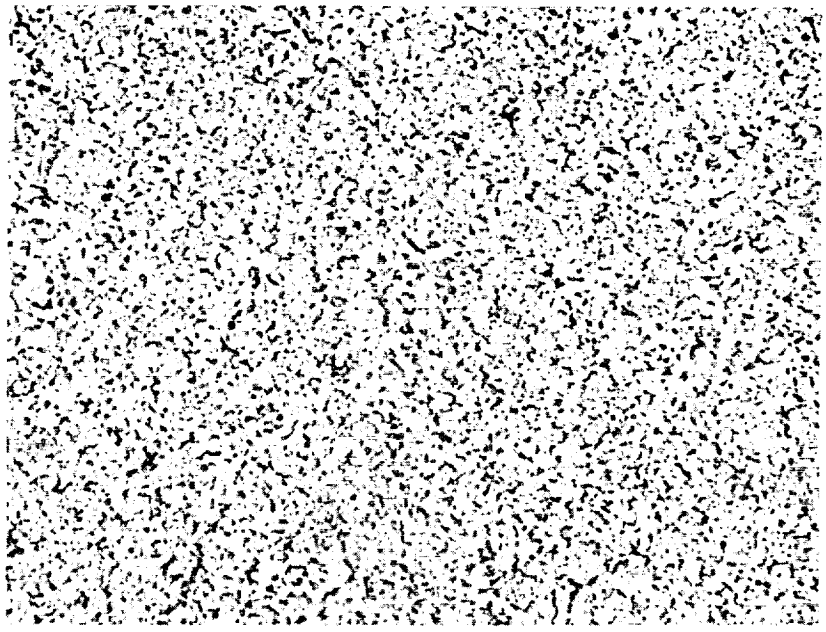

(b) Hardened, $R_c 61$ 500X

Figure 21. Microstructure of T440V.
Etchant: Electrolytic Chromic.

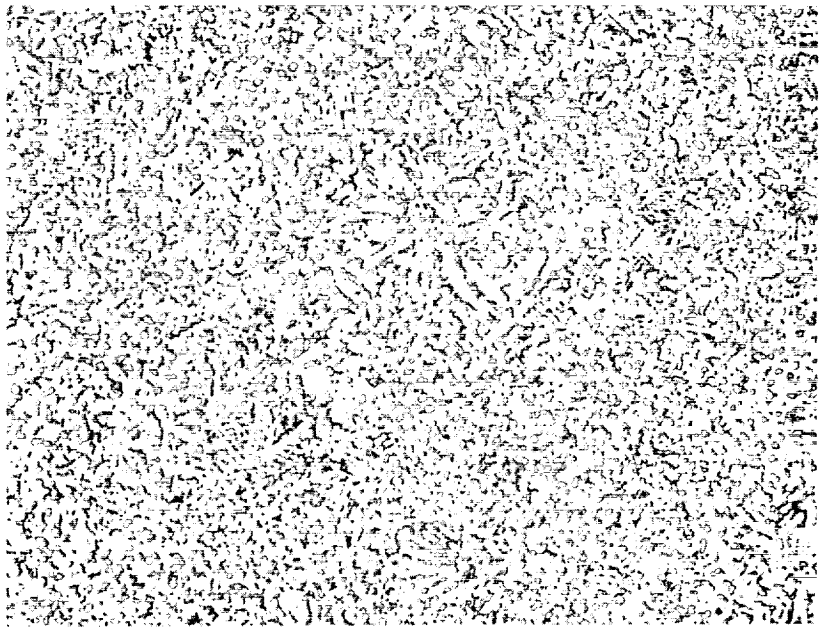

(a) As-HIP 500X

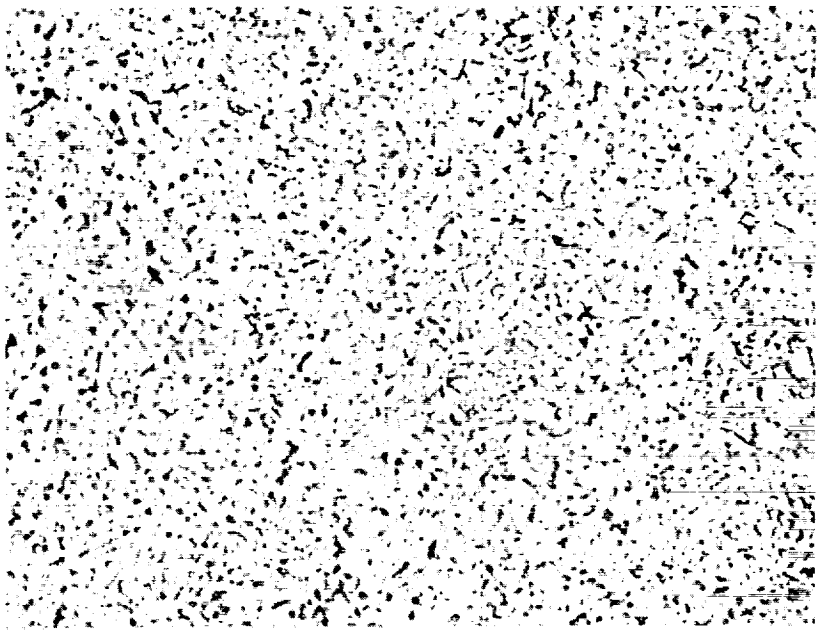

(b) Hardened, R_c61 500X

Figure 22. Microstructure of X-405.
Etchant: Electrolytic Chromic.

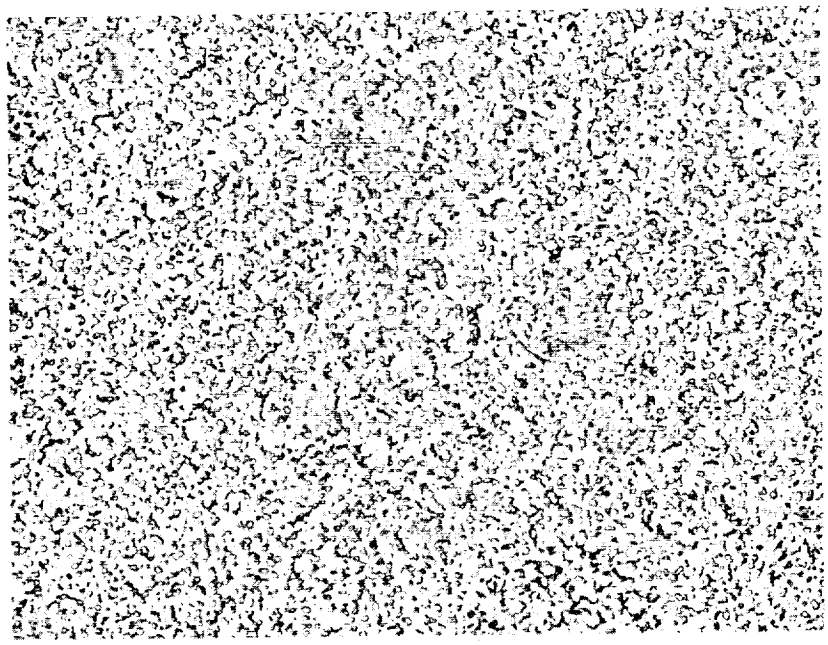

(a) As-HIP 500X

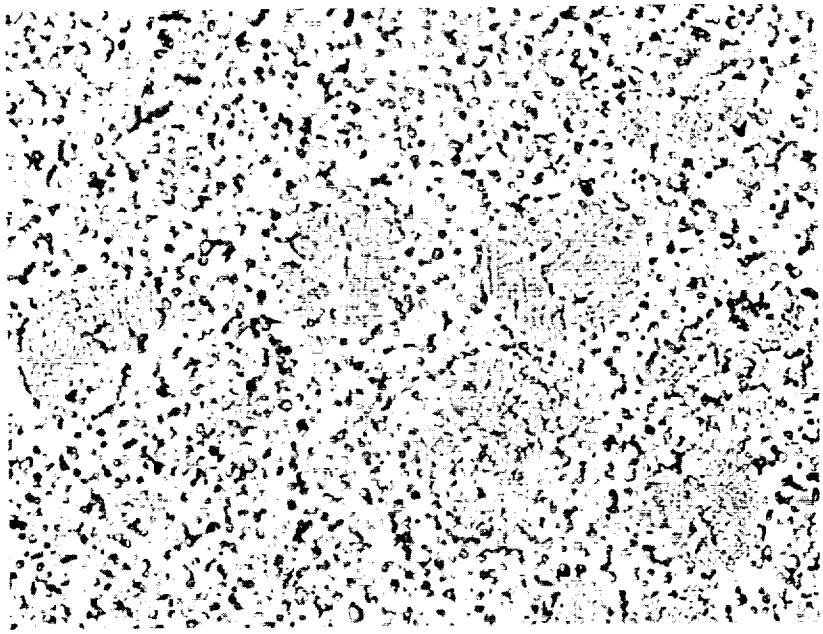

(b) Hardened, R_c62 500X

Figure 23. Microstructure of MRC-2001.
Etchant: Electrolytic Chromic.

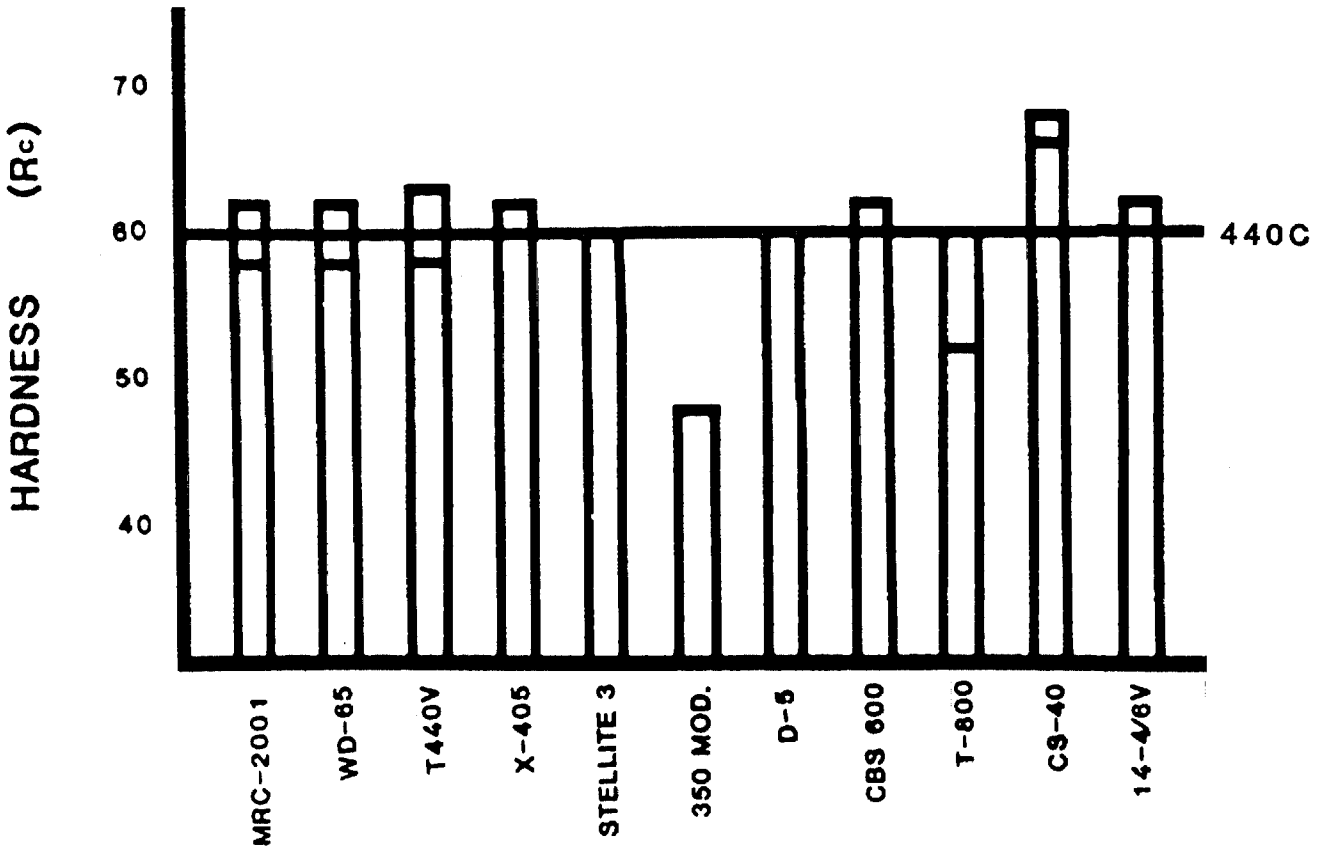

Figure 24. Comparison of Rockwell C hardness for the candidate bearing materials.

Table 5
Rockwell C Hardness of the Candidate Bearing Materials

Material	Rc Hardness
440C (Baseline)	59
V-Pyromet 350 MOD.	54(48)
Tribaloy 800	61
FerroTic (CS-40)	70
T440V	61
14-4/6V	63
X-405	61
MRC-2001	62
D-5	60
WD-65	62
Stellite 3	59
CBS-600	62

The third method consisted of a standard humidity test for each of the candidate materials. Tests were run at 39°C(102°F) between 95 and 100% relative humidity, for 30 days. The materials are ranked in the order of days to appearance of first visible oxidation.

Table 6 is a compilation of the data generated during corrosion testing of the candidate bearing materials. The CBS-600 was eliminated due to its poor corrosion resistance, as may have been expected considering its low 1.5 wt% chromium content. Also as expected, the baseline material, 440C, exhibited excellent corrosion resistance. Some of the other data presented is inconsistant in that one candidate material will outperform the other in one method and not fare all that well in a second test method.

(d) Rolling Contact Fatigue (RCF) Life. The fatigue endurance of the candidate bearing materials was evaluated through performance testing on a Polymet Corporation RCF-1 rolling contact fatigue and lubrication testing machine. In this screening test, half-inch diameter, three to four inch long test cylinders were rotated at 7000 RPM while loaded between two large idler disks, at a maximum Hertzian stress of 5058 MPa (733 Ksi). When a fatigue spall occurred, an accelerometer sensed the increased vibration and the test automatically ended. The results of these tests for the candidate bearing materials were plotted on Weibull charts. A comparison for candidate bearing materials is shown in Figure 25, with B^{10} lives (the point on the Weibull chart which represents failure of 10% of the test

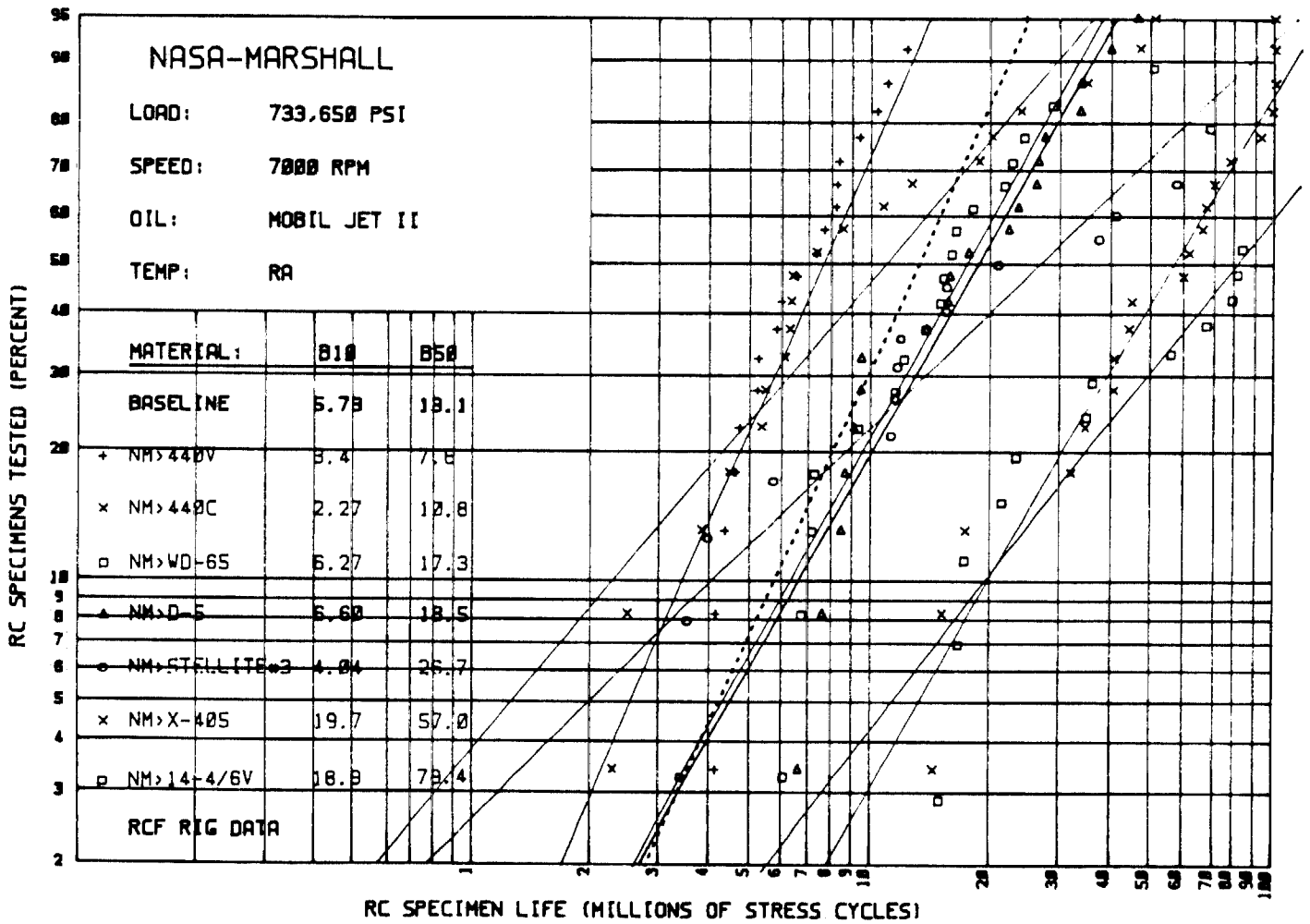

Figure 25. Rolling contact specimen life (millions of stress cycles) versus percent of rolling contact specimens tested for each of the candidate bearing materials.

Table 6
Corrosion Test Results for Candidate Bearing Steels

		Method 1 LN-Ambient Cycle		Method 2 Modified LN-Ambient Cycle		Method 3 High Humidity 30 Days	
Material	Chromium Content	Cycles to Oxidation	Test 1 Ranking*	Cycles to Oxidation	Test 2 Ranking	Days to Oxidation	Test 3 Ranking
440C	17.0	12	5			none-30 days	5
T440V	17.5			8	4		
14-4/6V	14.5			5	3		
X-405	19.0	5	1	5	3	17	4
MRC-2001	15.0	9	3	5	3		
WD-65	14.0	6	2	8	4	1	1
D-5	12.5	10	4	4	2	4	2
Tribaloy	17.0					none-30 days	5
FerroTic	17.5	12	5			9	3
CBS-600	1.5			<1	1		
V-Mod Pyro	17.0	Not tested, too soft					

*Ranking 1 = worst

specimens) for the individual materials shown in Figure 26. Weibull charts for the individual materials are shown in Figures 27 through 34. It should be noted that the "baseline" provided on each plot is that of M-50, due to the large amount of data available for this material. A straight-line function was assumed for the Weibull charts, though in actuality the plots exhibited dual slopes. In assuming the straight-line function, the plot addressed the possibility of very early failures, which were not experienced during testing. Table 7 is a compilation of the data generated during rolling contact fatigue testing of the candidate bearing steels.

FerroTic and Tribaloy were both eliminated from further testing due to their exceptionally poor endurance characteristics. Stellite 3 was also eliminated, since the conservative nature of the calculated Weibull slope predicted a possibility of very low RCF lives. The remaining alloys exhibited lives exceeding that of the 440C.

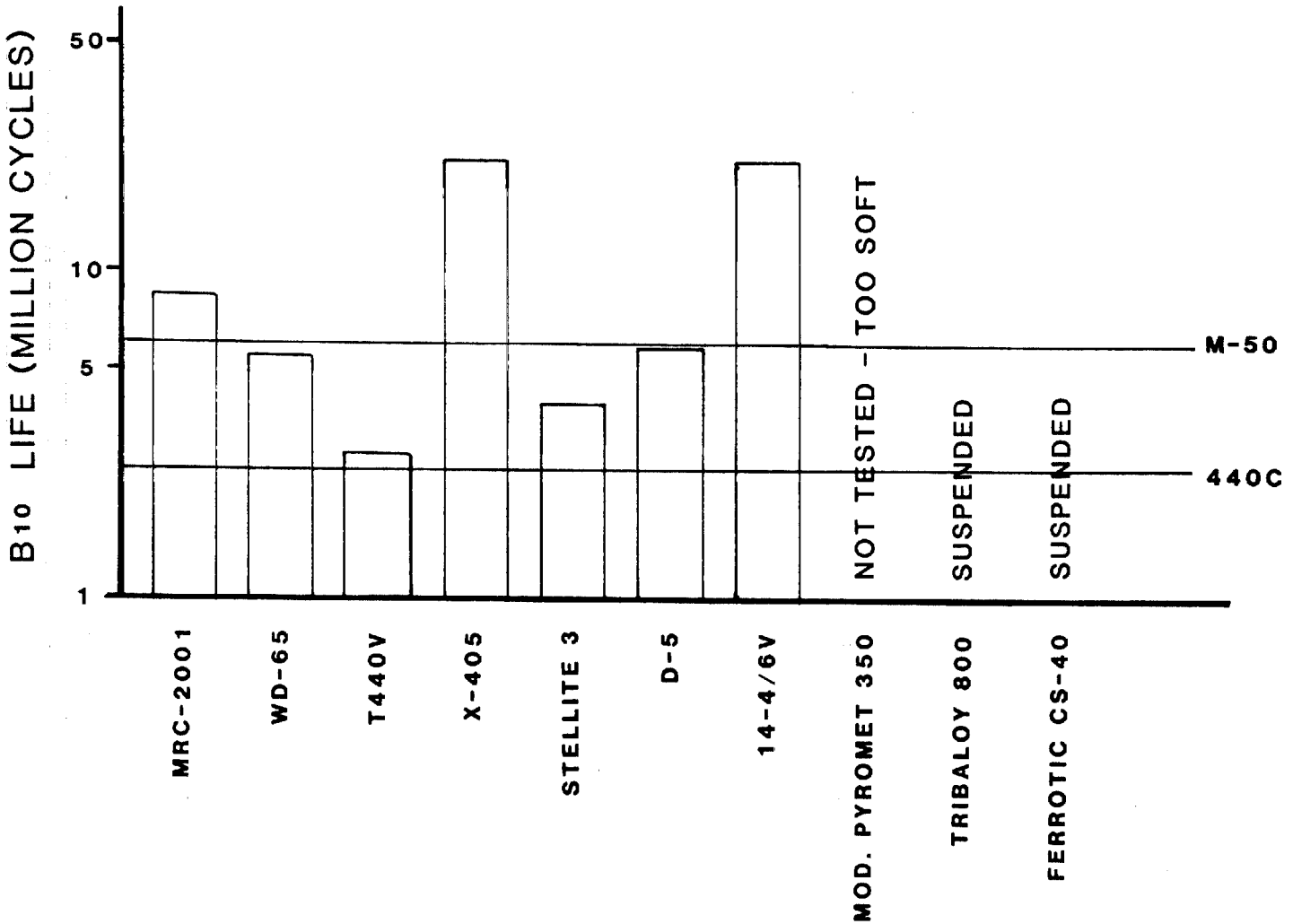

Figure 26. A comparison of the B_{10} lives for the candidate bearing materials.

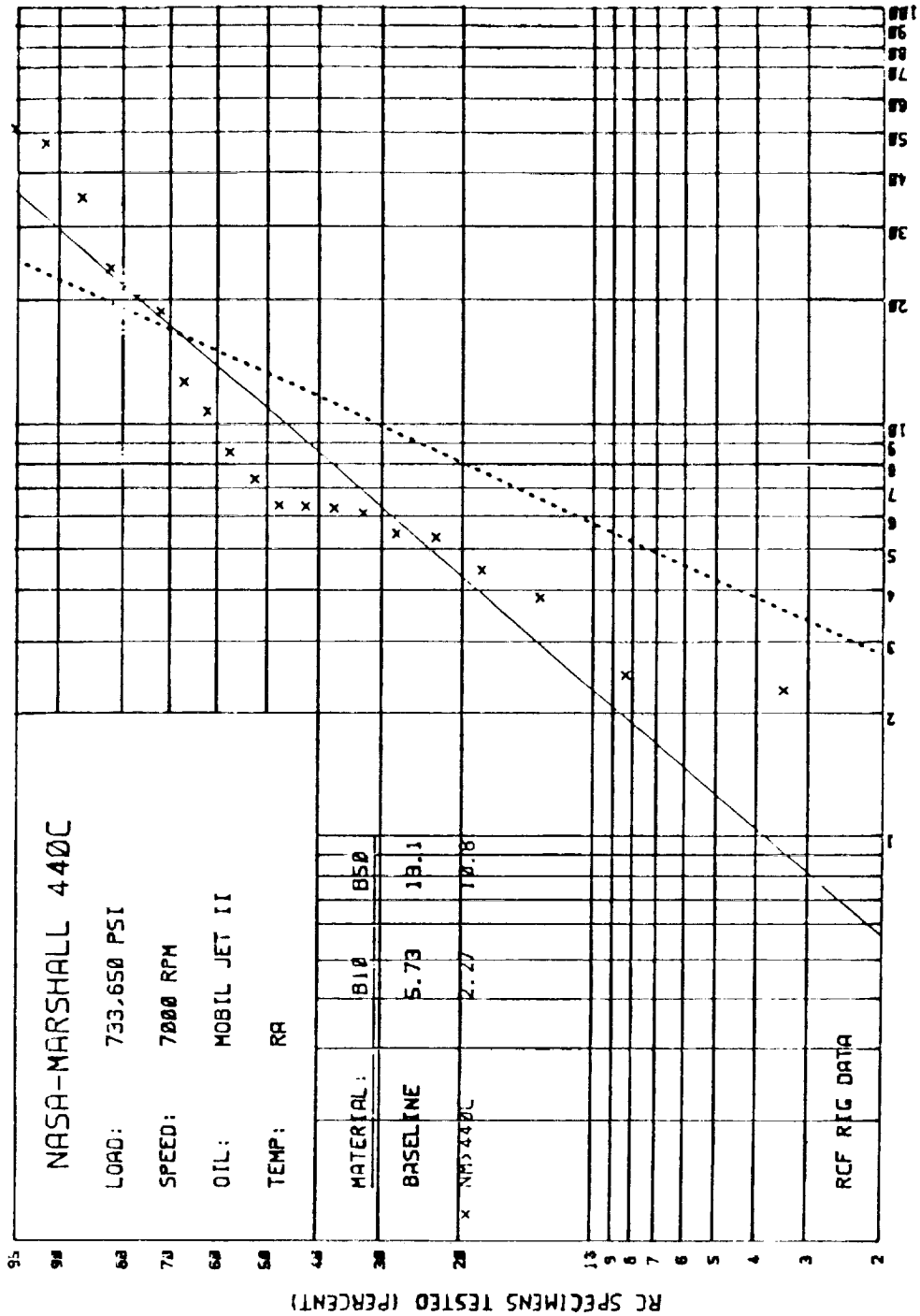

Figure 27. Weibull plot of 440C rolling contact fatigue test lives.

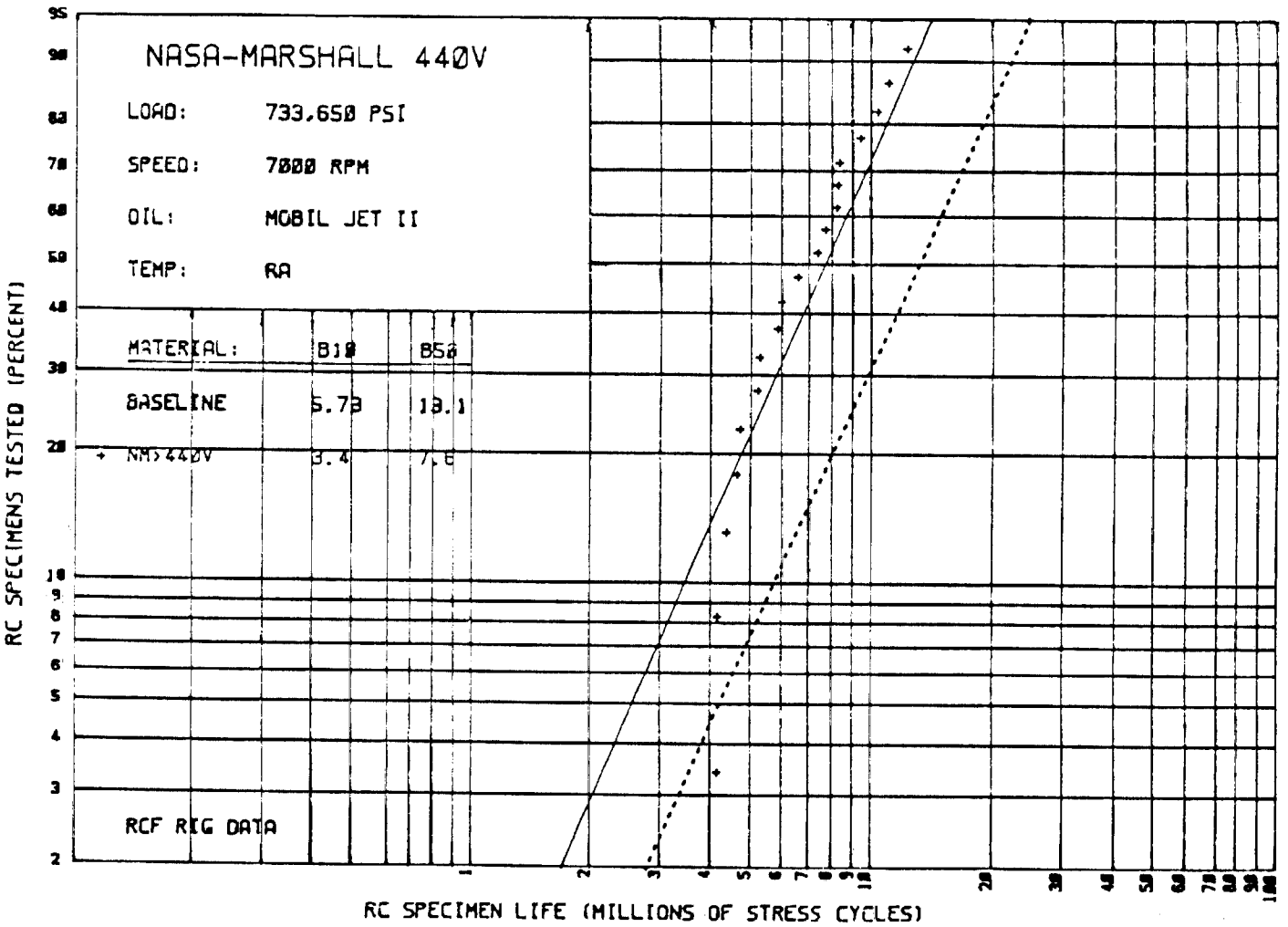

Figure 28. Weibull plot of T-440V rolling contact fatigue test lives.

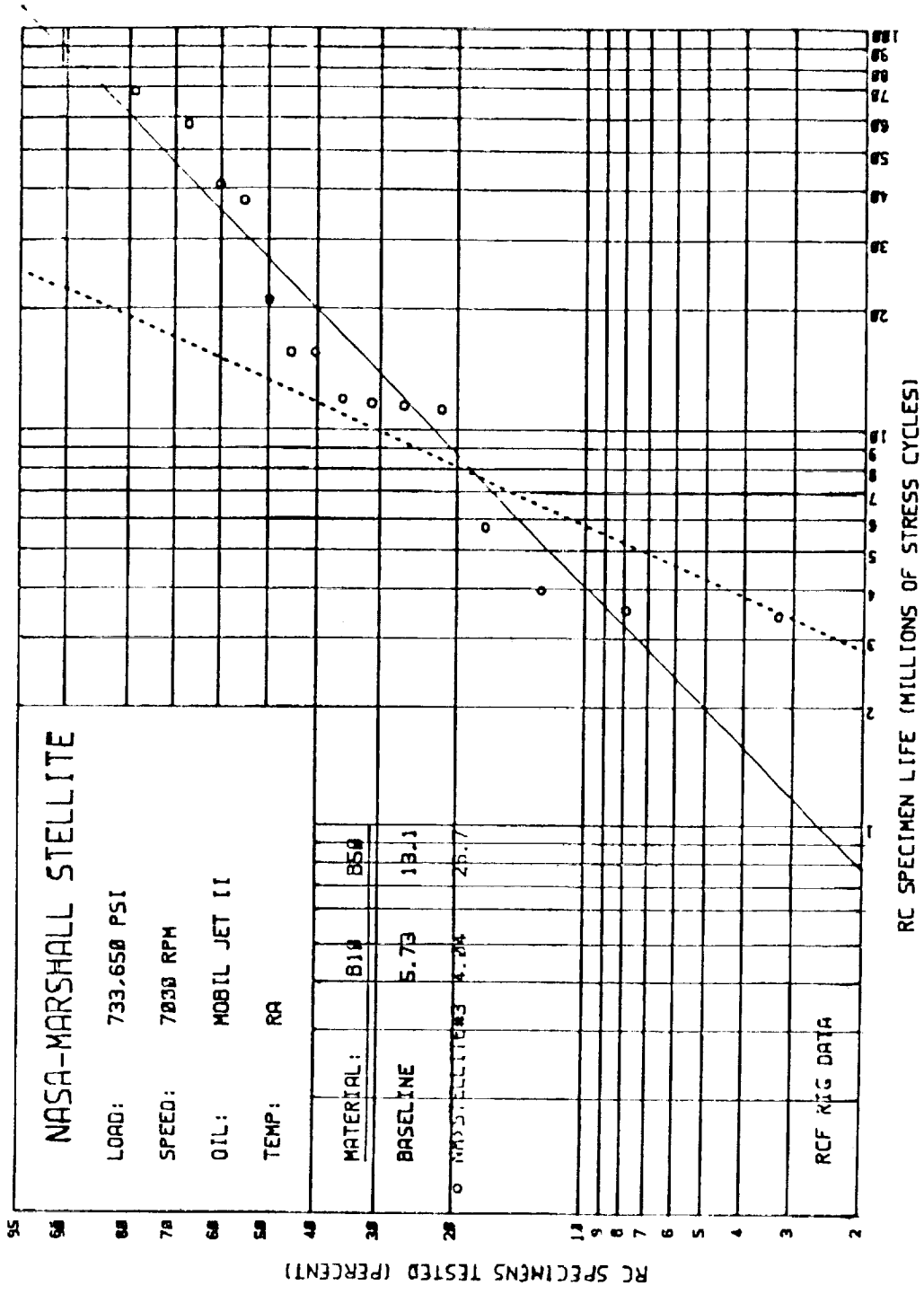

Figure 29. Weibull plot of Stellite 3 rolling contact fatigue test lives.

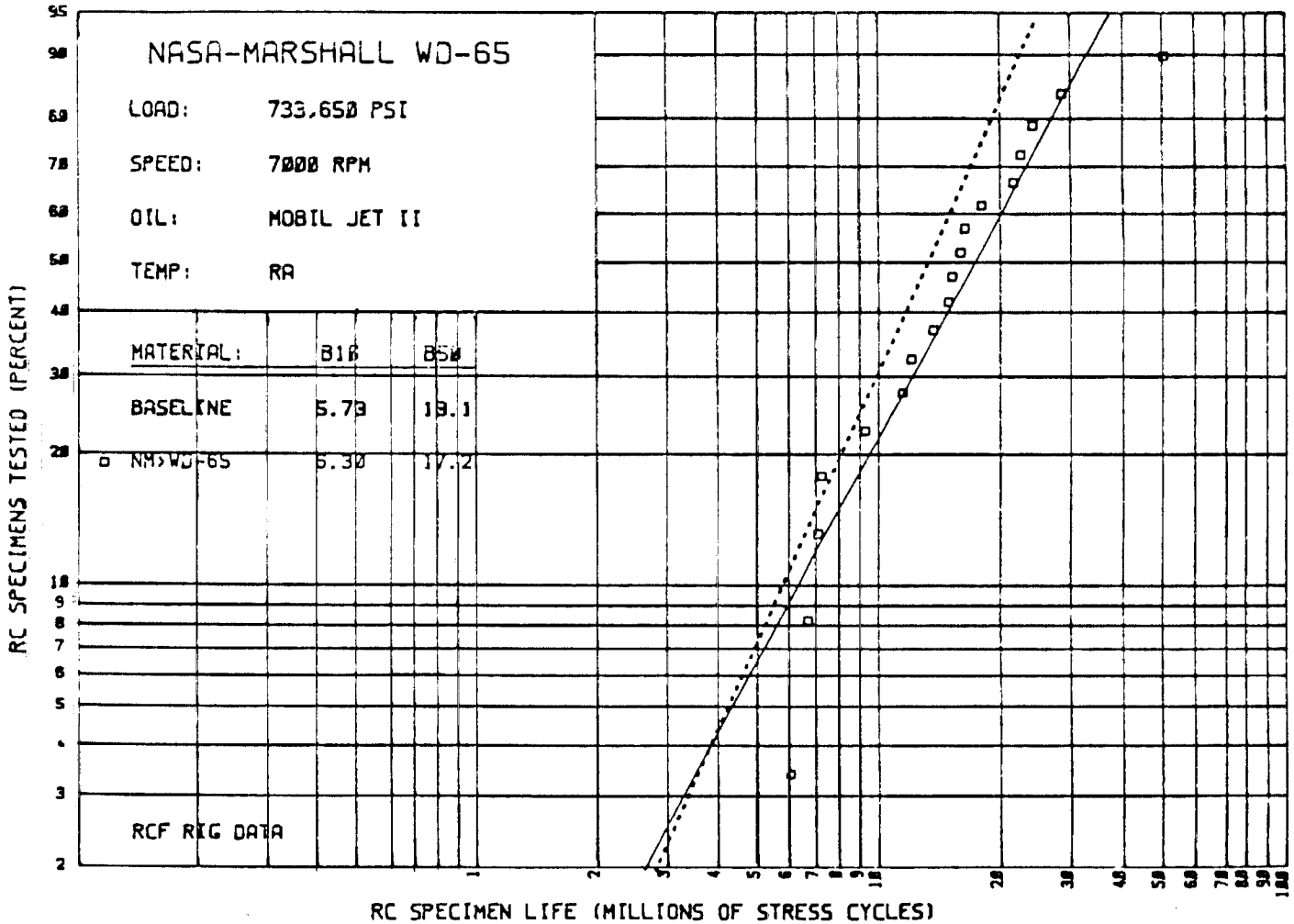

Figure 30. Weibull plot of WD-65 rolling contact fatigue test lives.

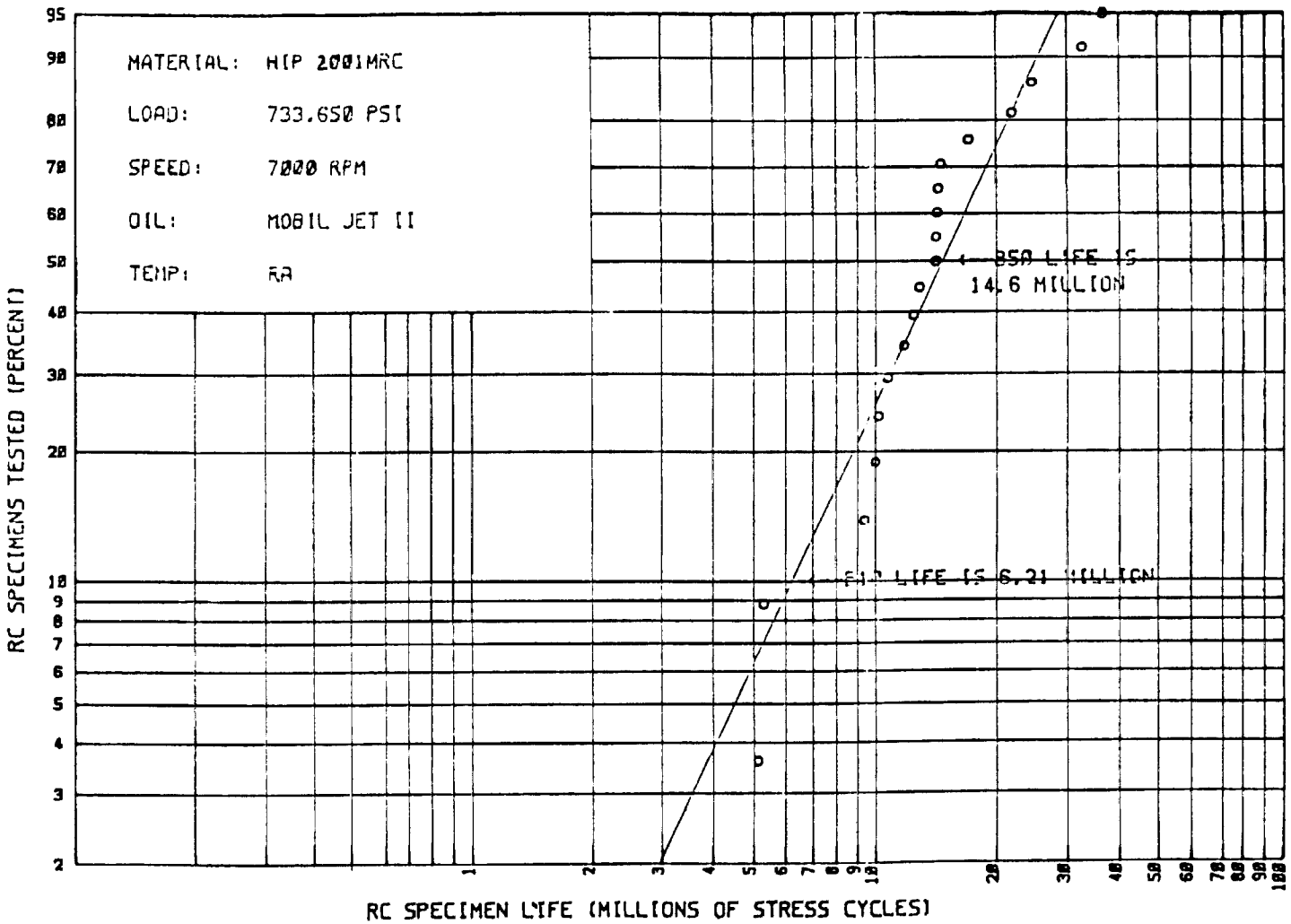

Figure 31. Weibull plot of MRC-2001 rolling contact fatigue test lives.

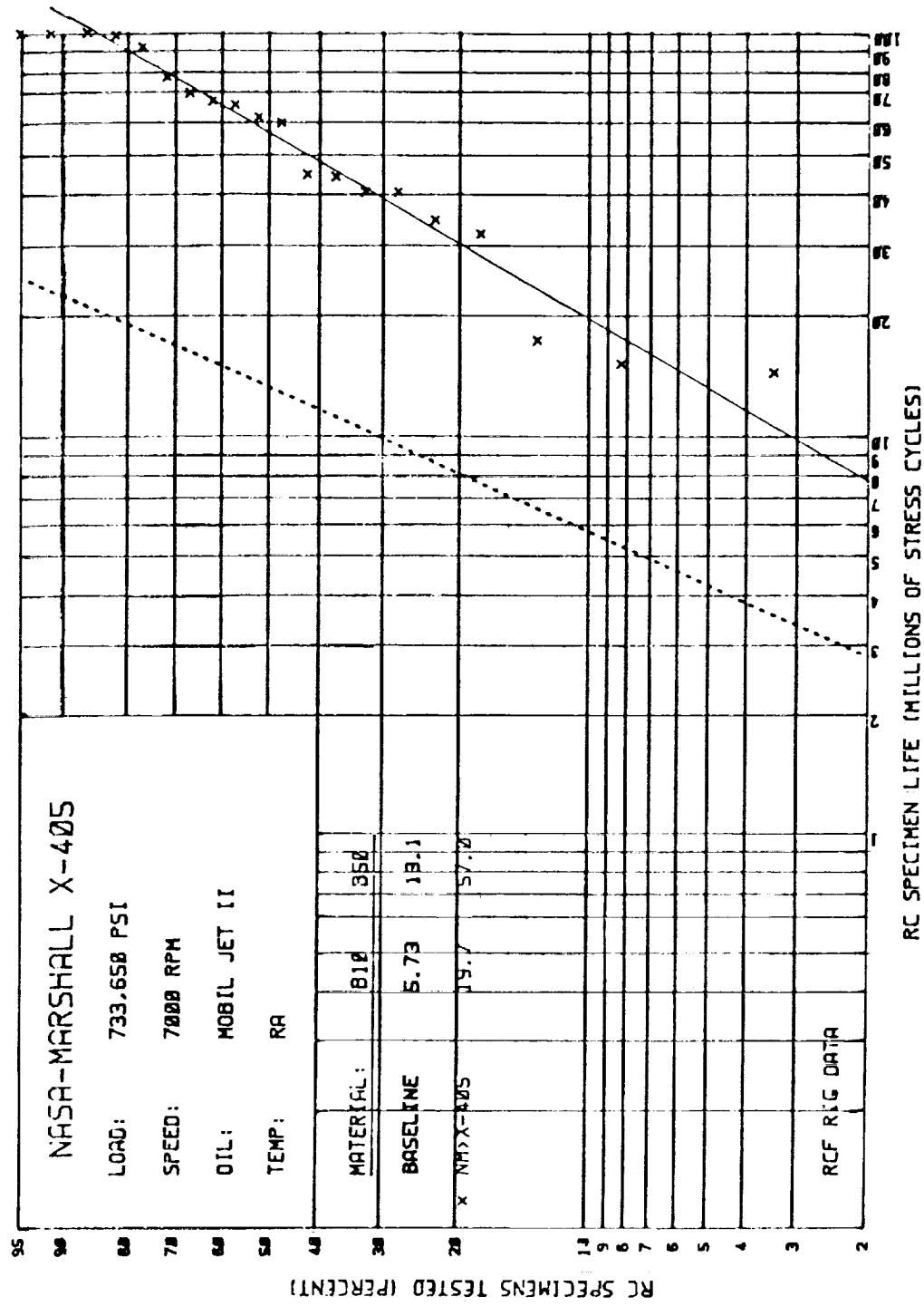

Figure 32. Weibull plot of X-405 rolling contact fatigue test lives.

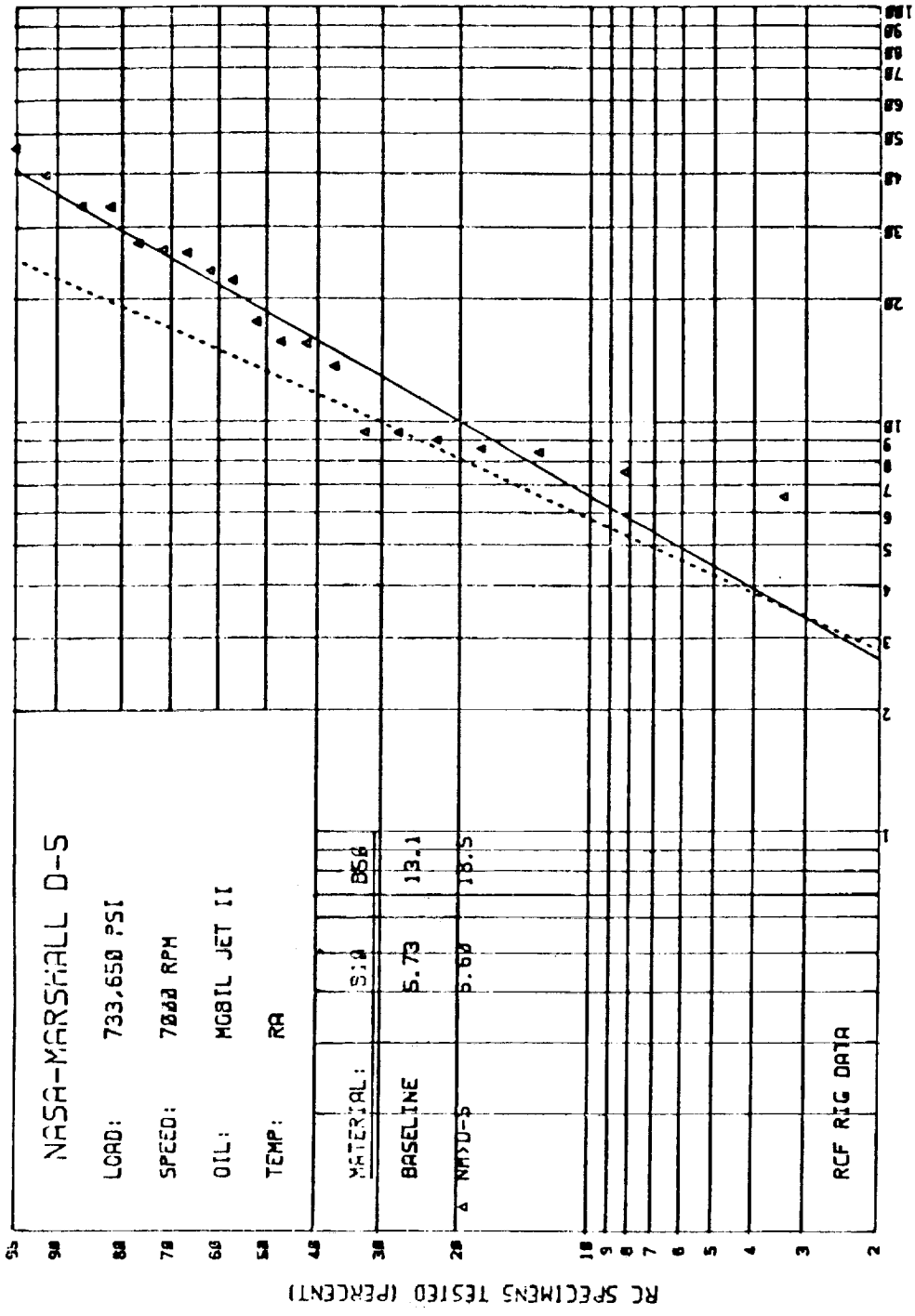

Figure 33. Weibull plot of D-5 rolling contact fatigue test lives.

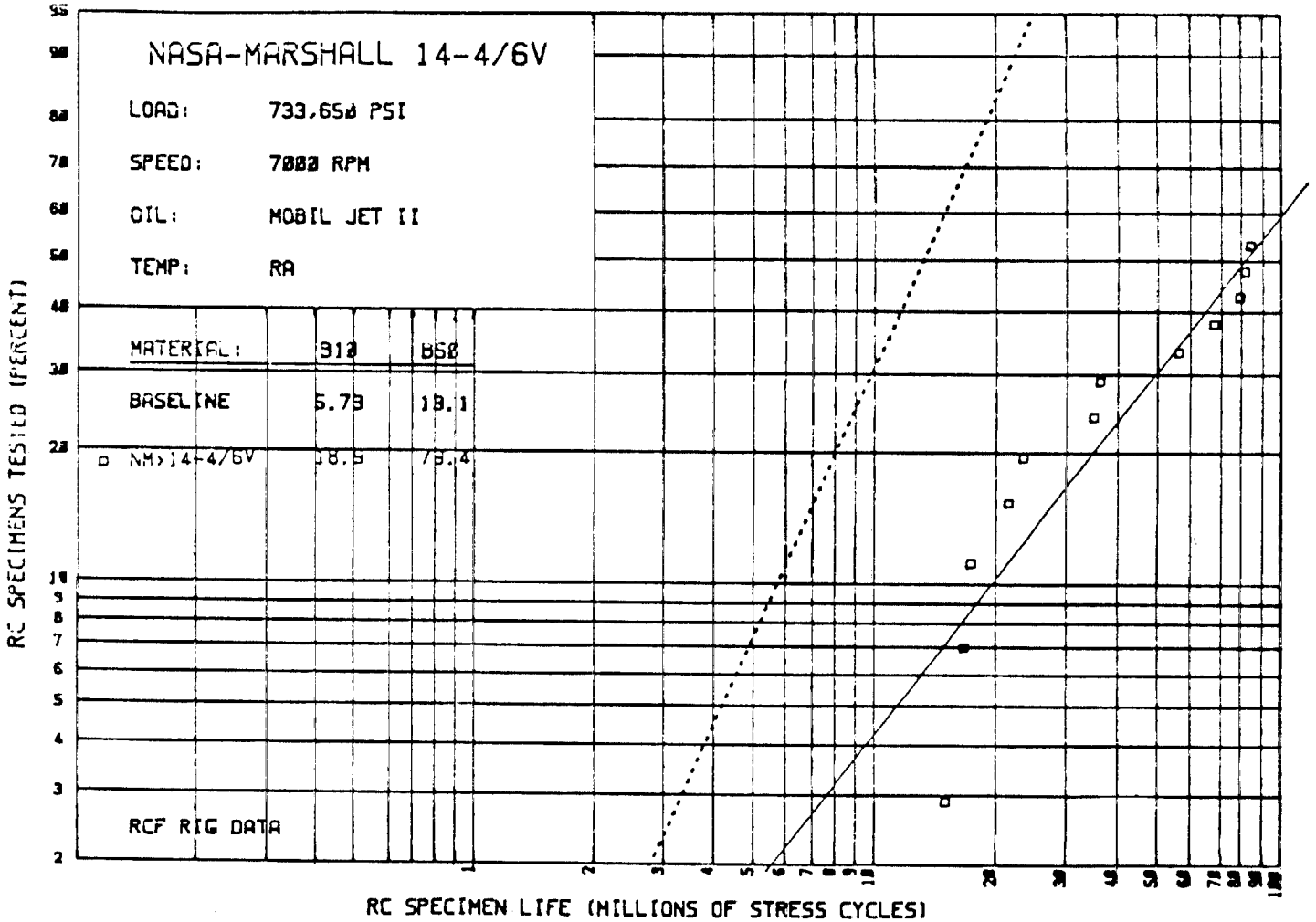

Figure 34. Weibull plot of 14-4/6V rolling contact fatigue test lives.

Table 7
Comparison of Data Generated During Rolling Contact Fatigue Testing of the Candidate Bearing Materials

Material	B-10 Life	B-50 Life	Slope	Rank by Slope*	Rank by B-10	Rank by B-50
V-Pyromet	Too soft					
FerroTic	Suspended				Eliminated	
Tribaloy	Suspended				Eliminated	
440C	2.27×10^6	10.8×10^6	1.21	2	1	2
T440V	3.40×10^6	7.6×10^6	2.34	9	2	1
Stellite 3	4.04×10^6	26.7×10^6	1.00	1	3	7
M-50	5.73×10^6	13.1×10^6	2.28	8	4	3
MRC-2001 as-HIP	6.00×10^6	12.7×10^6	2.20	7	5	4
WD-65	6.27×10^6	17.3×10^6	1.88	6	6	5
D-5	6.60×10^6	18.5×10^6	1.83	5	7	6
14-4/6V	18.9×10^6	79.4×10^6	1.31	3	8	9
X-405	19.7×10^6	57.0×10^6	1.77	4	9	8

* Ranking 1 = worst

(e) Fracture Toughness. Fracture toughness testing of the candidate bearing materials was performed by the short-rod technique; specimen geometry is shown in Figure 35. In Phase 1, specimens were tested at room temperature. Fracture toughnesses of the candidate materials are listed in Table 8. Results from cryogenic fracture toughness testing performed during the subsequent Phase 2 evaluation are also listed for comparison. In general, the candidate materials did not differ significantly with respect to either room temperature or cryogenic fracture toughness. All were poorer than 440C steel, with the exception of CBS-600. Due to an oversight, neither the X-405 or D-5 were evaluated at room temperature. However, based upon a comparison of the cryogenic results, the X-405 and D-5 were expected to have room temperature properties similar to those of 14-4/6V and T-440V, respectively. Tribaloy, FerroTic, and modified Pyromet were eliminated prior to fracture toughness testing.

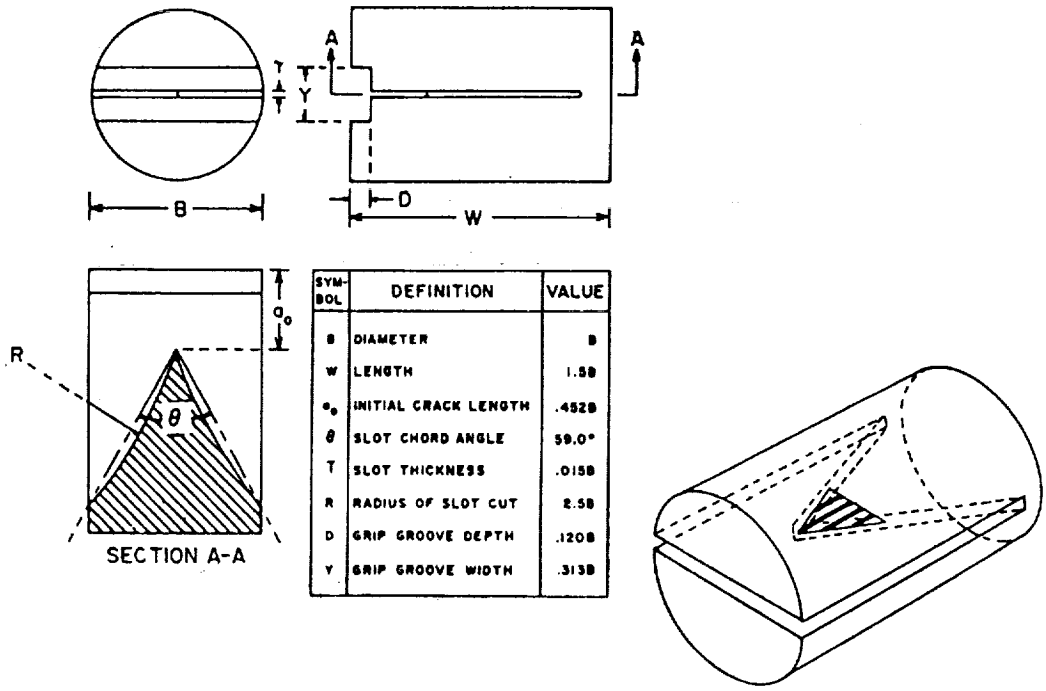

SYMBOL	DEFINITION	VALUE
B	DIAMETER	B
W	LENGTH	1.5B
a_o	INITIAL CRACK LENGTH	.452B
θ	SLOT CHORD ANGLE	59.0°
T	SLOT THICKNESS	.015B
R	RADIUS OF SLOT CUT	2.5B
D	GRIP GROOVE DEPTH	.120B
Y	GRIP GROOVE WIDTH	.313B

Figure 35. Schematic of short-rod $K_{Ic\text{-}SR}$ specimen. (B + 13 mm (0.5 in.)). The shaded triangle in the isometric view is the initial "crack", equivalent to a precrack in other fracture toughness tests.

Table 8
Short Rod Fracture Toughness Results of Candidate Bearing Materials

Material	Room Temp. MPa $\sqrt{m}$ (Ksi $\sqrt{in}$)	Cryogenic (Liq.N) MPa $\sqrt{m}$ (Ksi $\sqrt{in.}$)
T-440V	15.5 (14.1)	11.9 (10.8)
X-405	not tested	14.6 (13.3)
Stellite 3	13.2 (12.0)	not tested
CBS-600	48-54 (44-49)	not tested
MRC-2001 as-HIP	16.6 (15.1)	15.2 (13.8)
14-4/6V	15.9 (14.5)	14.8 (13.5)
WD-65	17.0 (15.5)	15.3 (13.9)
D-5 not tested	not tested	12.4 (11.3)
440C	27.7 (25.2)	21.6 (19.6)

(f) **Wear Resistance.** The response of candidate materials to rubbing and sliding under load was evaluated using a cross cylinder wear apparatus. Referring to the schematic in Figure 36, the stationary specimen is secured in a pivoted arm. At the free end of this arm, weights are suspended to provide a steady applied load. The rotating specimen is clamped inside an adjustable specimen holder. The character of wear resistance is measured in terms of weight loss of the stationary member plus visual analysis of the wear track on the rotating specimen. Figure 37 charts cross-cylinder weight loss for unlubricated metal-to-metal wear testing of the candidate bearing materials. (Modified Pyromet, FerroTic CS-40, Tribaloy, Stellite 3, and CBS-600 were eliminated prior to wear testing.) Table 9 is a ranking of the materials with respect to wear resistance. Elevated temperature wear, from the Phase 2 analysis, is listed for comparison.

2. Phase 1 Recommendations

Preliminary screening of the candidate bearing materials resulted in the elimination of the vanadium-modified Pyromet 350 due to insufficient hardness, and the elimination of the CBS-600 due to poor corrosion resistance. FerroTic CS-40, Tribaloy 800 and Stellite 3 were eliminated because of low RCF life. At the conslusion of Phase 1, it was recommended that 14-4/6V, X-405, MRC-2001, T440V, WD-65, and D-5 be evaluated in Phase 2. The status of the candidate bearings is summarized in Figure 38.

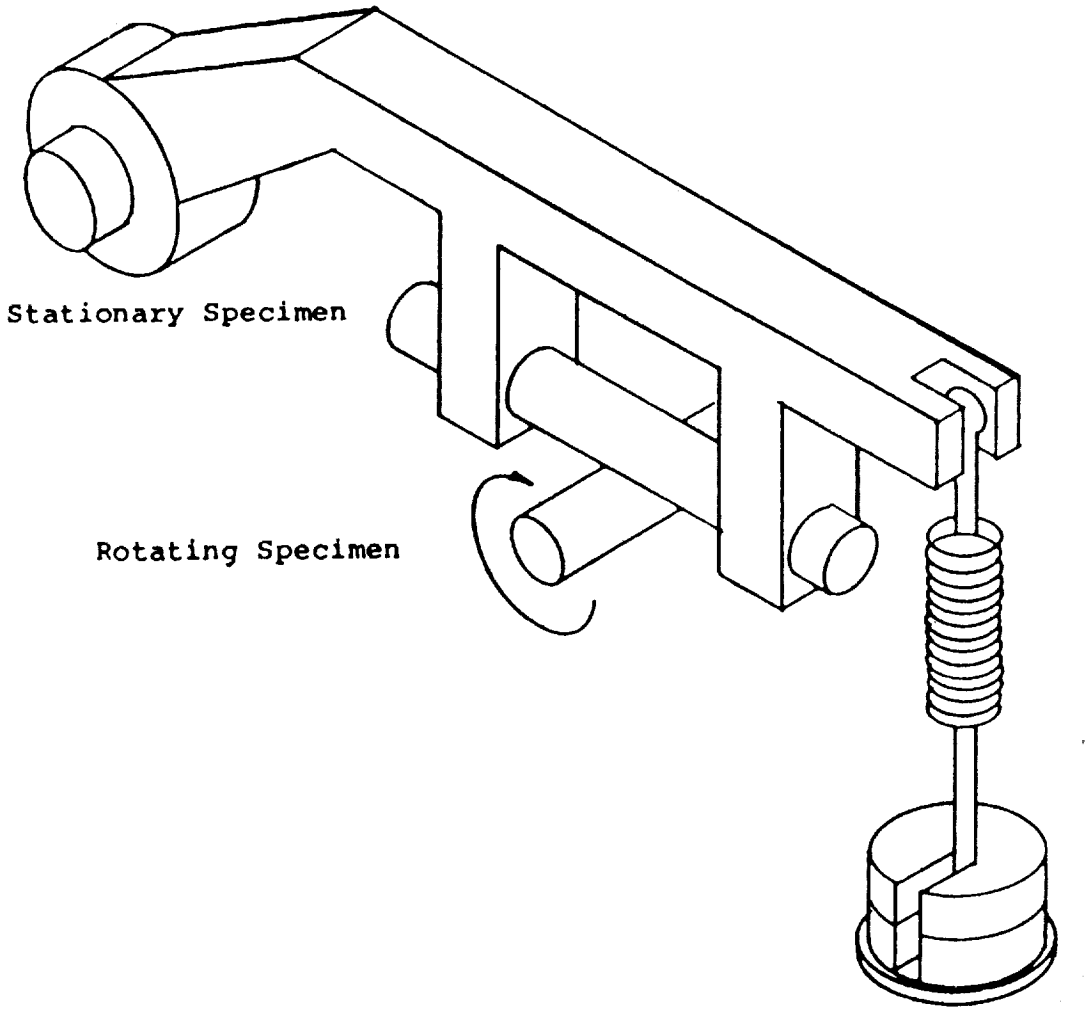

Figure 36. Schematic of cross-cylinder wear testing apparatus.

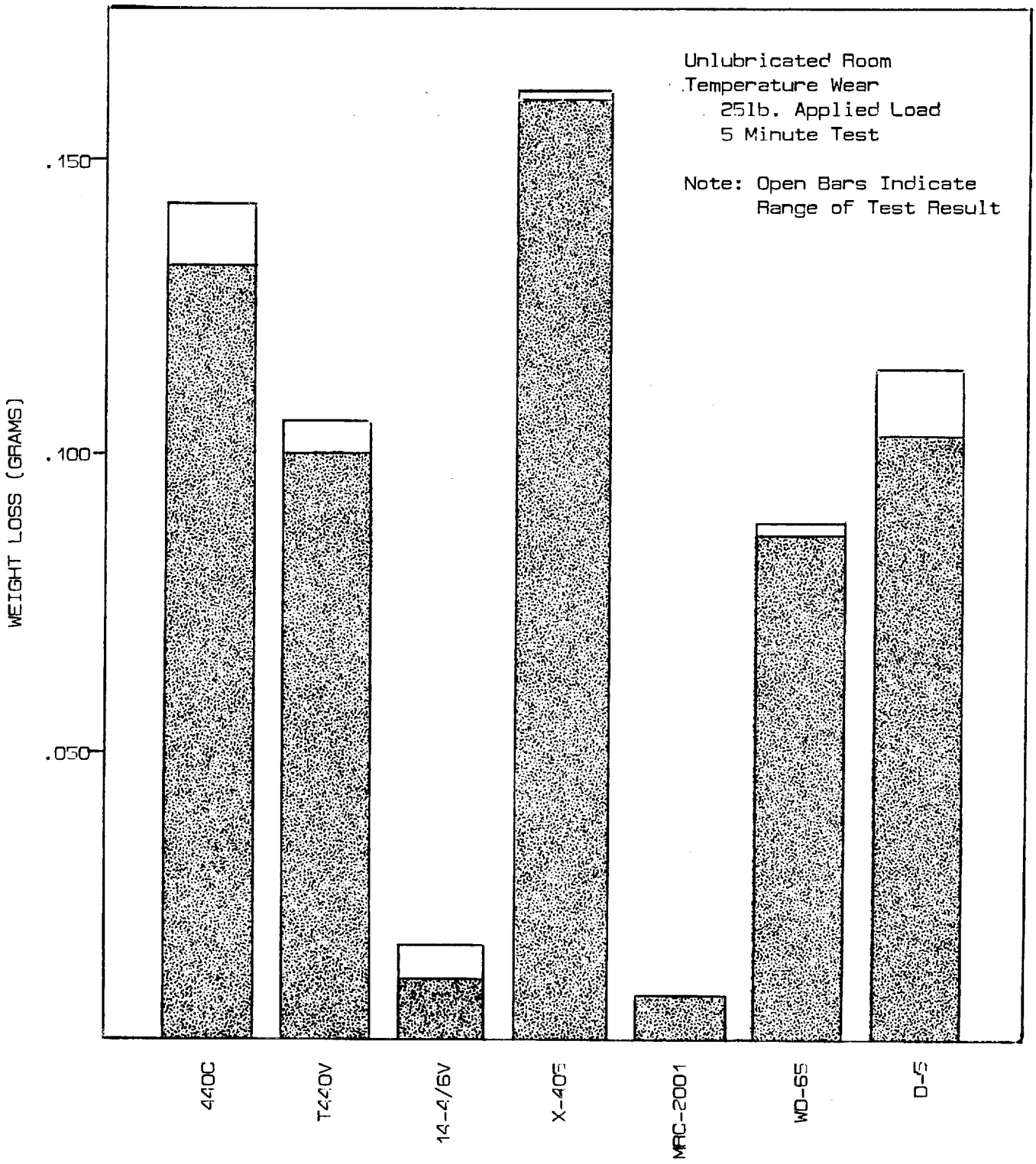

Figure 37. Unlubricated metal-to-metal wear as a function of weight loss for candidate bearing materials.

Table 9
Data Generated During Unlubricated Metal-to-Metal Wear Testing of Candidate Bearing Materials

	Room Temperature		Elevated Temperature	
Material	Weight Loss (grams)	Rank*	Weight Loss (grams)	Rank
440C	0.1321-0.1416 (ave. 0.1369)	6	0.064-0.113 (ave. 0.089)	6
T440V	0.0996-0.1053 (ave. 0.1025)	4	0.040-0.052 (ave. 0.046)	5
14-4/6V	0.0107-0.0166 (ave. 0.0137)	2	0.018-0.054 (ave. 0.036)	3
X-405	0.1597-0.1608 (ave. 0.1603)	7	0.058-0.115 (ave. 0.087)	7
MRC-2001	0.0080-0.0082 (ave. 0.0081)	1	0.010-0.014 (ave. 0.012)	1
WD-65	0.0859-0.0877 (ave. 0.0868)	3	0.040-0.048 (ave. 0.044)	4
D-5	0.1033-0.1143 (ave. 0.1088)	5	0.024-0.033 (ave. 0.029)	2
Pyromet 350 (V-Modified)	Too soft			
FerroTic	Eliminated after RCF tests			
Tribaloy	Eliminated after RCF tests			
CBS-600	Eliminated due to poor corrosion resistance			
Stellite 3	Eliminated after RCF tests			

* Ranking 7 = worst

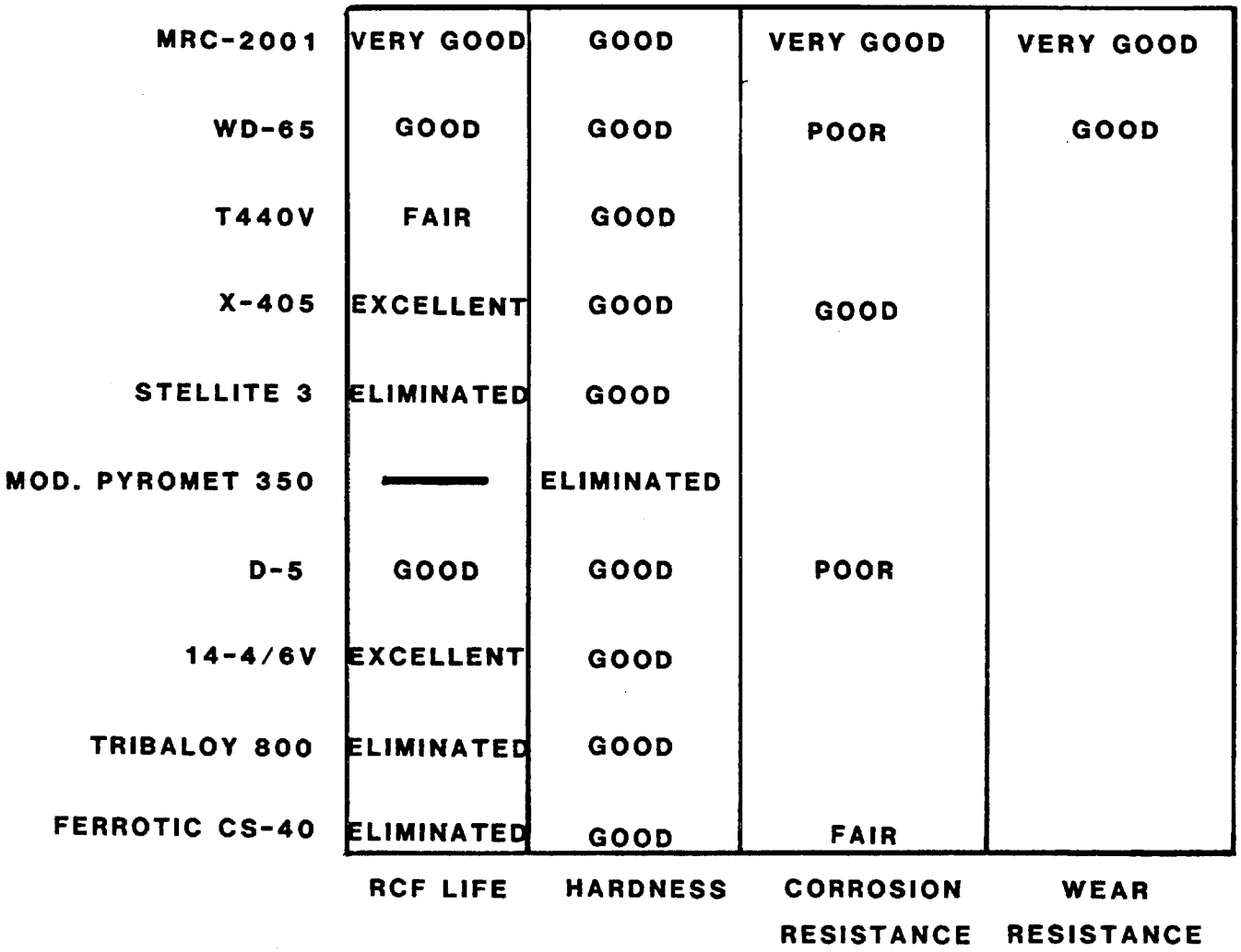

Figure 38. Status of candidate alloys at the end of Phase 1.

B. Phase 2 - Preliminary Material and Fabrication Technique Evaluation

The Phase 2 objective was to generate additional test data of the type conducted in Phase 1, and additional new tests including stress corrosion cracking and five-ball fatigue life tests. Phase 2 was essentially a three task effort. In Task 1 candidate materials were fabricated. Task 2 saw the testing of bearing materials prepared in Task 1. And, finally, Task 3 reviewed all data generated and made the selection of the bearing materials to be full scale tested in Phase 3. A review of the materials procured and the testing performed is presented below. As in Phase 1, the baseline for comparisons was the current 440C bearing material.

1. Experimental Procedures and Discussion of Results

a. Task 1. Fabrication of Candidate Materials. The chemical compositions of the P/M bearing alloys selected for Phase 2 are listed in Table 10. As indicated in the **Introduction**, this selection was developed in Phase 1 based on criteria which included corrosion resistance, rolling contact fatigue life, wear resistance, fracture toughness, and hardness. It should be noted that since the program was initiated, the carbon specification for the MRC-2001 alloy was changed. As shown in Table 1, the MRC-2001 powder evaluated in Phase 2 was procured to the new specification of 1.5 weight percent nominal carbon content. The previous specification, as recorded in the Phase 1 report, was 1.2 weight percent nominal carbon.

The WD-65 material was supplied as HIP (hot isostatic press) consolidated and rolled bar stock. All of the other program material was procured as nitrogen atomized powder. The powders were screened to -100 mesh (< 150 microns) and consolidated to full density by HIP at 1149°C/207 MPa/150 min (2100°F/30 ksi/150 min) in low carbon steel tubes. The sizes of the tubes were selected based on the required finish dimensions of the test specimens and the density of the loose powder in the can. The low carbon steel can material was removed after HIP by chemical leaching.

After HIP, the fully consolidated P/M bearing alloys were heat treated and finish machined to produce the required test specimen geometries. The details of the heat treatment for each alloy are given in Table 11. All of the heat treatments were performed in salt baths to maximize heat transfer and ensure uniform temperature cycles. Throughout the various heat treatments, the salt baths were monitored and maintained in the neutral condition by the addition of appropriate rectifiers. This prevented any adverse reactions of salt with metal. After the heat treatment was completed, the metallurgical microstructures of each alloy were evaluated and documented.

Table 10
Chemical Compositions of Phase 2 Selected P/M Bearing Alloys

		Typical Composition, weight percent							
Alloy	Base	Cr	Mo	V	Co	Mn	Si	C	Other
X-405	Fe	19.0	2.0	1.0				1.25	
MRC-2001		Fe	15.0	6.0	2.0		0.5	1.5	0.1Cb
T-440V	Fe	17.5	0.5	5.75		0.5	0.5	2.2	
D-5	Fe	12.5	1.5		2.75	0.3	0.3	1.25	
14-46V	Fe	14.5	4.5	6.0		0.5	0.5	2.0	
WD-65	Fe	14.0	4.0	2.75	5.75			1.15	2.5W

All of the consolidated powder microstructures were fully dense in the as-HIP condition. Figure 39 shows typical microstructures of the six candidate bearing alloys after heat treatment. All of the microstructures were well refined. No prior particle boundaries were detected. The microstructure of X-405 was noted to be somewhat coarser than some of the other microstructures, but there were no harmful effects associated with this in the subsequent testing.

b. Task 2. Testing of Bearing Materials from Task 1

(1) Corrosion, Rolling Contact Fatigue, and Stress Corrosion Tests. Test specimens were produced and shipped to the NASA Marshall Space Flight Center for evaluation of corrosion resistance, rolling contact fatigue life, and stress corrosion cracking resistance for each of the six candidate bearing alloys. The results of the NASA testing have been presented separately from this report (6,7). In general, the test data generated through Phase 2 testing were consistent with the results of Phase 1. All of the candidate powder metallurgy alloys were superior to the currently used 440C in rolling contact fatigue. They were all equal or superior to 440C in stress corrosion cracking resistance.

(2) Cryogenic Fracture Toughness. Fracture toughness was evaluated by the short rod technique for each of the six candidate bearing materials as well as for the currently used 440C. The specimen geometry is shown in Figure 35. Room (ambient) temperature fracture toughness values were determined in Phase 1. Cryogenic fracture toughness properties were tested at -196^{o}C (-320^{o}F) in Phase 2.

Table 11
Heat Treatments for Selected P/M Bearing Alloys

X-405

1149°C (2100°F), 30 min/Air cool
Deep Freeze: -79°C (-110°F), 2 hr
Temper: 204°C (400°F), 2 hr/Air cool
Deep Freeze: -79°C (-110°F), 2 hr
Temper: 204°C (400°F), 2 hr/Air cool
R_c: 60-63

MRC-2001

843°C (1550°F), 10 min
1121°C (2050°F), 20 min
Quench: 177°C (350°F), 20 min in low temperature drawing salt/Air cool
Wash
Deep Freeze: -79°C (-110°F), 1 hr
-196°C (-321°F) (liq. N), 1 hr
Temper: 538°C (1000°F), 2 hr
Deep Freeze: -196°C (-321°F) (liq. N), 1 hr
Temper: 538°C (1000°F), 2 hr/Air cool
R_c: 60-62

T-440V

843°C (1550°F), 5 min
1093°C (2000°F), 20 min
Quench: 593°C (1100°F), 5 min in barium chloride salt/Air cool
Martemper: 163°C (325°F) 5 min/Air cool
Wash
Deep Freeze: -79°C (-110°F), 1 hr
-196°C (-321°F) (liq. N), 1 hr
Temper: 149°C (300°F), 2 hr
Deep Freeze:
-196°C (-321°F) (liq. N), 1 hr
Temper: 149°C (300°F), 2 hr/Air cool
R_c: 60-62

D-5

843°C (1550°F), 5 min
996°C (1825°F), 20 min
Quench: 177°C (350°F), 5 min in low temperature drawing salt/Air cool
Wash
Deep Freeze: -79°C (-110°F), 1 hr
-196°C (-321°F) (liq. N), 1 hr
Temper: 468°C (875°F), 1 hr/Air cool
R_c: 60-62

14-46V

1093°C (2000°F), 30 min
Oil Quench
552°C (1025°F) Double Temper, 2 hr each/Air cool
R_c: 60-62

WD-65

843°C (1550°F), 10 min
1149°C (2100°F), 20 min
Quench: 177°C (350°F), 10 min in low temperature drawing salt/Air cool
Wash
Deep Freeze: -79°C (-110°F), 1 hr
Temper: 538°C (1000°F), 2 hr
Deep Freeze: -79°C (-110°F), 1 hr
Temper: 538°C (1000°F), 2 hr
R_c: 60-62

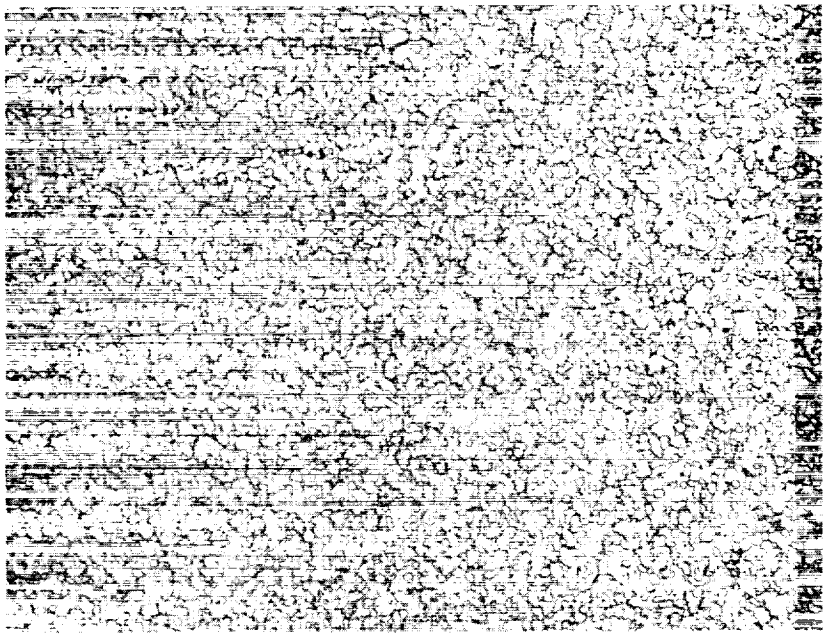

Electrolytic Chromic (a) X-405 500X

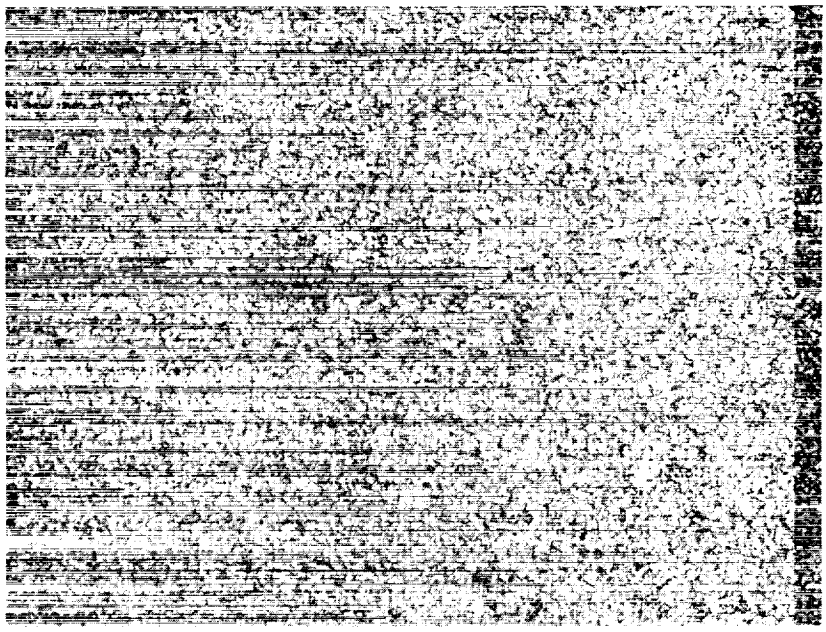

Electrolytic Chromic (b) MRC-2001 500X

Figure 39. Microstructures of candidate P/M bearing alloys after heat treatment.
Etchant: Electrolytic Chromic

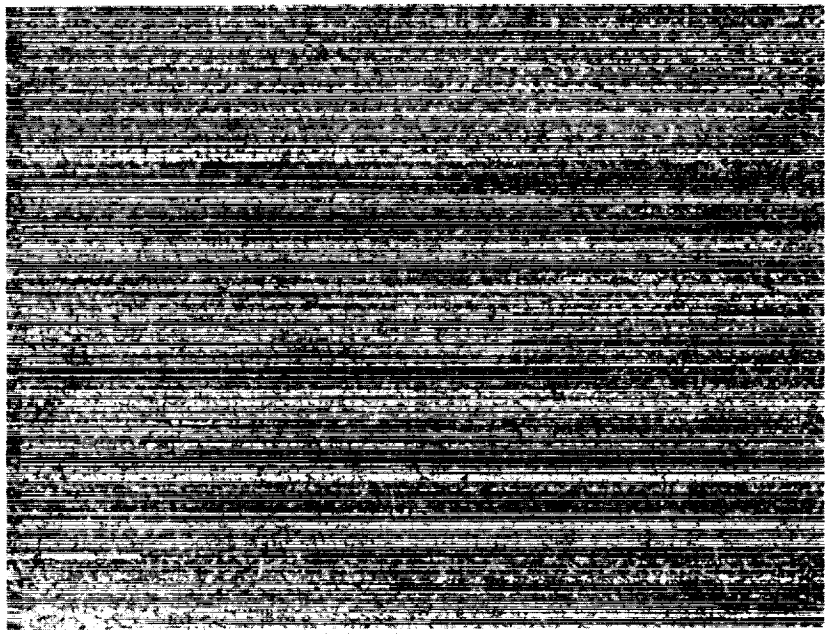

Electrolytic Chromic (c) T-440V 500X

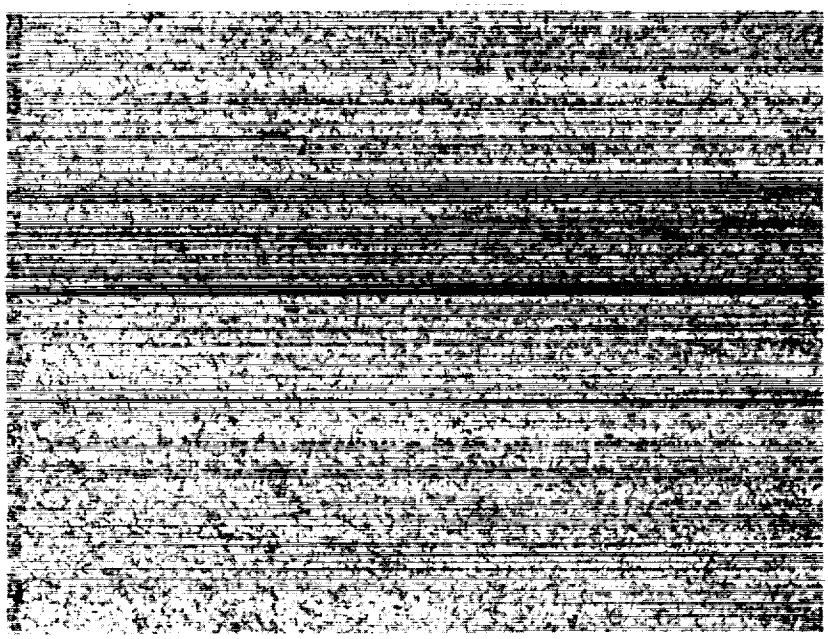

Electrolytic Chromic (d) D-5 500X

Figure 39. (continued) Microstructures of candidate P/M bearing alloys after heat treatment. Etchant: Electrolytic Chromic

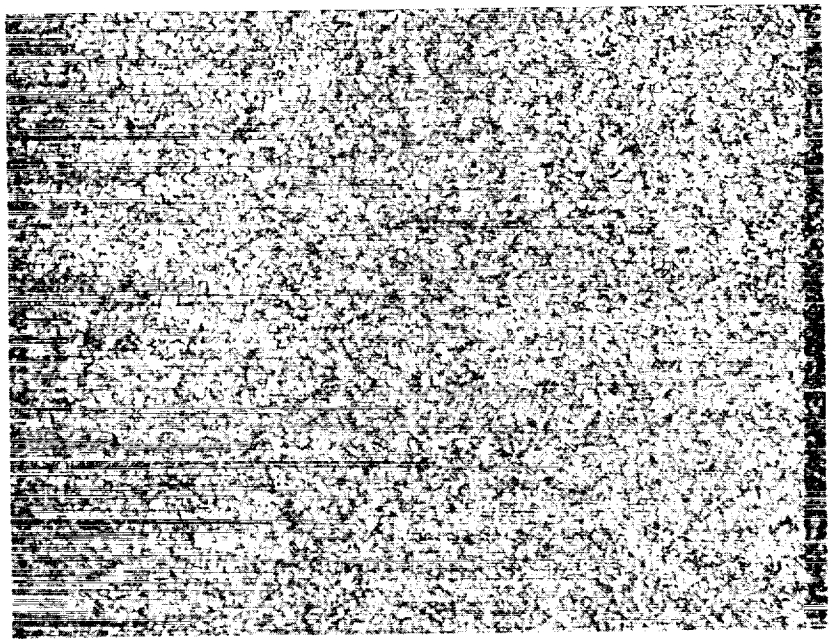

Electrolytic Chromic (e) 14-4/6V 500X

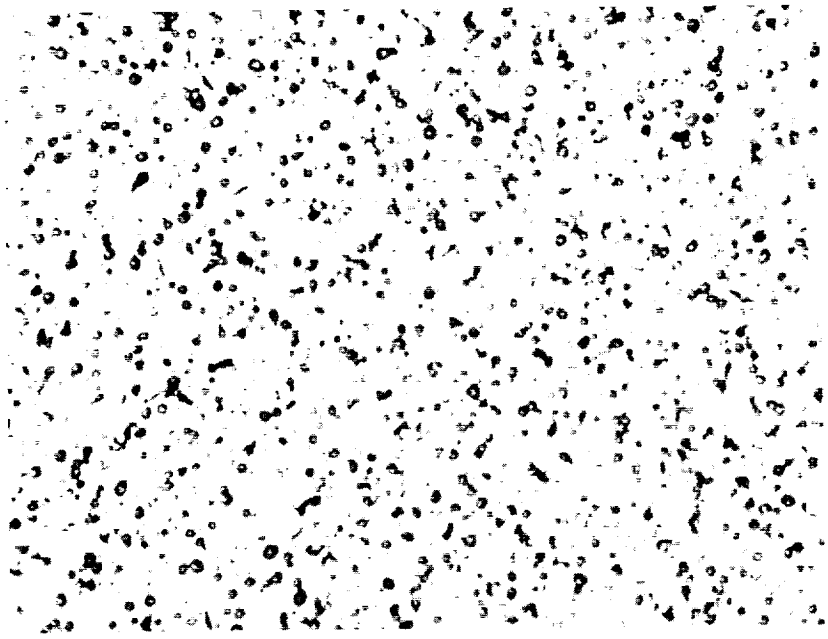

Electrolytic Chromic (f) WD-65 500X

Figure 39. (continued) Microstructures of candidate P/M bearing alloys after heat treatment Etchant: Electrolytic Chromic

The results of the Phase 2 cryogenic short rod fracture toughness tests are shown in Table 12. For comparison, results of room temperature tests conducted in Phase 1 are also listed. The six candidate materials did not differ markedly with respect to fracture toughness at either ambient or cryogenic temperatures. While T-440V and D-5 exhibited somewhat lower toughness at cryogenic temperatures than the other candidate materials, the most significant aspect of the data was that all of the candidates had lower toughness than the current bearing material, 440C.

For the materials which were tested at both ambient and cryogenic temperatures, all showed a decrease in toughness with decreasing temperature, ranging from 7 percent (14-4/6V) to 23 percent (T-440V) of the room temperature toughness value.

(3) Elevated Temperature Wear Resistance. Wear resistance was evaluated using a cross cylinder apparatus which is shown schematically in Figure 36. As shown in the figure, two specimens of the material to be evaluated are required. One specimen is held stationary and is secured in the pivoted arm. At the free end of the arm, weights are suspended to provide a steady applied load. The second specimen rotates and is clamped inside of an adjustable holder. No lubrication is used. Wear resistance is quantified in terms of the weight loss by the stationary member over a specified time interval. A low weight loss indicates high wear resistance.

As discussed previously, room (ambient) temperature wear tests were conducted in Phase 1 for each of the six candidate bearing alloys as well as for the current material, 440C. The applied load was 111 N (25 lb). The duration of each test was 5 minutes. Elevated temperature wear tests were conducted at 371°C (700°F) in Phase 2. The duration of each elevated temperature test was maintained at 5 minutes, but the applied load was reduced to 44.5 N (10 lb).

The results of the Phase 2 elevated temperature (371°C (700°F)) wear tests are shown in Table 13. For comparison, results of room temperature tests conducted in Phase 1 are also listed. At each temperature, the wear resistance of each alloy has been ranked based on the average weight of material lost over several tests.

Except for X-405, all of the candidate bearing materials exhibited wear resistance superior to the current 440C alloy at both ambient and elevated temperatures. The relative ranking of the alloys is the same at both test temperatures except that D-5 is significantly better, on a relative basis, at elevated temperature. The D-5 alloy was only fifth best at ambient temperature, but it was second best at 371°C (700°F). It is not possible to compare the effect of temperature on wear resistance on an absolute basis because, as noted above, a lower contact load was used at the higher temperature.

Table 12
Short Rod Fracture Toughness of Candidate Bearing Materials

Material	Room Temp.		Cryogenic (liq. N)	
	MPa $\sqrt{m}$	ksi $\sqrt{in}$	MPa $\sqrt{m}$	ksi $\sqrt{in}$
440C (Current Material)	27.7	25.2	21.5	19.6
X-405	not tested		14.6	13.3
MRC-2001	16.6	15.1	15.2	13.8
T-440V	15.5	14.1	11.9	10.8
D-5	not tested		12.4	11.3
14-4/6V	15.9	14.5	14.8	13.5
WD-65	17.0	15.5	15.3	13.9

Table 13
Unlubricated Metal-to-Metal Wear Data for Candidate Bearing Materials

Material	Room Temperature Test 111 N (25 lb) load				371°C (700°F) Test 44.5 N (10 lb) load			
	Weight Loss, g			Rank*	Weight Loss, g			Rank*
	Min.	Max.	Avg.		Min.	Max.	Avg.	
440C	0.1321	0.1416	0.1369	6	0.064	0.113	0.088	6
X-405	0.1597	0.1608	0.1603	7	0.058	0.115	0.096	7
MRC-2001	0.0080	0.0082	0.0081	1	0.010	0.014	0.012	1
T440V	0.0996	0.1053	0.1025	4	0.040	0.052	0.048	5
D-5	0.1033	0.1143	0.1088	5	0.024	0.033	0.029	2
14-4/6V	0.0107	0.0166	0.0137	2	0.018	0.540	0.032	3
WD-65	0.0859	0.0877	0.0868	3	0.040	0.048	0.043	4

* 1 - best, lowest wear (weight loss)

(4) Rolling Contact Fatigue (Five-Ball) Testing. Ten five-ball rolling contact fatigue tests were conducted for each of five of the candidate bearing alloys; i.e. X-405, MRC-2001, 14-4/6V, D-5, and T-440V. The sixth candidate bearing alloy, WD-65, was not five-ball tested.

Ball wires were produced as previously described by HIP consolidating powder in cans of 19 mm (3/4 in) initial diameter. The can material was removed by chemical leaching and the alloy wires were straightened and centerless ground to 11.2 mm (0.440 in). Balls were manufactured from the wires by heading and rough grinding prior to heat treatment. The balls were finish ground to the final diameter, 12.70 mm (0.5000 in), after heat treatment.

The basic configuration of a five-ball test apparatus is shown in Figure 40. The contact interface in a five-ball test more closely simulates the actual rolling-sliding contact in a thrust-loaded, angular contact bearing than any other simple element test. The basic configuration of the five-ball test apparatus is five balls, with four of them (support balls) located in a raceway, 90^0 apart and separated by a cage. The fifth (driving) ball rides on top of the four support balls. The support balls rotate about their own axes and orbit about the axis of the spindle. A dead weight is applied to the rotating spindle by a lever system with a knife edge fulcrum. This configuration is comparable to an axially loaded ball bearing in which the test (driving) ball represents the rotating inner ring.

For the five-ball testing of this program, the driver test ball was loaded to produce a maximum Hertzian stress of 5,516 MPa (800 ksi). It was rotated at 10,600 rpm. The balls were lubricated by means of an oil-mist constant density lubricator which dispensed 10 drops (approximately 6g) per hour. The lubricant itself was synthetic oil conforming to MIL-L-23699. Its kinematic viscosity was 28.4 centistokes (1.10 ft^2/hr) at 38^0C (100^0F).

A sharp increase in the amplitude of vibration of the test apparatus indicated that a failure had occurred. Upon failure of any of the five balls, the test was terminated. The total time to failure was recorded and the nature of the failure was characterized, including whether it was an upper or a lower ball that had failed. The balls which had not failed were not tested further. Thus, a total of fifty balls were involved in the ten five-ball tests conducted for each alloy.

Scanning electron microscope (SEM) and energy dispersive x-ray (EDAX) analyses were conducted on the fatigue and worn surfaces of the balls after completion of five-ball testing.

Table 14 summarizes the Weibull analysis of the five-ball rolling contact fatigue test results for the five alloys tested. The data is presented graphically in Figures 41 and 42. For comparison purposes, results for vacuum melted M-50 alloy (8) are also included in Table 14

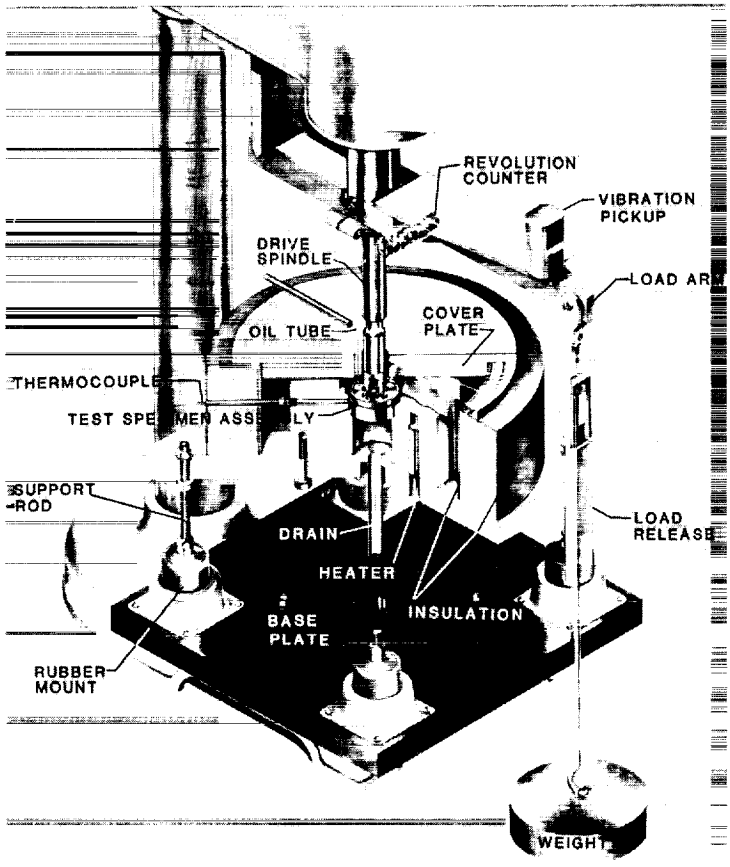

(A) FIVE-BALL FATIGUE TESTER

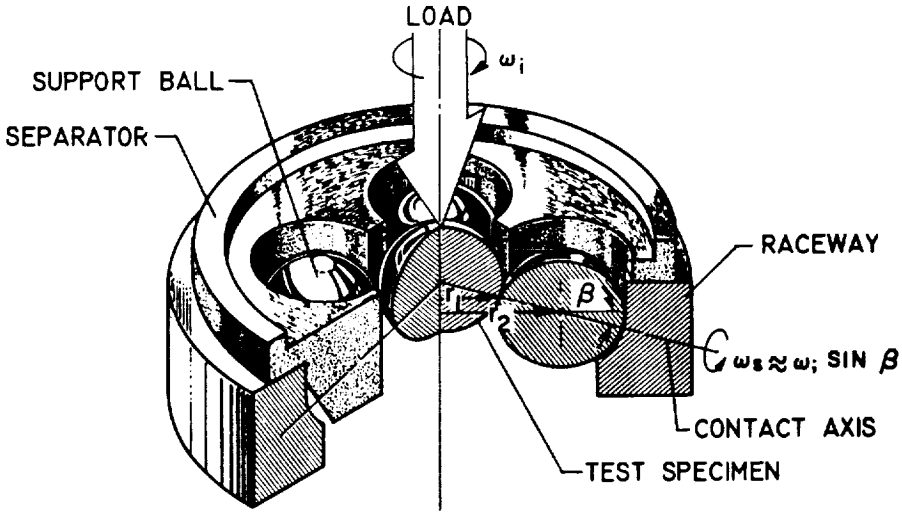

(B) SCHEMATIC, FIVE-BALL TESTER

Figure 40. Schematic of five-ball fatigue test apparatus.

Table 14
Weibull Analysis of Five-Ball Fatigue Test Results for Candidate Bearing Materials

	Failures of Test & Support Balls					Failures of Test Balls Only				
	L_{10}		L_{50}			L_{10}		L_{50}		
Material	Hours	Million Cycles	Hours	Million Cycles	Weibull Slope	Hours	Million Cycles	Hours	Million Cycles	Weibull Slope
X-405	33.8	64.5	181.3	345.9	1.12	55.7	106.2	109.2	208.3	2.80
MRC-2001	6.33	12.1	22.8	43.5	1.47	11.5	21.9	34.0	64.8	1.74
T-440V	3.39	6.5	12.6	24.0	1.43	2.34	4.5	13.1	24.9	1.09
D-5	8.24	15.7	22.4	42.7	1.88	6.51	12.4	21.8	41.6	1.56
14-4/6V	3.50	6.7	52.5	100.2	0.696	2.25	4.3	35.7	68.1	0.68
M-50*	7.77	14.8	21.0	40.1	1.89					

* For comparison purposes only

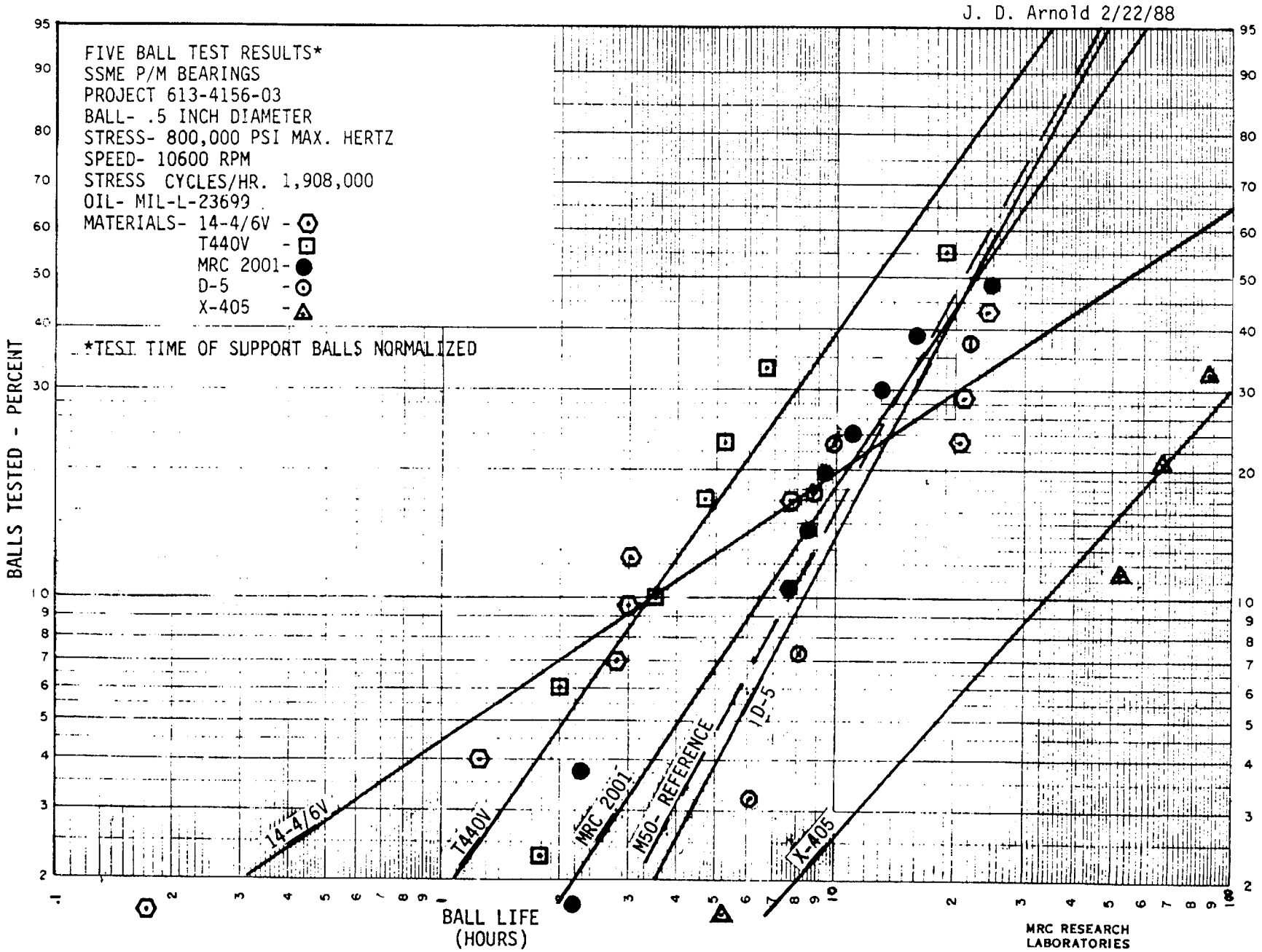

Figure 41. Five-ball test results for candidate bearing materials, including failures of support balls.

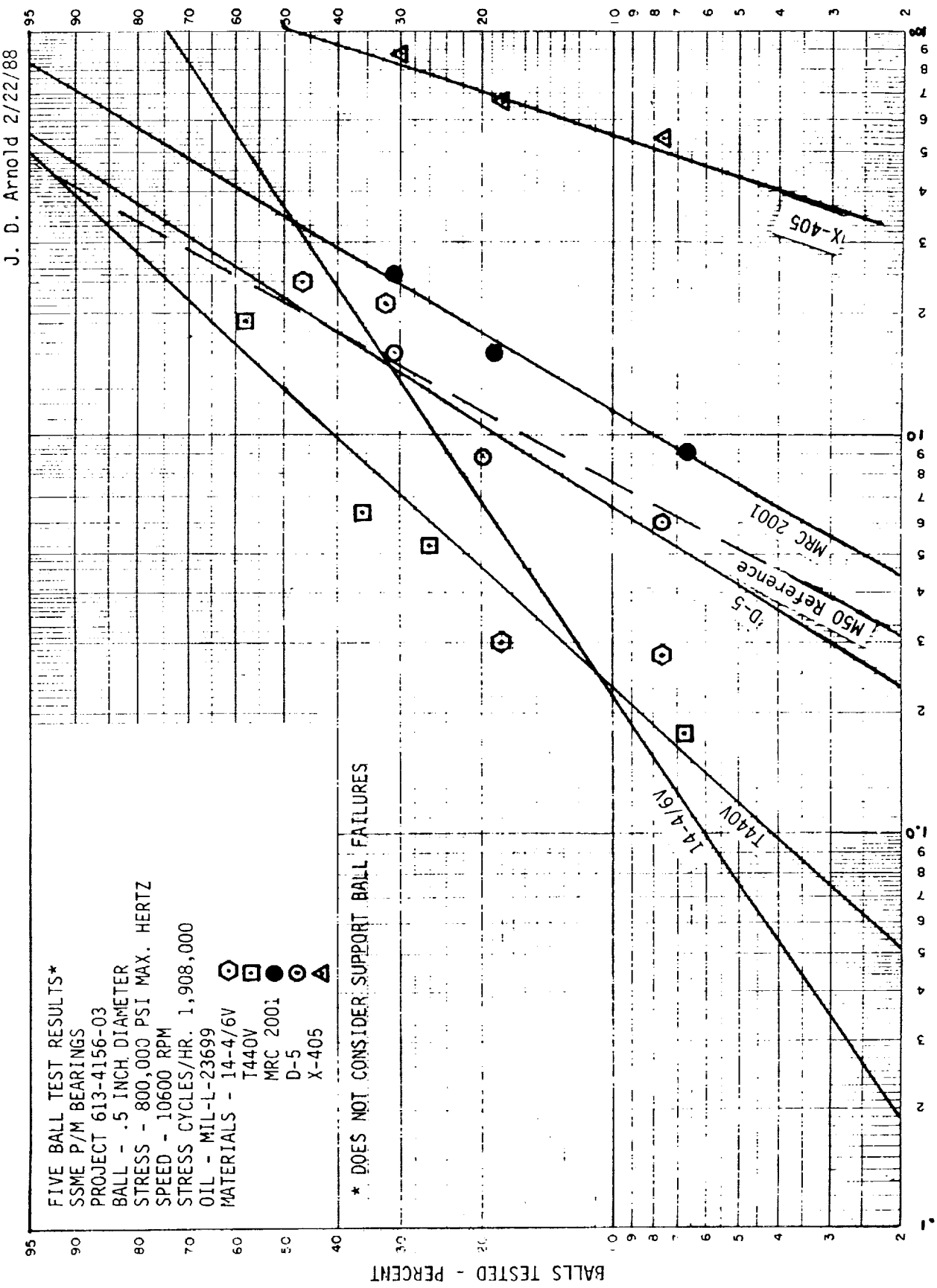

Figure 42. Five-ball test results for candidate bearing materials, excluding failures of support balls.

and Figures 41 and 42. (M-50 is a 4 weight percent chromium steel which lacks corrosion resistance and is used for aerospace applications in which corrosion is not a major concern.) The results of the testing indicated outstanding performance of two P/M alloys, X-405 and MRC-2001.

As shown in the table and figures, Weibull analysis is formulated in terms of the cumulative percentage of failures as a function of the severity of the test. In the case of the five-ball fatigue test, the severity is quantified by the total test time, which is proportional to the number of stress cycles.

The five-ball test performance of the candidate materials can be summarized by the L_{10} and L_{50} parameters. These indicate, respectively, the life time at which 10 percent and 50 percent of the balls have failed. The slope of the Weibull line is also significant, as it indicates the spread in the distribution of life times. A steep slope is preferred, as this indicates a relatively low probability of premature failures.

The analysis of the five-ball test data was complicated by an unexpected number of failures of the lower or support balls. Kinematic analysis, verified by stroboscope, has shown that a given contact point on the upper ball experiences 3.0 stress cycles per revolution. A contact point on one of the lower balls experiences only 0.65 stress cycles for each revolution of the upper test ball. It was expected that points on the upper balls should fail first because they accumulate stress cycles at a rate 4.62 times that for the lower balls.

However, contrary to expectation and as stated above, a number of lower ball failures were observed in the five-ball testing of the five candidate bearing alloys. The most extreme cast was MRC-2001. Of the 10 five-ball tests conducted on this alloy, 7 were terminated for lower ball failure versus only 3 upper test ball failures.

The significance of the apparently high number of support ball failures was not clear. It was speculated that marginal lubrication in at least some of the five-ball tests might have increased the number of support ball failures. Discoloration was evident on many of the test and support balls and this discoloration was attributed to lubrication distress.

Upon further investigation of the issue of support ball failures, it was found that lower ball failures are not especially unusual (9). While a preponderance of upper ball failures might be expected based on the higher number of stress cycles which the upper ball experiences in a given time, lower ball failures are favored by probability as there are four times as many lower balls as upper balls. Over large numbers of five-ball tests, the ratio of lower ball failures to upper ball failures is close to 50:50 (9).

Given the number of lower ball failures in the five-ball test data for the five candidate bearing alloys, it did not not seem reasonable to neglect the distribution between upper and lower balls in the Weibull analysis. The five-ball test data were analyzed in two ways. In the first case, all of the ball failures were analyzed together. The lives (time to failure) of the support balls were normalized (reduced) by the factor of 4.62 to account for the lower rate at which points on the support balls accumulate stress cycles.

Table 14 and Figure 41 show the results of analyzing the data in this way. The X-405 alloy is clearly superior to all of the other alloys tested as well as to the M-50 reference material. Only 4 points are plotted for X-405 because the other tests were suspended when no failures had occurred. One of the X-405 tests was suspended at 67.9 hours and the other 5 were suspended at times ranging from 99.2 to 110 hours.

The Weibull lines for MRC-2001, D-5, and M-50 are very close, indicating similar performance in the five-ball test. While MRC-2001 exhibited somewhat shorter life, on average, than D-5, it is not certain if this difference is significant in light of the high percentage of support ball failures in MRC-2001.

As shown in Figure 41, the performance of the T440V and 14-4/6V alloys in five-ball testing was significantly worse than the others. It was also noted that the slope of the 14-4/6V Weibull line in Figure 41 was the shallowest, indicating that, while this alloy exhibited some relatively long lived samples, there also were premature failures.

The ranking of alloys in five-ball testing is consistent with the results of the Phase 2 rolling contact fatigue (RCF) testing conducted by NASA at the 5,420 MPa (786 ksi) maximum Hertzian stress level (1). This stress was close to the 5,520 MPa (800 ksi) maximum of the five-ball testing. The ranking seemed somewhat dependent on the stress level. At 4,040 MPa (586 ksi), the top three alloys in RCF L_{10} lives were MRC-2001, T-440V, and X-405 (1).

In contrast to the comparison with the Phase 2 RCF data, the five-ball test ranking of the alloys is somewhat inconsistent with the rolling contact fatigue testing conducted in Phase 1 at 5,050 MPa (733 ksi). The ranking from best to worst L_{10} life had been X-405, 14-4/6V, D-5, M-50, MRC-2001, and T440V. Thus, in Phase 1 RCF, the 14-4/6V alloy was second best while in five-ball testing it was one of the worst.

The second way in which the five-ball test data was treated was to exclude the lower ball failures from the anlaysis entirely. Only the upper ball performance was considered. Table 14 and Figure 42 show the results of analyzing the data in this way. The relative ranking of the alloys is essentially unchanged, except that MRC-2001 now appears to be significantly better than both the M-50 reference and the D-5 powder metal alloy material.

SEM images of the wear track surfaces of the balls are shown in Figures 43 through 47. The balls of X-405 and MRC-2001 material, shown in Figures 43 and 44 respectively, failed through spalling, a fatigue mechanism. Microspalls which developed during testing were detected along the wear tracks. Elemental analysis by the energy dispersive x-ray method (EDAX) revealed no difference in chemical composition between the spall areas and the matrix material.

A mixed mode of failure, characterized by both wear and microspalling, was observed in the 14-4/6V and T-440V balls. This mode of failure is shown in Figures 45 and 46. Multiple damage sites were detected in the case of a D-5 alloy ball which failed after only 4.7 hours, Figure 47.

Suggestions of inadequate lubrication during the five-ball tests were previously noted. In the balls examined in the SEM, however, there was evidence of lubrication distress only in the ball of alloy D-5, which exhibited a short life and the multiple damage sites seen in Figure 47. The balls of the other alloys exhibited no lubrication distress. In particular, the grooves produced by ball grinding were undamaged and are still visible around the spall on the MRC-2001 alloy ball, Figure 44. While the SEM examination found little evidence of lubrication distress, it should be noted that the possibility of inadequate lubrication in the five-ball tests was based on the visual appearance of some of the 250 test and support balls. As discussed above, only a few balls were examined in the scanning elecron microscope.

2. Task 3. Selection of Bearing Materials and Fabrication Techniques

Outstanding fatigue resistance was observed in five-ball testing of P/M X-405 bearing steel. This steel exhibited an excellent rolling-element fatigue life, substantially better than that of the high-performance vacuum-melted M-50 bearing steel as well as all of the other candidate bearing alloys.

The P/M MRC-2001 alloy exhibited the highest wear resistance of any of the candidate bearing alloys, at both ambient and elevated temperatures. The fatigue life of MRC-2001 in five-ball testing was similar to that obtained with wrought M-50 bearing steel. However, in comparison with M-50, P/M MRC-2001 material has improved corrosion resistance, thus making it more desirable for aerospace cryogenic systems in which corrosion is a major concern.

The MRC-2001 alloy was recommended for full scale bearing testing in Phase 3. This selection was based on its superior combination of wear resistance, fatigue life, and corrosion resistance. Performance at elevated surface temperatures and resistance to wear caused by poor lubrication conditions were considered the most critical properties for performance in the high pressure oxygen turbopump of the space shuttle main engine.

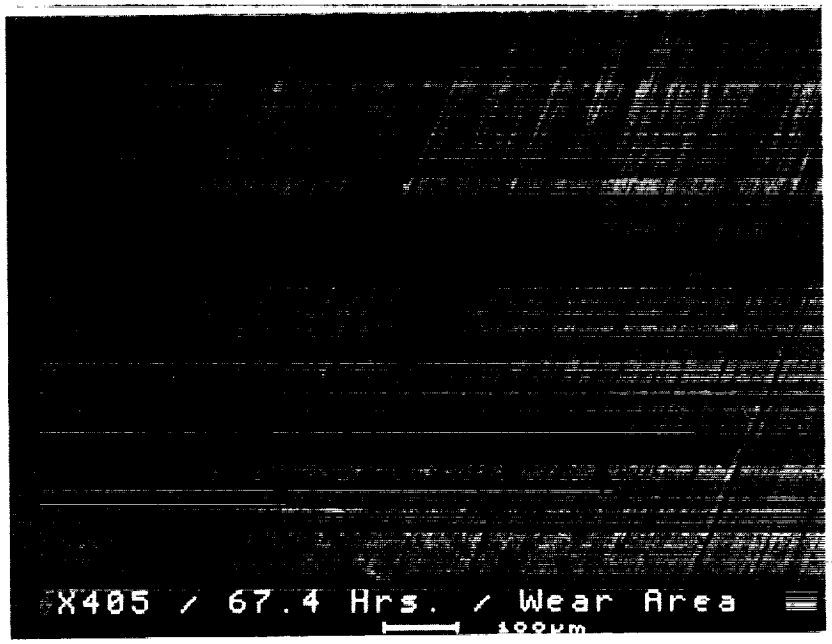

(a) Wear Track ↓ 100X

(b) Wear Track at Higher Magnification ↓ 980X

Figure 43. Scanning electron microscope (SEM) image of wear track surface of P/M X-405 alloy ball which failed after 67.4 hours.

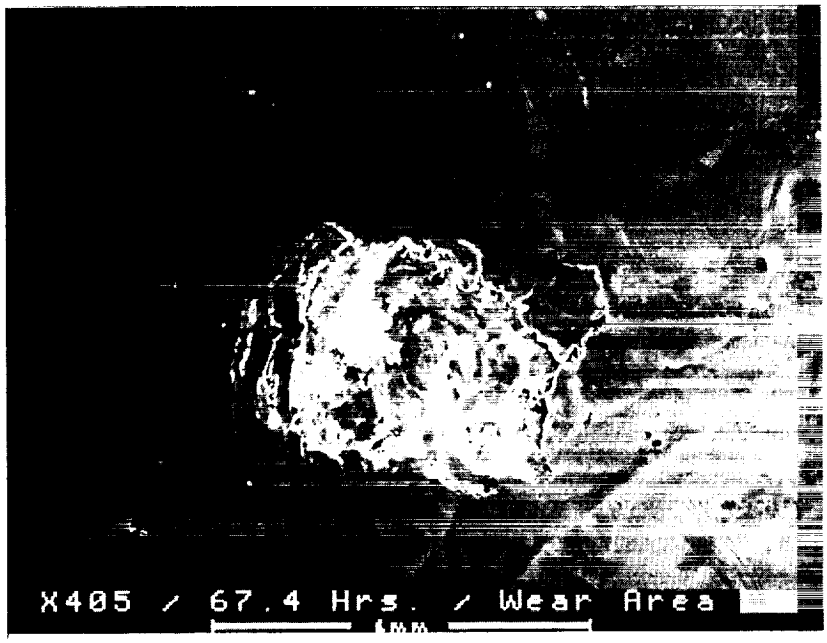

(c) Spall Which Caused the Failure 50X

Figure 43. (continued) Scanning electron microscope (SEM) image of wear track surface of P/M X-405 alloy ball which failed after 67.4 hours.

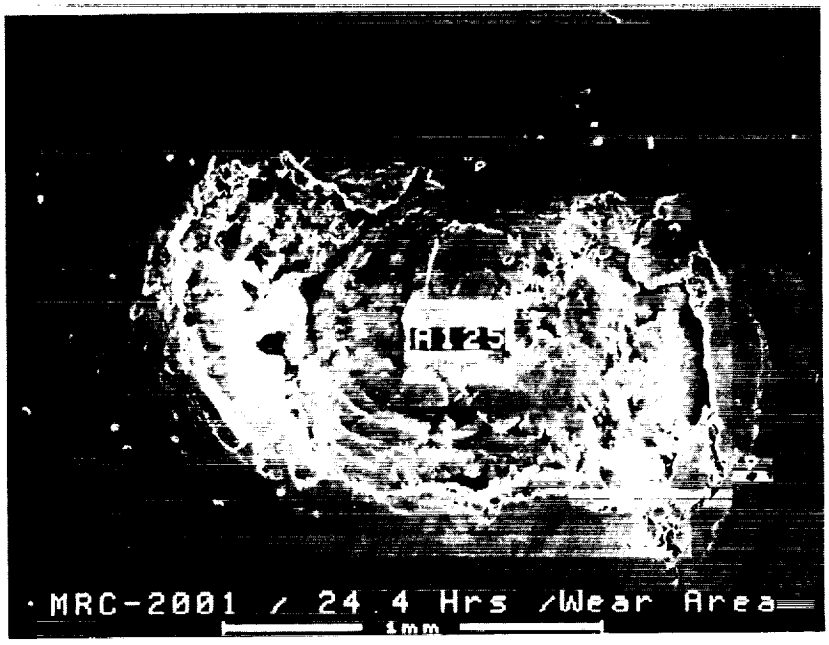

(a) Spall in Wear Track 50X

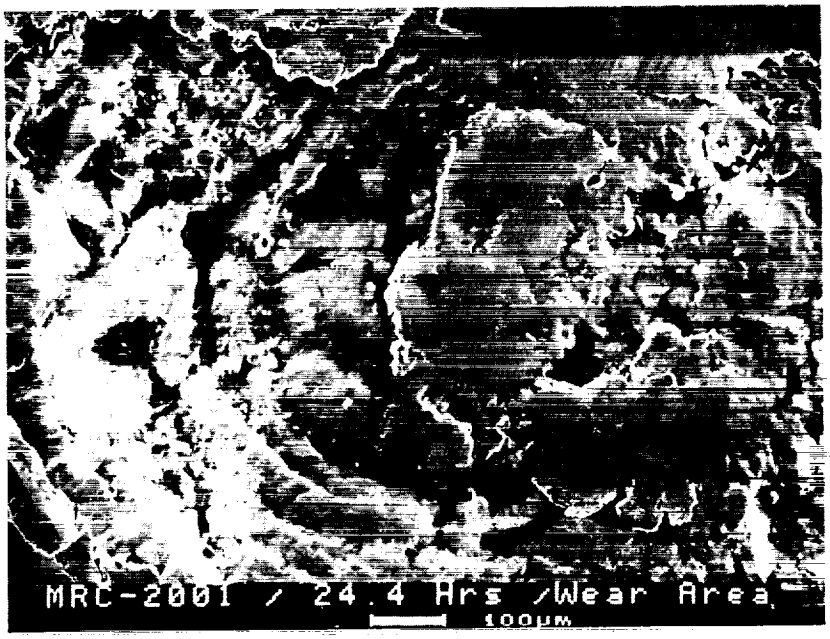

(b) Spall at Higher Magnification 100X

Figure 44. Scanning electron microscope (SEM) image of wear track surface of P/M MRC-2001 alloy ball which failed after 24.4 hours.

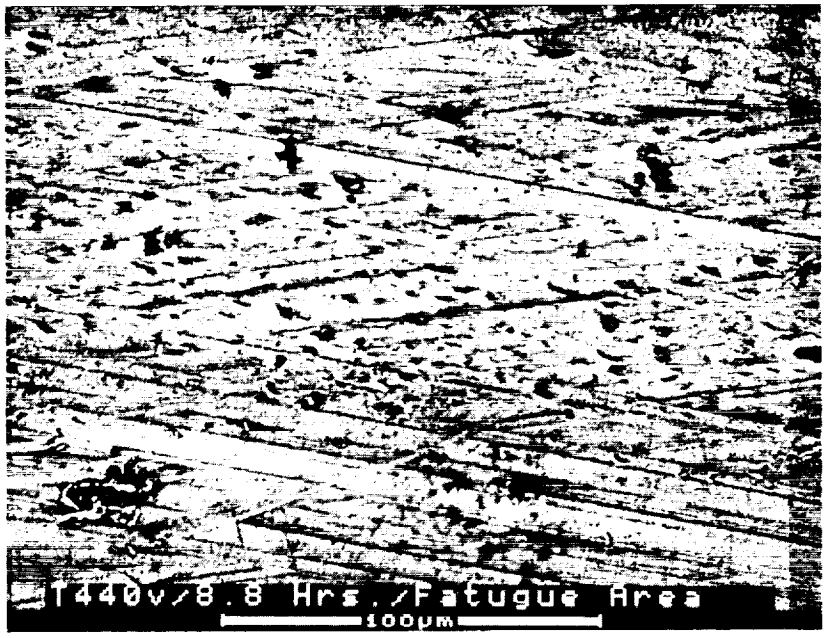

(a) Wear Track ⟶ 500X

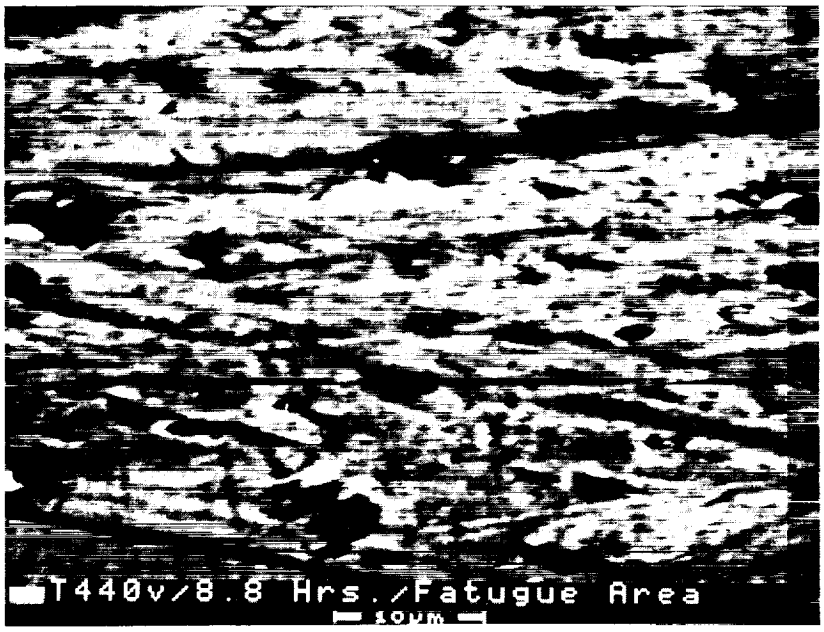

(b) Wear Track at Higher Magnification ⟶ 1,990X

Figure 45. Scanning electron microscope (SEM) image of wear track surface of P/M T-440V alloy ball which failed after 8.8 hours.

(Note that microspall failure mechanism is dominant.)

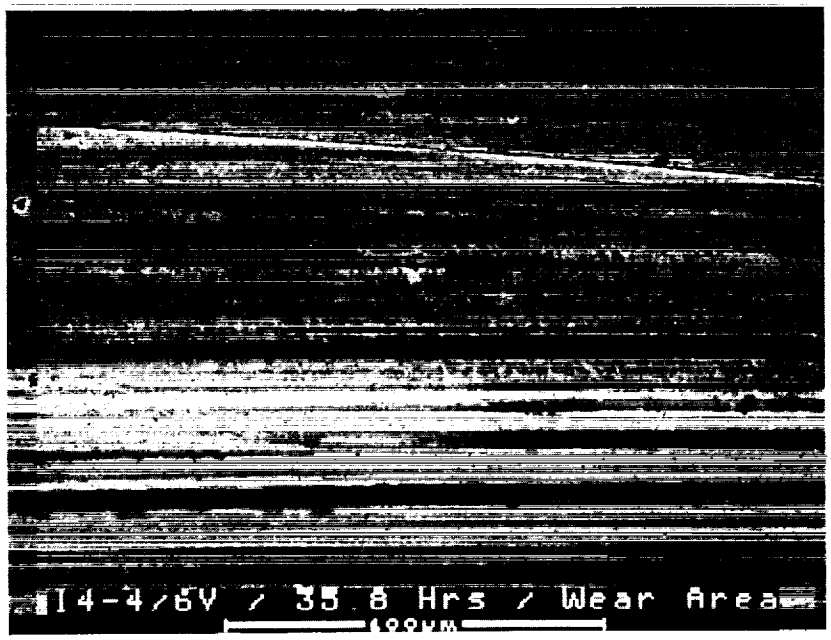

(a) Wear Track ⟶ 500X

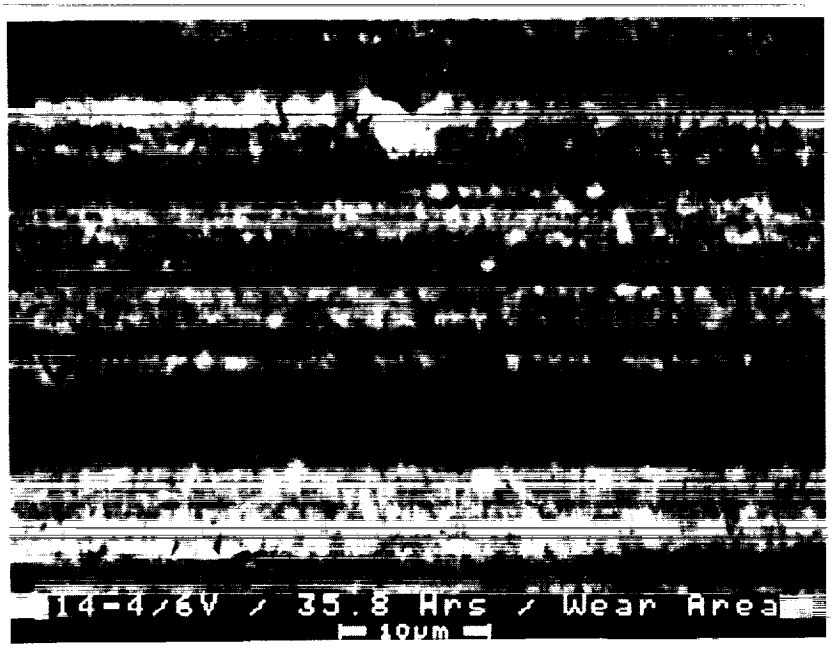

(b) Wear Track at Higher Magnification ⟶ 2,000X

Figure 46. Scanning electron microscope (SEM) image of wear track surface of P/M 14-4/6V alloy ball which failed after 35.8 hours.

(Note mixed mode of failure of wear lines and microspalls.)

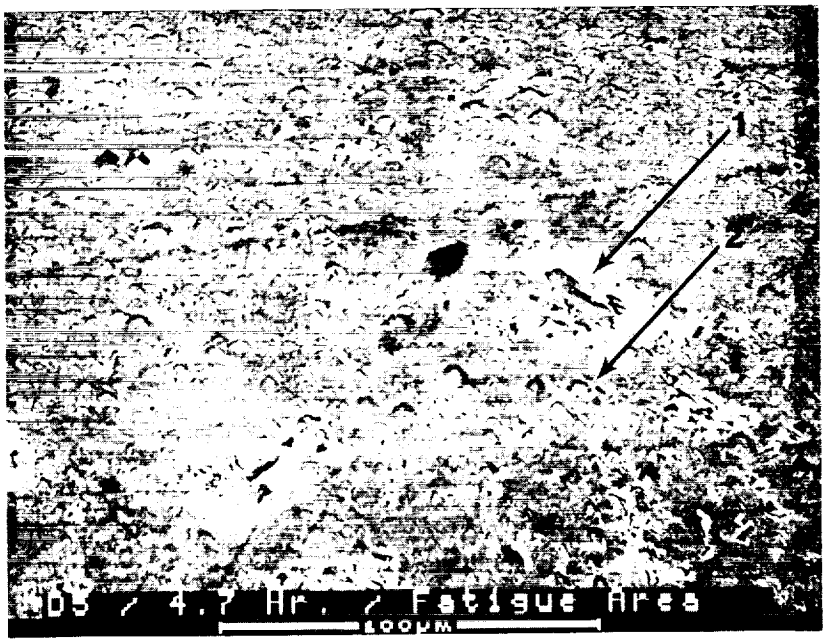

(a) Wear Track ⟶ 500X

(b) Spall Area (No. 1) at Higher Magnification ⟶ 2,000X

Figure 47. Scanning electron microscope (SEM) image of wear track surface of P/M D-5 alloy ball which failed after 4.7 hours.

(c) Area of Multiple Fatigue Damage Sites (No. 2) at Higher Magnification ⟶ 2,000X

Figure 47. (continued) Scanning electron microscope (SEM) image of wear track surface of P/M D-5 alloy ball which failed after 4.7 hours.

C. Phase 3 - Full-Scale Bearing Development and Testing

The objective of Phase 3 was to conduct full-scale bearing tests to evaluate the performance of the material selected, MRC-2001, in Phase 2. There were three tasks as part of this phase. Task 1 was directed towards the fabrication of the candidate bearings. Task 2 efforts required the actual testing of the candidate bearings and was the responsibility of NASA/MSFC. NASA/MSFC would rate the performance of the bearings and recommend whether further consideration should be given to additional evaluation in advanced propulsion systems. Results of the testing are not included as part of this report. The last task, Task 3, required the preparation of a specification for the material and associated fabrication techniques. Discussions of candidate bearing fabrication and the resultant material specification are presented below.

1. Task 1. Fabrication of Candidate Bearings. The task objective was to manufacture candidate bearings from MRC-2001 for full-scale bearing tests. Two bearing designs were used, Rockwell Rocketdyne drawings RS007955-261 and 7R032203-1, Rev. E. Twenty bearings were to be manufactured from each design. In addition, sixty (60) liquid oxygen (LOX) test specimens, twenty (20) rolling contact fatigue (RCF) specimens, and wire material for gaseous oxygen (GOX) flammability tests also were produced during this task.

a. Candidate Bearing Material Procurement. Besides the MRC-2001 alloy, X-405 also exhibited superior performance in the Phase 2 evaluation trials. Because of these results, consolidation of X-405 powder also was included in this task; however, only preform shapes suitable for bearing manufacture were to be made for future requirements for prototype bearings of X-405.

The powders for this task were procured from Crucible Research Center. The powders were made by nitrogen gas atomization and only powders finer than -150 mesh were used. Larger particle sizes were considered scrap. The heat numbers and chemical composition of each heat used in this task are shown in Table 15.

As discussed in the Phase 2 section of this report, the carbon content of the MRC-2001 alloy specification had been increased from 1.2 weight percent carbon at the beginning of the program to 1.5 weight percent. The weight percentages of some of the other alloying elements also were slightly changed. This had been done to address problems that had been experienced in Phase 1 in achieving consistent hardness levels after heat treatment. The carbon level in an alloy such as MRC-2001 must be great enough to form sufficient carbides and harden the matrix, but must not be so great that it significantly depletes the chromium level in the matrix and diminishes the corrosion resistance. No problems were found in Phase 2 relating to the increased carbon level in the MRC-2001.

Table 15
Chemical Composition of Bearing Materials for Phase 3

Alloy	Heat No.	Base	Cr	Mo	V	Cb	B	Mn	Si	C	O	N	P	S
MRC-2001(1)	518-536	Fe	15.54	7.39	2.05	0.12	0.10	0.40	<0.02	1.45	0.009	0.069	0.03	0.004
X-405(2)	517-910	Fe	19.57	2.05	1.08	-	-	<0.1	<0.1	1.27	0.006	0.12	<0.01	0.004

(1) Determined on -150 mesh powder
(2) Determined on -10 mesh powder

b. Consolidation of Preform Shapes for Bearings. This task required the consolidation of two preform shapes for the bearings, ball wires for the balls and rings for the races. Consolidation of the ball wires was relatively straightforward as long as attention was placed on the welding parameters and techniques in sealing the hot isostatic press (HIP) cans. All consolidation was performed by HIP.

The dimension of the cans for ball wire were 1.4 cm (9/16 inch) inside diameter, 1.9 cm (3/4 inch) outside diameter by approximately 68 cm (27 inches) long. A yield of approximately 61 cm (24 inches) was anticipated. The can material was low carbon mild steel to obtain maximum weldability and good flow during consolidation.

The can components, especially the insides of the tubes were thoroughly cleaned with solvent during preparation. All powder handling was performed under Class 100 clean room conditions (see Figure 48). During filling the cans were "tapped" on the side to maximize the loose powder density. Densities greater than 70% were measured after filling and tapping. The final sealing of the cans was done via electron beam (EB) welding. A can top was welded (similarly as the bottom) to the tubular cans after powder filling. The top had a small hole in the center. The cans were placed in the EB weld chamber which was then evacuated. The cans outgassed through a small hole in one end until the vacuum level in the chamber was 2.0×10^{-5} torr or less. Then the small hole was EB welded to seal the can, removed from the chamber and helium leak checked to verify the absence of leaks. A total of 21m (approximately 70 feet) of 1.12 cm (0.440 inch) diameter bar was prepared for the manufacture of the balls for 40 prototype bearings. This quantity was a conservative estimate to allow for losses in setup, processing, etc.

All sealed cans were HIP'ed at $1149^{o}C$ ($2100^{o}F$)/207 MPa (30 Ksi)/150 minutes. Metallographic evaluations were perfomed on HIP bar ends to ensure complete densification. Several specimens indicated some porosity attributed to can leaks and were removed from the lot to be used for ball wires. The can material then was leached off, the wires warm straightened at approximately $260^{o}C$ ($500^{o}F$) and centerless ground to the required 1.12 cm (0.440 inch) diameter.

For the manufacture of the bearing raceways, approximately 150 cm (60 inches) of ring stock, 10.8 cm (4.25 inch) outside diameter by 5 cm (2 inch) inside diameter was required. The fabrication of suitable ring stock was found to be more difficult than originally anticipated. Some detail of the trials is presented here to allow duplication of this effort in the future without any extensive development.

Several initial trial runs were planned and conducted utilizing "scrap" MRC-2001 powder. The first ring stock was produced using a can with a 12.7 cm (5 inch) outside diameter and a 12.1 cm (4.75 inch) inside diameter with a 5 cm (2 inch) solid bar in the center. The can was 30 cm (12 inches) in length. Handling of the powder (filling, etc.)

Figure 48. Filling of ballwire cans in Class 100 clean room conditions.

C-2

and sealing of the raceway cans was handled similarly as described for the ball wire cans. All HIP was conducted at 1149°C (2100°F)/207 MPa (30Ksi)/150 min. Evaluation after HIP indicated that sectioning of the ends using an abrasive cutoff wheel generated thermal cracks (heat checks) due to overheating. This was not a problem with the smaller ball wire material. After modification of the cutoff process, a good section was obtained that had no heat checks. It was found, however, that a circular crack still remained around the center mandrel, on average approximately 0.25 cm (0.1 inch) offset from the mandrel/MRC-2001 interface. Initially it was believed that this crack developed due to the differential thermal expansion between the mild steel mandrel and the MRC-2001 ring surrounding it. The basis for this conclusion was that the average coefficient of thermal expansion of mild steel between ambient temperature and 1149°C (2100°F) is approximately $13.5 \times 10^{-6}\ ^{o}C^{-1}$ ($7.5 \times 10^{-6}\ ^{o}F^{-1}$). The thermal expansion coefficient of MRC-2001 was determined by MMTC to be $12.6 \times 10^{-6}\ ^{o}C^{-1}$ ($7.0 \times 10^{-6}\ ^{o}F^{-1}$). Because the mild steel mandrel has a higher coefficient of thermal expansion than the MRC-2001, it would generate a tensile stress in the radial direction as it cooled from the HIP temperature.

MMTC decided that a hollow core tube may be the best solution to solving the cracking problem. A trial can was produced having a core tube 5 cm (2 inches) in outside diameter with a 0.8 cm (0.3 inch) wall. The outer tube was 13.3 cm (5.25 inches) outer diameter with a 0.3 cm (0.125 inch) wall thickness. The outer diameter was increased based on the results of the previous trial in order to meet the outside diameter ring stock dimension requirements. After successful HIP of the can filled with MRC-2001 powder, sections were taken from the bar. Again some heat checks were found but, initially, no major cracks. However, it was disconcerting to examine the parts several days later and find major cracks on opposite sides of the core and reaching, in one case, to the outer can shell as shown in Figure 49. The delayed nature of their appearance indicates that the cracks are a result of accumulated stress on the untempered martensite of the microstructure. Previous conjecture that the cracks were the result of thermal expansion differentials were unfounded. Computations commonly used in the welding industry to compute residual stresses, show that the contraction of the core bar would only have applied a stess level of approximately 100 to 138 MPa (15 to 20 Ksi) to the surrounding alloy steel. Such a stress level is inadequate to account for the cracks observed.

A third trial was conducted using a modified HIP run. Utilizing the same procedures for can making as described in trial two with a solid mandrel, the can was HIP'ed under the previously described HIP conditions. However, the cooling cycle was carefully controlled to achieve an annealed condition. The temperature was allowed to drop normally from 1149°C (2100°F) to 843°C (1550°F), but was then held six hours at 843°C (1550°F). A cooling rate of 11°C (20°F) per hour was established from 843°C (1550°F) to 649°C (1200°F). The can was held an additional five hours at 1200°F, and then allowed to cool normally to room temperature. The pressure in the HIP vessel dropped as the

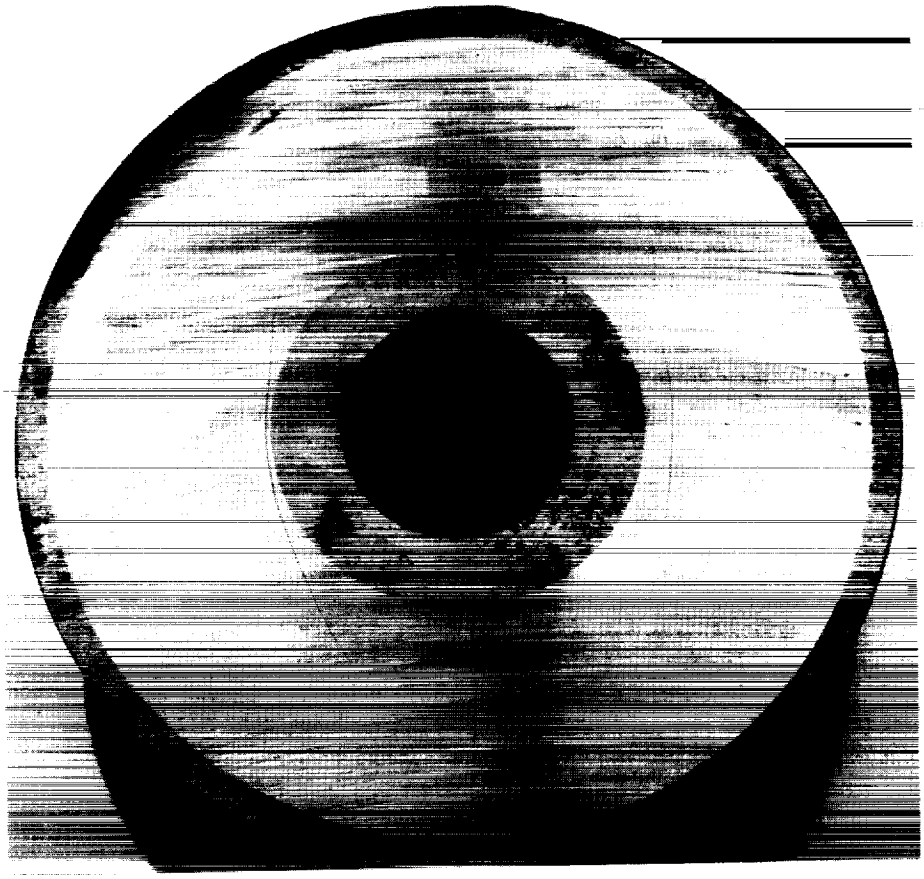

Figure 49. Section of hollow core raceway compact. Bottom cut-off wheel cut is at top, showing heat checks which were visible immediately after cutting. The arc shaped cracks on each side of the core did not appear until several days had elapsed after cutting.

temperature dropped, but was still approximately 120 MPa (17.5 Ksi) at the end of the 649°C (1200°F) hold. Sectioning of the can showed no evidence of any cracks.

Although the consolidation of the raceway was successful with the modified HIP cycle, there now was concern that the slow cooling cycle may promote the formation of carbide networks, instead of the fine spherodized structure expected. Figure 50 shows the microstructure obtained from the slow HIP cycle, as revealed by two different etches. The specimen was made from -10 mesh, MRC-2001 powder for this trial. The usual molybdic acid etch shows what appears to be a continuous link of carbide (white). A combination of picral followed by Beraha's etch colored the matrix and left the carbides clear. The size of the areas surrounded by the white carbides in the lower part of Figure 51 are only 0.0005 to 0.002 cm (0.0002 to 0.0005 inch) across, and probably do not correspond to the prior austenite grain size.

The as-HIP material was subjected to an austenitizing treatment at 1121°C (2050°F) for hardening. Figure 51 shows the results of this treatment compared to the as-HIP condition. There appeared to be no continuous networks present as a result of the austenitizing treatment indicating that the hardening treatment will render any as-HIP carbide continuity harmless in the final bearings. The carbides that agglomerated as a result of the HIP operation were high chromium carbides which then dissolved at the austenitization temperature and reformed during the quench as independent particles. It was concluded that the material would offer the same properties as found for all previous HIP MRC-2001.

Based on the compaction results for the raceway stock, HIP cans were prepared to the dimensions described previously at a length of 61 cm (24 inches)(See Figure 52). They were fabricated with a hollow center and utilized a slip fit mandrel to maintain straightness and dimensions. Three cans for each alloy, MRC-2001 and X-405, were fabricated, cleaned, filled, sealed and leak checked as described previously for the ball wires. -150 mesh powder was used for all cans except for one X-405 can. Since inadequate -150 mesh powder was available, -60 mesh powder was used with the approval of NASA-MSFC. The sealed cans were HIP using the modified HIP cycle.

Evaluation of the six HIP cans indicted complete consolidation. There were some fine cracks at the ends that did not propagate for the MRC-2001 alloy only. Possibly thinner end caps may reduce the tendency for cracking. The canning material was leached and machined off. Typical microstructures of the as-HIP material are shown in Figures 53 and 54. The structures are typical of what is found in the annealed condition.

All ball wires and raceway rings were ultrasonically inspected prior to shipment to the ball bearing vendor and were found to be completely sound. It should be noted that MIL-STD-2154 was called out

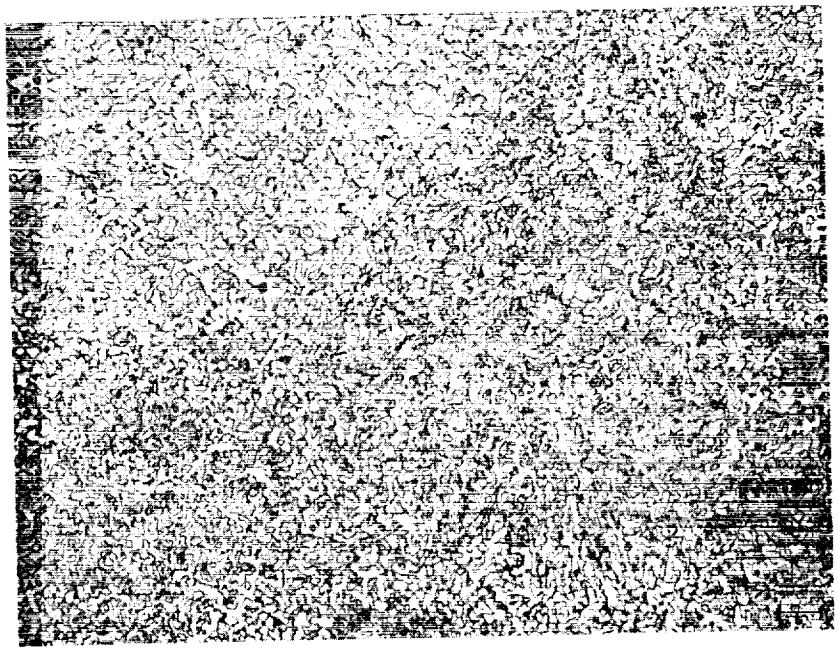

MOLYBDIC ACID SLOW COOL FROM HIP 500X
HRC 30-31

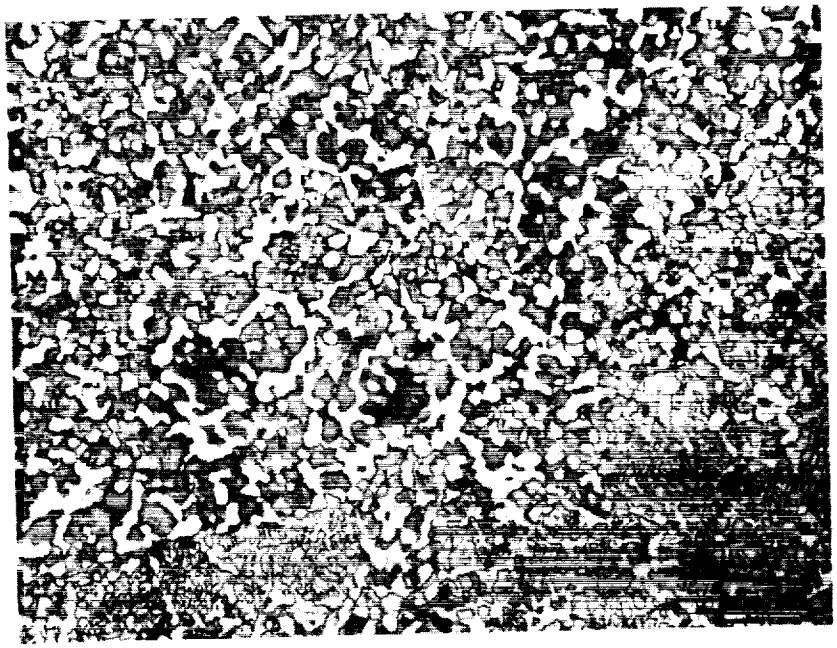

PICRAL + BERAHA'S SLOW COOL FROM HIP 1000X
HRC 30-31
White area is carbide

Figure 50. MRC-2001 microstructure-slow cool from HIP.

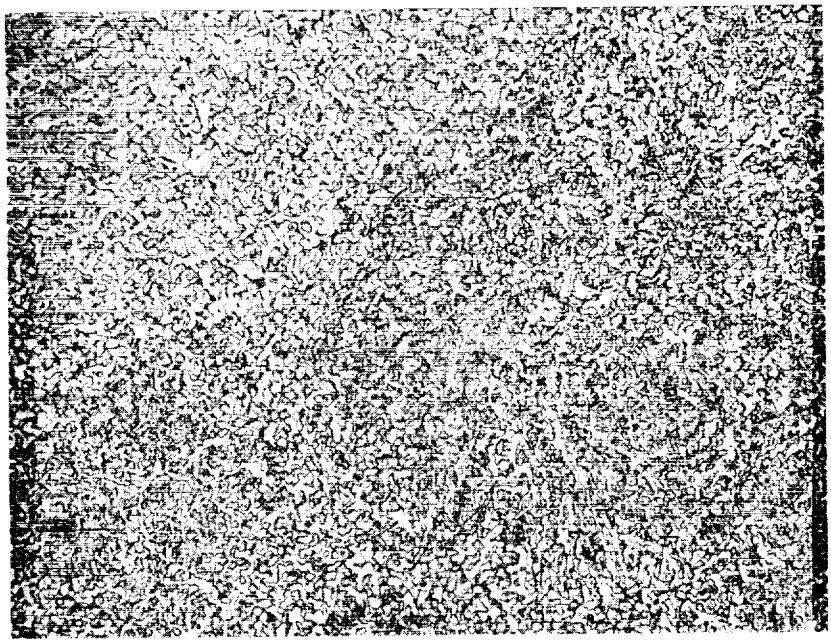

MOLYBDIC ACID SLOW COOL FROM HIP 500X
HRC 30-31

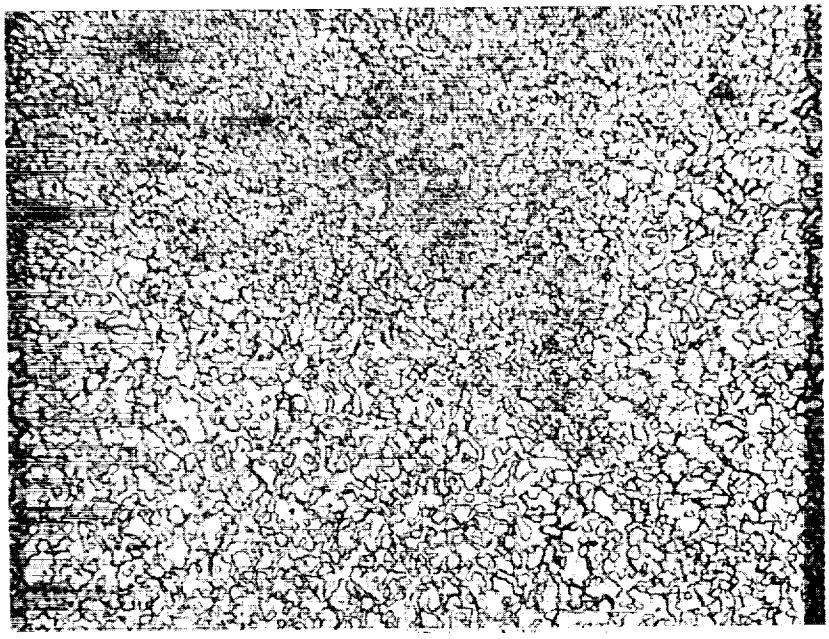

MOLYBDIC ACID HARDENED FROM 2050F 500X
HRC 60-62

Figure 51. Microstructural comparison of MRC-2001 after an austenitizing treatment.

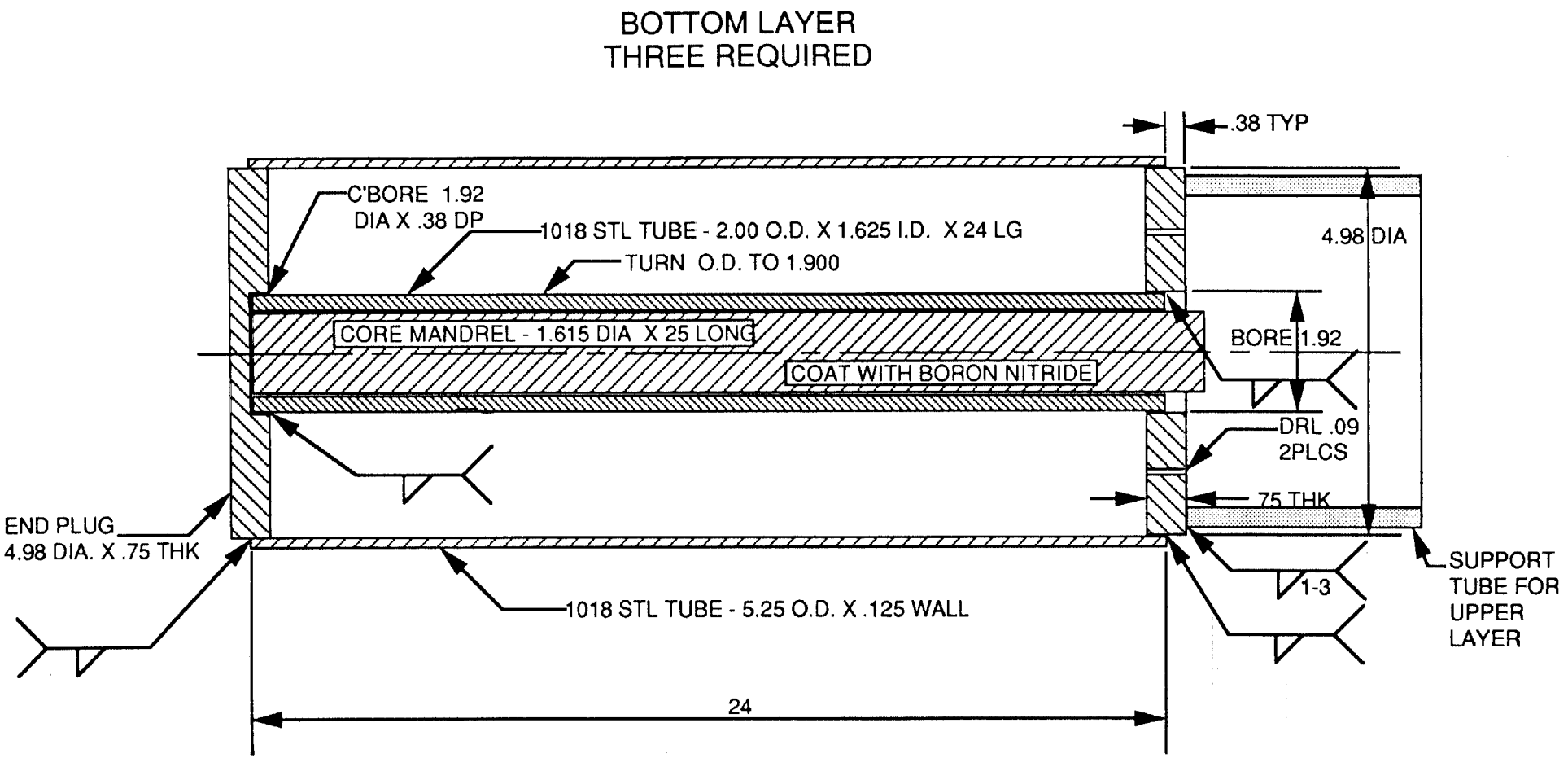

NOT TO SCALE

Figure 52. Raceway HIP can.

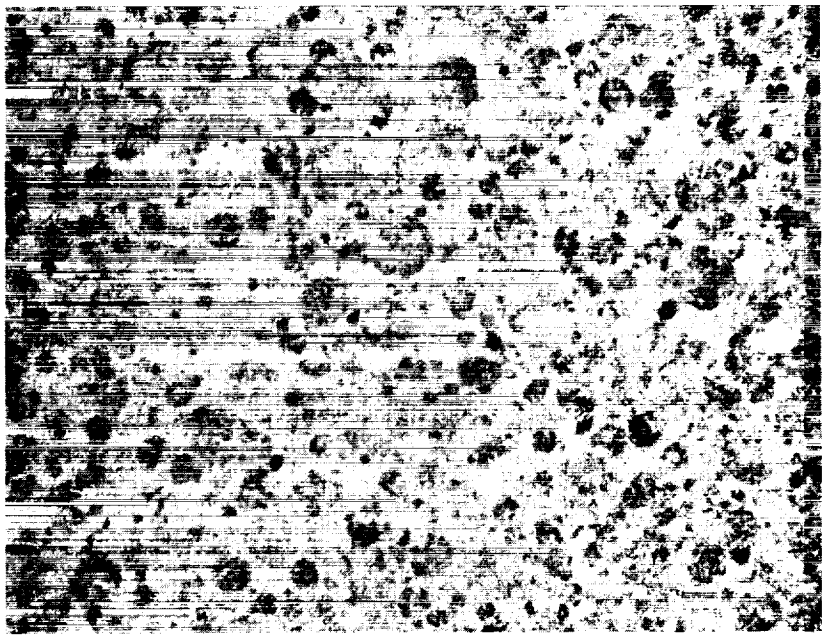

MOLYBDIC ACID 100X

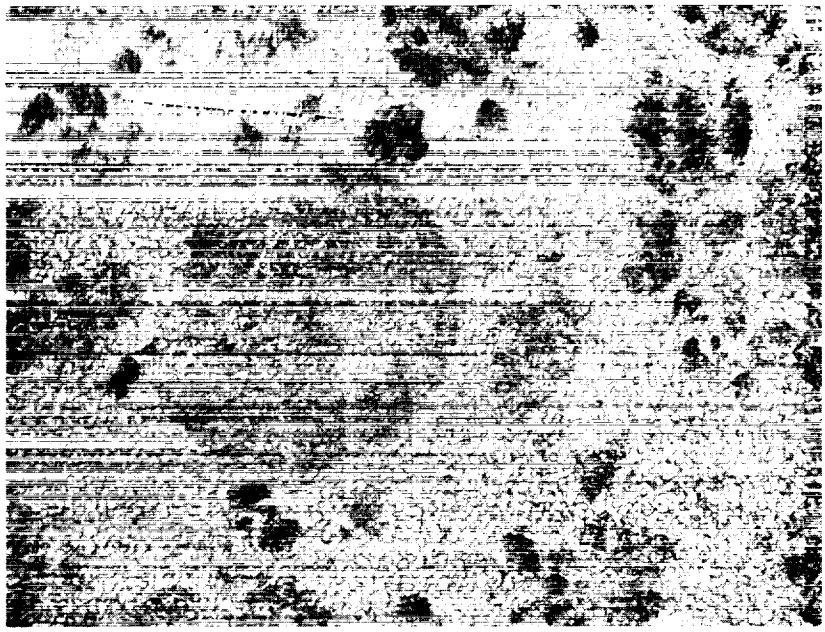

MOLYBDIC ACID 500X

Figure 53. As-HIPped microstructure of MRC-2001 utilizing modified HIP procedures.

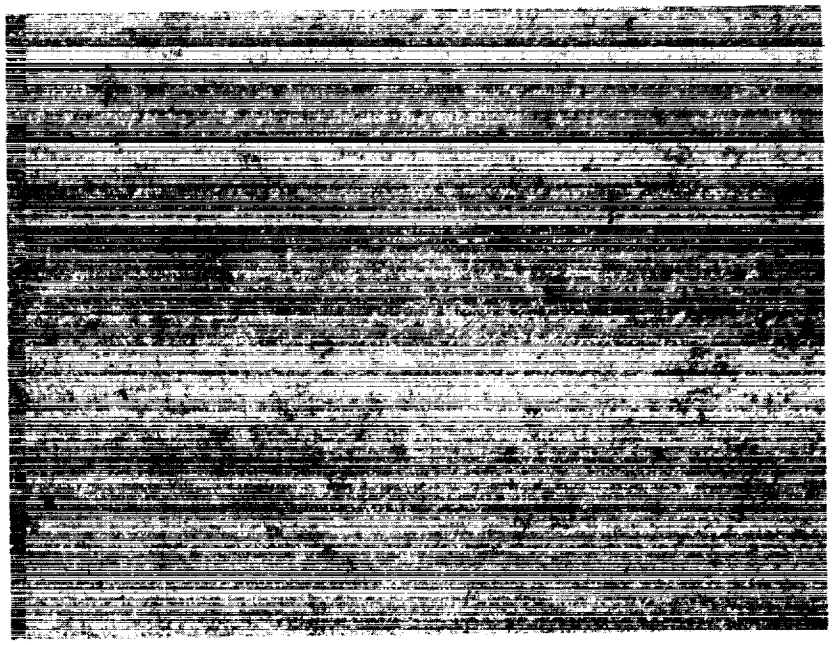

MOLYBDIC ACID 100X

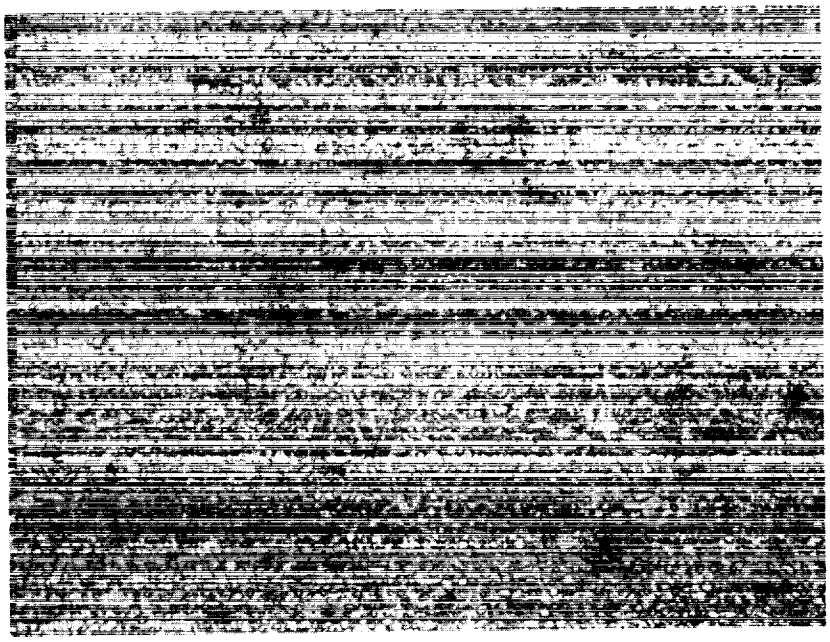

MOLYBDIC ACID 500X

Figure 54. As-HIPped microstructure of X-405 utilizing modified HIP procedures.

on the Rocketdyne drawings specifically identified as a process for "Wrought Metals" and, therefore, is of limited applicability to the powder metallurgy product of this program. After inspection, the ball wire and raceway ring stock were shipped to Split Ballbearing (SBB) to be used in the manufacture of the bearings.

As part of the above effort, material for rolling contact fatigue (RCF) specimens and liquid oxygen (LOX) tests also was consolidated. The RCF specimens were removed from twenty of the ball wires for each alloy so that the testing would include specimens from all of the ball wire HIP runs. A separate bar was HIP'ed for the LOX impact specimens for MRC-2001. Material was rough machined, heat treated and then final machined to the required dimensions for both specimens. Twenty (20) machined blanks of each alloy were prepared for the RCF test specimen. Sixty (60) machiend blanks (1.71 cm (0.674 inch) diameter by 0.16 cm (0.063 inches)) of the MRC-2001 alloy were prepared for the LOX impact specimens. In addition NASA-MSFC requested material for gaseous oxygen (GOX) flammability tests. MRC-2001 ball wires that were found to be porous as previously discussed were suitable for this test. MMTC shipped to NASA-MSFC twenty (20) each alloy RCF specimens, sixty (60) MRC-2001 LOX specimens and seven (7) MRC-2001 ball wires for GOX flammability tests. All testing and results will be reported by NASA-MSFC.

c. Bearing Manufacture. As previously mentioned, the task objective was to manufacture forty (40) bearings, twenty (20) each of two Rocketdyne designs. The bearings were 57mm in size and were defined by design drawings RS007955-261 and 7R032203-1, Rev. E. MMTC contracted the bearing manufacture with Split Ballbearing (SBB) a Divison of MPB Corporation located in Lebanon, New Hampshire. The MRC-2001 ball wire and ring preform stock prepared in this program was shipped to SBB for bearing manufacture.

Processing of the ball wire into the required 1.27 cm (0.5 inch) diameter balls was done by hot heading. Normally balls are cold headed to the required diameter; however, MRC-2001 does not respond to cold heading as it will crack upon working. The hot heading of the balls was performed for SBB by MRC Specialty Ball in Winstead, Connecticut. MRC along with MMTC had conducted numerous processing trials of the MRC-2001 alloy in the early 1980's and were familiar with the materials characteristics. MRC apparently is the only ball manufacturer in the United States capable of hot heading. A simplified routing used to process the wire into balls is given below in Table 16.

All operations listed above were conducted by MRC except for the heat treatment inspections performed at SBB called out as NDT inspection which was the responsibility of SBB. The hot heading operation yielded 677 pieces from the ball wire supplied. The yield at shipment from MRC was 622 balls or 92% which is considered excellent for an alloy that has little processing history. Processing of the ring preform stock for the raceways was straightforward. Essentially the ring stock was abrasive saw cut, heat treated and ground to the required dimensions. The process routing for raceway manufacture is presented in Table 17.

Table 16
Typical Process Routing for MRC-2001 Balls from 1.12 cm Ball Wire

Operation	Comment
Hot Head	1149°C (2100°F)/1.43 cm (9/16 in) die
Place Balls in Lime	Minimizes cracking and oxidation
Stress Relieve	Place in furnace below 149°C (300°F), heat to 593°C (1100°F), hold 1 hour and air cool
Clean, Weight, Count	-
Inspection	-
Anneal	Heat to 816°C (1500°F), hold 1 hour minimum, cool to 538°C (1000°F) at a rate less than 10°C (50°F) per hour, air cool
Soft Grind and Inspect	-
Macro Etch	-
Clean, Weigh, Count	-
Heat Treat	See Appendix
Metallography	-
Clean, Weigh, Count	-
Hard Grind and Inspect	-
Clean, Weigh, Oil	-
Rough Lap and Inspect	-
Clean	-
Finish Lap	-
Inspection	Dimensions, Sphericity, Waviness, Diameter and Lot Variation, Surface Roughness
Clean	-
Size Check	-
30X Visual Inspect	-
Passivation	MRC Spec. PS-16
Sample Size	-
Sample Alloy Ident.	-
NDT Inspection	Passivation (SBB EPS 11), Penetrant (SBB ECS 30.6), Etch (SBB ECS 30.5A), Penetrant (SBB ECS 30.6A), Hardness, Visual

Table 17
Typical Process Routing for MRC-2001 Raceways

Operation	Comment
Mark	Heat Code
Heat Treat	See Appendix
Magnaflux	SBB EPS 22
Rough & Finish Grind Surface	-
Mark	Transfer Heat Code
Rough Grind OD, Bore, Race and Dam	-
Rough and Finish Grind Chamfer OR	-
Radius I.D. Bore Corner	-
Bore Misc., Bore Corner	-
Stress Relieve	135°C (275°F)/2 hours min.
Finish Grind OD, Bore Race and DAM	-
Rough and Finish Grind Chamfer OD, B.T. Corner	-
Stress Relieve	135°C (275°F)/2 hours min.
S.L. Deburr	-
Rough and Finish Hone	-
Inspect all Race Characteristics	-
Mark	Transfer Heat Code
Surface Grind OR OD Misc	-
Zyglo	SBB ECS 30.6
S.L. Deburr	-
Eddy Current	SBB ECS 30.9
Passivate	SBB ERS-121
Final Inspect	-

The finished balls and raceways were subjected to additional processing beyond what is described in Tables 16 and 17. This processing is required to meet all specifications on the Rocketdyne drawings. These final major operations for final bearing assembly are described in Table 18.

Photographs of a typical MRC-2001 bearing assembly and the forty bearing assemblies that were shipped to NASA/MSFC for further testing are shown in Figures 55 and 56.

2. Task 3. Material Specification. As part of the final report, a material specification for MRC-2001 has been included. Very little is available in the literature on this alloy since it is a relatively new alloy conceived in the late 1970's by TRW Inc. personnel of the Materials and Manufacturing Technology Center (MMTC) and MRC Bearings. A patent (Patent Number 4,767,456) on this alloy was issued in 1988 entitled, "Corrosion and Wear Resistant Metal Alloy Having High Hot Hardness and Toughness," to Ronald F. Spitzer (MRC Bearings Incorporated).

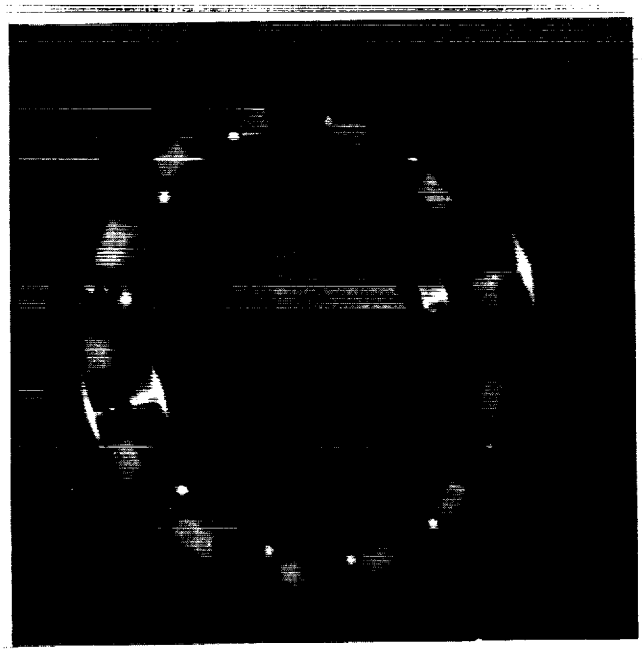

Figure 55. Typical MRC-2001 bearing assembly shipped to NASA-MSFC.

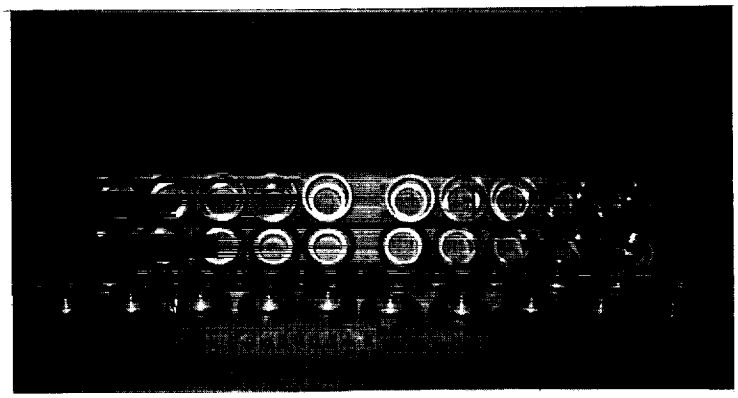

Figure 56. Forty MRC-2001 bearing assemblies shipped to NASA-MSFC.

Table 18
Typical Process Routing for MRC-2001 Bearing Assemblies

Operation	Comment
Process Balls	See Table 16
Process Raceways	See Table 17
Wash and Gage Inners	Match Grind of Outers
Wash and Gage Outers	-
Assemble	Match Inner & Outer Dummy retainers and balls
Wash and Inspect	-
Wash	-
Preload	Measure Flatness
Preload Grind	-
Preload	Measure
Wash and Inspect	-
Mark	-
Wash and Final Inspect	Visual
Inspect	Assign serial numbers
Mark	-
Wash and Final Inspect	Marking
Inspect	Alloy
Wash	-
Lube	Dry film lube inners and outers
Inspect	-

The objective of the material specification is to present data that will allow others skilled in the art to process MRC-2001 successfully. Processing of MRC-2001 is somewhat unique. Although not previously discussed, consolidation by hot extrusion was not entirely successful at MMTC. The extruded product often cracked after extrusion. Further development of this consolidation method is required to yield good quality materials. Possibly a slow cooling after extrusion similar to that used for the race material after HIP would solve the cracking problems. HIP of the powder is the optimum consolidation method at this time; however, as described earlier, a modified HIP cycle that allows slow cooling to yield an essentially annealed product is required. Finally, heading of the material into balls must be performed hot because of the composition. The composition of MRC-2001 includes elements that does not allow one to use conventional procedures to produce the alloy. The advantage of powder metallurgy is to design a unique alloy especially useful for bearing applications such as the SSME.

The material specification is presented separately as an Appendix.

SECTION III. CONCLUSIONS AND RECOMMENDATIONS

The mechanical property testing conducted in this program has indicated two alloys, MRC-2001 and X-405, as being superior to the current SSME alloy, 440C. The program has shown that a technology such as powder metallurgy can be used to design alloys for very demanding applications that cannot be produced by conventional ingot metallurgy approaches.

Testing of the alloys in this program were performed on material in the as-HIP plus heat treated condition except for five-ball testing. Material for five-ball testing was hot headed prior to heat treatment. To improve yields, reduce cost and possibly improve the microstructure, it is recommended that consolidation by extrusion be more extensively investigated. Since the initiation of the program there have been substantial improvements in powder production. Although MRC-2001 has many superior properties, the fracture toughness is not as high as one would want ideally. It is recommended that more emphasis and development be directed at the powder processing end to minimize oxygen and other impurities and to look at higher nitrogen contents to improve toughness. Some of these evaluations are being pursued in a new NASA-MSFC contract (10).

SECTION IV. APPENDIX

MATERIAL SPECIFICATION FOR MRC-2001

MRC-2001 steel is a corrosion and wear resistant powdered metal alloy. For maximum toughness considerations, the powder is nitrogen gas atomized. The alloy is ideally suited for use in bearing applications at cryogenic, ambient and elevated temperatures. MRC-2001 has demonstrated superior hot hardness, toughness, corrosion resistance and wear resistance for bearing applications.

Chemical Composition

	Base	Cr	Mo	V	Mn	Cb
MRC-2001	Fe	14-16	6-8	1.75-2.25	0.4-0.6	0.05-0.15

C	Si	O	S/P
1.4-1.55	0.1 max.	50ppm max.	0.03 max.

Martensitic Transformation Temperature

Ms 70-80°C (160-175°F)

Powder Size

Powder screened to -150 mesh is preferred

Consolidation

A preferred method of consolidation for the MRC-2001 powder is hot isostatic pressing (HIP). Standard HIP can manufacture, cleaning, filling, sealing, and leak checking are employed. HIP can material is low carbon steel for maximum ductility during consolidation. HIP parameters will depend upon size. Large diameter bar essentially has to be annealed as part of the HIP cycle. Recommended HIP cycle parameters are as folows:

Up to 2.54 cm (1 inch) in diameter or cross-section

1149°C (2100°F)/207 MPa (30 Ksi)/150 min.
Normal cool from 1149°C (2100°F) to unload

Greater than 2.54 cm (1 inch) in diameter or cross-section

1149°C (2100°F)/207 MPa (30 Ksi)/150 min.
Normal cool from 1149°C (2100°F) to 843°C (1550°F)
Hold at 843°C (1550°F) for 6 hours
Cool from 843°C (1550°F) to 649°C (1200°F) at a rate of 11°C (20°F) per hour
Hold at 649°C (1200°F) for 5 hours
Normal cool from 649°C (1200°F) to unload

Forging

Heat material thoroughly to 1149°C (2100°F) prior to forging or hot heading. Do not forge below 1121°C (2050°F). Reheat as necessary. After forging, cool slowly in vermiculite or lime.

Annealing

Heat uniformly to 843°C (1550°F), and hold at temperature for 2 hours. Cool from 843°C (1550°F) to 649°C (1200°F) at a rate of 11°C (20°F) per hour, then air cool. Typical hardness is Rc 32.

Stress Relieving

Stress relieving is normally performed after hot working to allow a visual inspection without the scale that would form from a full anneal. Place in furnace which is below 149°C (300°F) and heat to 593°C (1100°F). Hold for 1 hour and air cool.

Hardening

Preheat to 843°C (1550°F) and soak for 10 minutes. Transfer to a furnace at 1121°C (2050°F) and soak for 20 minutes. Soaking times will depend upon section size.

Quenching

Quench in salt at 177°C (350°F) and hold for 10 minutes, then air cool.

Cryogenic Treat/Tempering

Double deep freezing and tempering are performed to eliminate retained austenite. The process includes a deep freeze at -79°C (-110°F) for one hour plus -196°C (-321°F) in liquid nitrogen for one hour followed by a tempering cycle.

Typically MRC-2001 is tempered at 538°C (1000°F) for 2 hours and air cooled. The deep freeze and tempering cycles are repeated for a second time. Typical hardness after the second temper is Rc 60-62.

SECTION V. REFERENCES

1. Bhat, B.N., Humphries, T.S., Thom, R.L., Friedman, G.I., Moxson, V.S.: "Powder Metallurgy Bearings for Advanced Rocket Engines," Proceedings of Advanced Propulsion Technology Conference, NASA Publications, NASA/MSFC Huntsville, Alabama, May 13-15, 1986.

2. "HPOTP Bearing Consultant Review," Rockwell International Report BC 81-52, March 25, 1981

3. Bhat, B.N.: "Fracture Analysis of HPOTP Bearing Balls," NASA TM- 82428.

4. Dufrane, K.D. and Kannel, J.W.: "Evaluation of Shuttle Turbo Pump Bearings," NASA CR 150906.

5. Bhat, B.N. and Dolan, F.J.: "Past Performance Analysis of HPOTP Bearing," NASA TM-82470, March, 1982.

6. Friedman, G.I. and Bhat, B.N.: "Advanced Bearing Materials for Cryogenic Aerospace Engine Turbopump Requirements," Proceedings of AIAA/ASME/SAE/ASEE 22nd Joint Propulsion Conference, Alabama, June, 1986.

7. Moxson, V.S., Friedman, G.I., Bhat, B.N.: "Application of Powder Metallurgy Techniques to Produce Improved Bearing Elements for Liquid Rocket Engines", Powder Metallurgy in Defense Technology Seminar," Annapolis, Maryland, December, 1986.

8. Parker, Richard J., Zaretsky, Erwin V. and Dietrich, Marshall W.: "Rolling-Element Fatigue Lives of Four M-Series Steels and AISI 52100 at 150^{O}F, "NASA TN D-7033, February 1971.

9. Zaretsky, Erwin V., NASA Lewis Research Center, personal communication to Fred Dolan, NASA Marshall Space Flight Center, June, 1989.

10. Moracz, D.J. and Benn, R.C.: "Application of Powder/Wrought Composite Metallurgy Techniques to Produce Fracture-Tough Bearing Elements," Monthly Report No. 6, April 1992 under Contract NAS8-38977.